

A SYSTEM DYNAMICS APPROACH FOR
CLIMATE CHANGE IMPACT ANALYSIS IN THE SNAKE RIVER BASIN

By

David Jerome Hoekema

A thesis

submitted in partial fulfillment

of the requirements for the degree of

Master of Science in Civil Engineering

Boise State University

May 2011

BOISE STATE UNIVERSITY GRADUATE COLLEGE

DEFENSE COMMITTEE AND FINAL READING APPROVALS

of the thesis submitted by

David Jerome Hoekema

Thesis Title: A System Dynamics Approach for Climate Change Impact Analysis in the Snake River Basin

Date of Final Oral Examination: 11 January 2011

The following individuals read and discussed the thesis submitted by student David Jerome Hoekema, and they evaluated his presentation and response to questions during the final oral examination. They found that the student passed the final oral examination.

Venkataramana Sridhar, Ph.D., P.E. Chair, Supervisory Committee

George A. Murgel, Ph.D., P.E. Member, Supervisory Committee

Gary S. Johnson, Ph.D., P.E. Member, Supervisory Committee

Sudhir Goyal, Ph.D. Member, Supervisory Committee

The final reading approval of the thesis was granted by Venkataramana Sridhar, Ph.D., P.E., Chair of the Supervisory Committee. The thesis was approved for the Graduate College by John R. Pelton, Ph.D., Dean of the Graduate College.

DEDICATION

I dedicate this thesis to my wife, Bethany, my three children, Andrew, Abigail, and Benjamin, as well as my father, Dr. Dale Hoekema, who has inspired me with his life-long pursuit of learning.

ACKNOWLEDGEMENTS

Special thanks to my advisory committee members Dr. Sudhir Goyal, a Hydrologist with the Idaho Department of Water Resources, and Dr. Gary Johnson, Associate Professor with the University of Idaho.

Support of this project by the NSF-Idaho EPSCoR Program and the National Science Foundation under award number EPS-0814387, and a student scholarship from the United States Society on Dams are gratefully acknowledged.

ABSTRACT

Warming temperatures throughout the Western United States due in part to human-induced climate change caused by the emission of greenhouse gases has been found to be responsible for 60% of the hydrologic change in the Western United States over the last half century. The hypothesis of the research is that climatic change will make planning and management based on historic climate conditions less reliable in the future. Therefore, there is a need for water management planning tools that capture feedback loops within the water-resource system so that management plans are developed that perform optimally under a wide array of inputs. This thesis explores the use of system dynamics framework to model the feedback loops associated with water management in the Snake River Basin.

The Snake River Planning Model (SRPM) was developed by the Idaho Department of Water Resources (IDWR) in FORTRAN in the 1970s, as a tool for planning and managing water resources in the Snake River Basin. The following research presents the conversion of SRPM from FORTRAN to a system dynamics platform using Powersim Studio 8. The new model is referred to as System Dynamics—Snake River Planning Model (SD-SRPM). New features in the model are a dynamic link between reservoir operations and groundwater/surface water interactions between 6 reaches of the Snake River and the East Snake Plain Aquifer through use of response functions. The response functions were generated using IDWR's East Snake Plain Aquifer Model. SD-SRPM replicates end-of-month reservoir with an r^2 value of greater

than 0.70 for most reservoirs and critical reaches within the Henry's Fork, Snake River, Boise River, and Payette River.

In addition to developing a new platform for the SRPM, this thesis explores the historic response of canal diversions in response to changes in temperature, precipitation, and streamflow within the Snake River during the period 1971-2005. The analysis of temperature and precipitation at ten climate stations throughout the basin indicates a highly significant ($P < 0.10$) increase in average annual temperatures. The greatest temperature increase is occurring in the spring (3.0°C) and winter (3.2°C). Due to the high natural variability of precipitation, few significant trends were found. This increase in winter and spring temperatures is driving increased springtime diversions in the basin. The early season diversions correspond to early season soil moisture conditions as represented to a strong correlation of early season diversions to the Palmer Drought Severity Index and Palmer's z-index. Based on this analysis, a new method of determining diversion demand was developed, referred to as minimum full-supply demand.

In order to test the usefulness of the SD-SRPM model for climate impacts analysis, the model was run using bias corrected, projected flow generated by the Variable Infiltration Capacity (VIC) hydrologic model. The flow from the VIC model was based on downscaled temperature and precipitation data from three global climate models using the A1B emission scenario. The results indicate under future climate change we should expect to see a shift in the unregulated flow hydrograph, more difficulty in filling reservoirs, and perhaps a shift in where shortages occur in the basin and increased flood risk. These impacts seem to be amplified in global climate models

that project greater temperature increases. The analysis of climate impacts indicates that the impacts of climate change based on the historic record may be inadequate for planning future water resource management.

TABLE OF CONTENTS

DEDICATION	iv
ACKNOWLEDGEMENTS	v
ABSTRACT	vi
LIST OF TABLES	xiv
LIST OF FIGURES	xvi
LIST OF ABBREVIATIONS	xxi
CHAPTER ONE: INTRODUCTION	1
Purpose	1
Problem Statement	1
Historical Development of Irrigated Agriculture in Idaho	8
Climatic Variability and Water Conflict	10
System Dynamics Modeling	13
CHAPTER TWO: PHYSICAL DESCRIPTION OF THE SNAKE RIVER BASIN	17
Climate, Geology, and Irrigation within the Snake River Basin	17
Surface Water Diversion Infrastructure and Institutions in the Snake River Basin	21
Out of Priority Delivery in the Eastern Snake River Basin	21
Out of Priority Delivery in the Western Snake River Basin	22
Interbasin Transfers	23

Groundwater/Surface Water Interactions in the Boise and Payette River Basins	23
Groundwater/Surface Water Interactions in the Eastern Snake River Basin	24
CHAPTER THREE: RECENT HISTORIC TRENDS IN SURFACE WATER DIVERSIONS AND CLIMATE IN THE SNAKE RIVER BASIN	26
Current Representation of Diversions in Water Resource Planning and Management	27
Declining Surface Water Supply Since 1967	29
Methods and Materials	30
Mann-Kendall Nonparametric Trend Analysis	30
Surface Water Supply Index Correlation to Canal Diversions	33
Palmer Drought Severity Index Correlation to Canal Diversions	34
Results	37
Mann-Kendall Trend Analysis	37
Temperature Trend Analysis	37
Precipitation Trend Analysis	41
Canal Diversion Trend Analysis	42
Diversion Comparison with Supply and Soil Moisture Indices	47
Comparison of Diversions with SWSI	47
Correlation of April Diversions with PDSI and the Z-index	49
Discussion	51
Conclusions	54
CHAPTER FOUR: MODEL DESCRIPTION OF THE SYSTEM DYNAMICS – SNAKE RIVER PLANNING MODEL	56
Existing Models and Model Selection	56

Components of the System Dynamics Model in Powersim Studio 8	57
The Basic Structure of SRPM and SD-SRPM	58
Modeling Reservoirs	60
Modeling Diversions	64
Modeling Return Flow	66
Modeling Assigned Flow	69
Modeling Flood Control Operations	71
Modeling Reservoir Evaporation	72
Modeling Interbasin Transfers	73
Groundwater Modeling SRPM	74
Brief History of the East Snake River Plain Model and Response Functions	75
Linking SD-SRPM Dynamically to the East Snake Plain Aquifer	76
Modeling Groundwater Recharge in SD-SRPM	77
Determining the Parameters for the Recharge Calculation	85
Determining Non-Modeled Groundwater Contributions from the ESPA to Six Reaches	86
CHAPTER FIVE: MODEL VALIDATION AND HISTORIC SHORTAGE ANLYSIS	88
Model Validation	88
Validation of SD-SRPM Being Linked to the East Snake Plain Aquifer through Use of Response Functions	92
Assessing Historic Shortages Based on Minimum Full-Supply Demand	93
Conclusions	97
CHAPTER SIX: CLIMATE CHANGE IMPACT ANALYSIS USING SD-SRPM	99

Bias Correction of VIC Generated Streamflow Using Quantile Mapping	102
Reach Gain Distribution Method	104
Validating the Reach Gain Distribution Method Using Historic Flow	107
Validating the Use of VIC Redistributed Flow	109
Climate Change Impact Analysis	110
Climate Change Impacts on Unregulated Flow	110
Climate Change Impacts on Reservoir Storage and Shortage Calculations	113
Climate Change Impacts on Groundwater/Surface Water Interactions	117
Climate Change Impacts on Regulated Flow and Flood Risk	120
CHAPTER SEVEN: CONCLUSIONS	121
Selection of Model Platform	121
Modeling Groundwater/Surface Water Interactions	122
Modeling Flood Control Operations	123
Modeling Land-use Changes and Water Rights	123
Modeling Return Flow and Canal Seepage	124
Research on Historic Impacts of Climate Change	124
Conclusion of Study	125
REFERENCES	126
APPENDIX A	134
APPENDIX B	137

APPENDIX C	148
APPENDIX D	155

LIST OF TABLES

Table 1.1	Global Climate Model Descriptions (also see, http://gdo-dcp.ucllnl.org/downscaled_cmip_projections)	7
Table 1.2	Federally Operated Irrigation Projects in Idaho	10
Table 3.1	Significance of and Percent Decline in Annual Flow from Unregulated Streams in the Snake River Basin from 1967-2007 (Clark, 2010)	30
Table 3.2	Location and Elevation of Weather Stations used in Trend Analysis	32
Table 3.3	Average Monthly, Annual, and Seasonal Temperature Trends from 1971-2005 by Climate Station	38
Table 3.4	Trend Analysis of Canal Diversions in the Eastern Snake River Basin above Milner Dam, Average Annual Diversions (kaf) from 1971-2005 are Shown in Brackets after the Annual Trend, Diversion Codes are Described in Appendix A	43
Table 3.5	Trend Analysis of Canal Diversions in the Western Snake River Basin from the Boise River and Payette River, Average Annual Diversions (kaf) from 1971-2005 are Shown in Brackets after the Annual Trend	44
Table 3.6	Crop Emergence Dates at Agrimet Stations	45
Table 3.7	The Correlation of PDSI and Palmer's Z-index to Diversions in the Snake River Plain Based on Spearman's Rank Correlation Coefficient	50
Table 4.1	Call Orders in the Snake River Basin as Represented in SD-SRPM	62
Table 4.2	Irrigation Entities in SD-SRPM and Location of the ESPAM Grid Cells Used to Generate Response Functions for each Entity	78

Table 4.3	Base Reach Gains (kaf) in the Snake River along the East Snake Plain Aquifer	87
Table 5.1	Description of Streamflow Gages Used in Validation of SD-SRPM	89
Table 5.2	Statistical Validation that SD-SRPM Replicates SRPM Operations over the Period from 1991-2005 where Mean Bias is Expressed in kaf	90
Table 5.3	Statistical Validation of SD-SRPM with Response Functions ..	93
Table 5.4	Comparison of Shortages in SD-SRPM based on Average Demand and Minimum Full-Supply Demand	95
Table 5.5	Comparison of Shortages in the Snake River Basin by Region under Minimum Full-Supply Demand	96
Table 5.6	Statistical Comparison of SD-SRPM Runs based on Historic Diversions, Average Demand Diversions (AD), and Minimum Full-Supply Diversions (MFS)	97
Table 6.1	Monthly Flow Ranges on which Hydrologic States are Based in SD-SRPM	105
Table 6.2	October and November Reach Gain Distribution Table for the Boise River	107
Table 6.3	Shortages (kaf) by Decade Based on Actual and Redistributed Flow	108
Table 6.4	Average Annual Historic and Projected Flow Volumes (kaf) ...	112
Table 6.5	Average June and October EOM (kaf) for Palisades and the Boise River Storage Triplex	115
Table 6.6	Changes in Shortages Between Historic Drought and CCSM3 Drought on the Snake River (kaf)	117
Table 6.7	Peak Historic and Projected Monthly Flows Showing the Frequency and Magnitude (in Brackets) of Monthly, Modeled, Regulated Streamflow	120
Table A	Source, Diversion Identification, and Canals Associated with Each Diversion Entity in SRPM and SD-SRPM	135

LIST OF FIGURES

Figure 1.1	Study Area Map of the Snake River Basin Upstream of Hells Canyon Dam Showing Hydropower Dams and Irrigation Reservoirs	3
Figure 1.2	Change in Mean Annual Temperature from 2011-2099 based on the 1949-1999 Mean (Jin and Sridhar, unpublished)	5
Figure 1.3	Percent Change in Mean Annual Precipitation from 2011-2099 based on the 1949-1999 Mean (Jin and Sridhar, unpublished) ..	5
Figure 1.4	Boxplot of Naturalized Flow at Heise, ID (1930-2005) and Unregulated Flow on the Boise River near Twin Springs, ID (1911-2009)	13
Figure 1.5	Three-Hundred Year Reconstruction (1700-2003) of Summer PDSI based on a Gridded Tree-ring Dataset (Cook et al., 1999)	13
Figure 2.1	Map Showing Five Major Surface Water Irrigation Regions in Southern Idaho	18
Figure 3.1	Location Map of Weather Stations Used in Study	32
Figure 3.2	1971-2005 Canal Diversion Correlation with SWSI on the Burgess Canal	34
Figure 3.3	Climate Divisions within Southern Idaho (www.cpc.noaa/monitoring/regional_monitoring/CLIM_DIVS/idaho.gif)	36
Figure 3.4	Average Decadal Temperature at Nampa and Jerome USHCN Stations	39
Figure 3.5	January Monthly Temperature Trends for Daily Average Temperature (green), Maximum Average Daily Temperature (red), Minimum Average Daily Temperature (blue) at the (a) Dubois and (b) Parma Weather Stations from 1971 to 2005	40
Figure 3.6	Annual Diversions of the Burgess Canal	47

Figure 3.7	Monthly Correlation of Burgess Canal Diversions to SWSI	49
Figure 4.1	Side View of How Pool Levels are Represented in SRPM and SD-SRPM	61
Figure 4.2	Pool Levels within the Palisades Reservoir	62
Figure 4.3	Example of Call Order 8 from SD-SRPM	63
Figure 4.4	SD-SRPM Diversion Calculation Structure	66
Figure 4.5	Calculation Method for Determining Return Flow	67
Figure 4.6	SD-SRPM Return Flow Calculation Structure	69
Figure 4.7	SD-SRPM Required Flow Structure	71
Figure 4.8	Flood Control Release Curve for Palisades Reservoir as Determined by IDWR for SRPM	72
Figure 4.9	SD-SRPM Flood Control Curves	72
Figure 4.10	Map of Groundwater (G) and Surface Water (S) Irrigation Entities Described in Table 4.2	76
Figure 4.11	SD-SRPM Recharge Calculation Structure for S10 in SD-SRPM	81
Figure 4.12	Aging Loop Structure Used in SD-SRPM to Calculate Groundwater/Surface Water Interactions for S10	84
Figure 5.1	Comparison of SD-SRPM, SRPM, and Observed Values	91
Figure 5.2	SWSI Supply for the (a) Snake River near Heise and the (b) Boise River near Boise	94
Figure 6.1	A Comparison of GCM Projected (a) Precipitation and (b) Temperature Changes Used in this Study (ECHO-red dotted, CCSM3-red dashed, and PCM1-red solid) versus 13 Other GCM Trends	100
Figure 6.2	Bias Correction of VIC Generated Streamflow	103

Figure 6.3	SD-SRPM Modeled and Observed EOM at (a) Jackson Lake, $r^2 = 0.82$ and (b) Palisades Reservoir, $r^2 = 0.81$ Using Historic, Redistributed Flow	108
Figure 6.4	SD-SRPM Modeled and Observed EOM at (a) Jackson Lake, $r^2 = 0.55$ and (b) Palisades Reservoir, $r^2 = 0.75$ Using VIC Generated, Historic, Redistributed Flow	109
Figure 6.5	Monthly, Bias Corrected, Mean Natural Flow Generated by the VIC Hydrologic Model for the (a) Henry's Fork, (b) Teton River, (c) Snake River at Heise, (d) Boise River, (e) Payette River, (f) and the Snake River near Oxbow Dam Based on the CCSM3, A1B Climate Scenario	111
Figure 6.6	June and October Average, Decadal EOM for Palisades Reservoir and the Boise River Storage Triplex Based on the ECHO, CCSM3, and PCM1 for the A1B Emission Scenario	114
Figure 6.7	June and October EOM from 1929-2099 based on Historic and CCSM3, A1B Climate Scenario at (a) Palisades Reservoir and (b) the Boise River Storage Triplex	116
Figure 6.8	Mean Monthly Estimates of Discharge from the ESPA to the Snake River above King Hill by Decade	117
Figure 6.9	A Comparison of ESPA Discharge at the Snake River with PDSI 1991-2005	119
Figure B.1	Schematic of SRPM Provided by Dr. Sudhir Goyal of IDWR Showing the Eastern Snake River Basin	138
Figure B.2	Schematic of SRPM Provided by Dr. Sudhir Goyal of IDWR Showing the Western Snake River Basin	139
Figure B.3	Schematic of Natural Flow Structure in SD-SRPM above Lake Walcott, Excluding the Southern Tributaries	140
Figure B.4	Schematic of Natural Flow Structure in SD-SRPM of Southern Tributaries above Lake Walcott	141
Figure B.5	Schematic of the Natural Flow Structure in SD-SRPM below Lake Walcott	142
Figure B.6	Schematic of the Regulated Flow Structure for the Henry's Fork, Falls River, and Teton River	143

Figure B.7	Schematic of the Regulated Flow Structure for the South Fork of the Snake River, Willow Creek, Blackfoot River, and Mainstem of the Snake River above Blackfoot	144
Figure B.8	Schematic of the Regulated Flow Structure for the Blackfoot River and Mainstem of the Snake River below Blackfoot	145
Figure B.9	Schematic of the Regulated Flow Structure for the Boise River	146
Figure B.10	Schematic of the Regulated Flow Structure for the Payette River	147
Figure C.1	Reservoir EOM within the Henry's Fork Basin at (a) Henry's Lake, (b) Island Park, and (c) Flow in the Henry's Fork near Rexburg	149
Figure C.2	Reservoir EOM within the South Fork and Mainstem of the Snake River at (a) Jackson Lake, (b) Palisades Reservoir, (c) American Falls Reservoir, and (d) Lake Walcott	150
Figure C.3	Streamflow within the Snake River (a) near Irwin, (b) below Milner Dam, and (c) near Weiser	151
Figure C.4	Reservoir EOM within the Minor Tributaries at (a) Grassy Lake on Falls River, (b) Grays Lake on Willow Creek, (c) Ririe Reservoir on Willow Creek, and (d) Blackfoot on the Blackfoot River	152
Figure C.5	Reservoir EOM within the Boise River Basin at (a) Anderson Ranch Reservoir, (b) Arrowrock Reservoir, (c) Lucky Peak Reservoir, and (d) Streamflow near Parma	153
Figure C.6	Reservoir EOM within the Payette River Basin at (a) Lake Cascade and (b) Deadwood Reservoir with Streamflow near (c) Horseshoe Bend and (d) Payette	154
Figure D.1	Mean, Monthly, Historic, and Projected Flow of the Henry's Fork near Ashton for the (a) PCM1, (b) CCSM3, and (d) ECHO GCMs	157
Figure D.2	Mean, Monthly, Historic, and Projected Flow of Falls River near Squirrel for the (a) PCM1, (b) CCSM3, and ECHO GCMs	158
Figure D.3	Mean, Monthly, Historic, and Projected Flow of the Teton River near St. Anthony for the (a) PCM1, (b) CCSM3, and (c) ECHO GCMs	159

Figure D. 4	Mean, Monthly, Historic, and Projected Flow of the South Fork of the Snake River near Heise for the (a) PCM1, (b) CCSM3, and (c) ECHO GCMs	160
Figure D.5	Mean, Monthly, Historic, and Projected Flow of the Boise River near Parma for the (a) PCM1, (b) CCSM3, and (c) ECHO GCMs	161
Figure D.6	Mean, Monthly, Historic, and Projected Flow of the Payette River near Payette for the (a) PCM1, (b) CCSM3, and (c) ECHO GCMs	162
Figure D.7	Mean, Monthly, Historic, and Projected Flow of the Snake River near Oxbow Dam for the (a) PCM1, (b) CCSM3, and (c) ECHO GCMs	163

LIST OF ABBREVIATIONS

- CAMP – Comprehensive Aquifer Management Plan
- COOP – Cooperative Weather Station
- EOM – end-of-month reservoir content
- ESPA – East Snake Plain Aquifer
- ESPAM – East Snake Plain Aquifer Model
- ESRP – East Snake River Plain
- ET – Evapotranspiration
- GCM – global climate model
- IDWR – Idaho Department of Water Resources
- ISHS – Idaho State Historical Society
- kaf – thousand acre-feet (= 1233.5 m³)
- NCDC – National Climatic Data Center
- NOAA – National Oceanic and Atmospheric Administration
- NRCS – Natural Resources Conservation Service
- PDSI – Palmer Drought Severity Index
- SD-SRPM – System Dynamics-Snake River Planning Model
- SRBM – Snake River Basin Model
- SRPM – Snake River Planning Model
- SWSI – Surface Water Supply Index
- USACE – United States Army Corps of Engineers

USBR – United States Bureau of Reclamation (or Bureau of Reclamation)

USDA – United States Department of Agriculture

USGS – United States Geological Survey

USHCN – United States Historical Climatology Network

CHAPTER ONE: INTRODUCTION

Purpose

The purpose of this research was to develop and test a system dynamics based reservoir operations model of the Snake River basin to be used for the analysis of climate change impacts on surface water diversions within the Snake River basin. The model has been dynamically linked to the East Snake Plain Aquifer (ESPA) through the use of response functions generated from a groundwater model of the aquifer. Historically, the model was found to be able to adequately represent end-of-month (EOM) reservoir content and streamflow at critical locations within the basin using two different means of estimating current diversion practices. The model was also tested using projected flows based on three climate change scenarios. The following thesis introduces the physical setting of the research, the institutions developed to manage surface water diversions, and climatic trends within the basin. The introductory material is followed by a description of the model, the validation of the model, and findings of how climate change may impact surface water diversions based on three climate change scenarios. The last chapter discusses the conclusions of the research, as well as, identifies areas for further research.

Problem Statement

Idaho, with 3.3 million acres of irrigated land, is ranked fifth in the nation for the state with the most irrigated crop land in 2007 (USDA, 2007). Most of this irrigation

occurs in the Snake River Plain, which covers most of southern Idaho and stretches into eastern Oregon (see Figure 1.1). Most of the infrastructure built to support surface water diversions in this region was built under the principle of stationarity, which assumes that climate will vary within the envelope of the historic variability of the instrumental record (Lettenmaier, 2008). Gaged streamflow and climate records in Idaho extend back about 100 years. The assumption of stationarity has always been a topic of debate in the hydrologic community, but recent research in the fields of paleoclimate and climate change have led researchers to declare the *death* of stationarity, and to seek a new paradigm for water resource management (Milly et al., 2008; Rogers, 2008; Lettenmaier, 2008). Paleoclimate research indicates that climate in the western United States has varied dramatically over the past two millennium with droughts much more severe than indicated by the instrumental record (Cook et al., 2007, Meko et al., 2007). Climate change studies indicate that greenhouse gases added by humans to the atmosphere are causing, and will continue to cause, a significant increase in global temperature (Barnett et al., 2008; Bates et al., 2008), regardless of whether or not we are able to reduce or eliminate the emission of greenhouse gases (Solomon et al., 2009).

At the time irrigated agriculture was being established in the western United States, initial climate change research, which was focused on explaining the Ice Ages, was just beginning to speculate that emissions of carbon dioxide and other greenhouse gases could alter the Earth's atmosphere and thus climate (Weart, 2008). Although crude scientific models based on physics have long indicated that greenhouse emissions could alter the climate (Arrhenius, 1896; Callendar, 1938), it was not until the development of computationally intense global climate models (GCMs), which include atmospheric

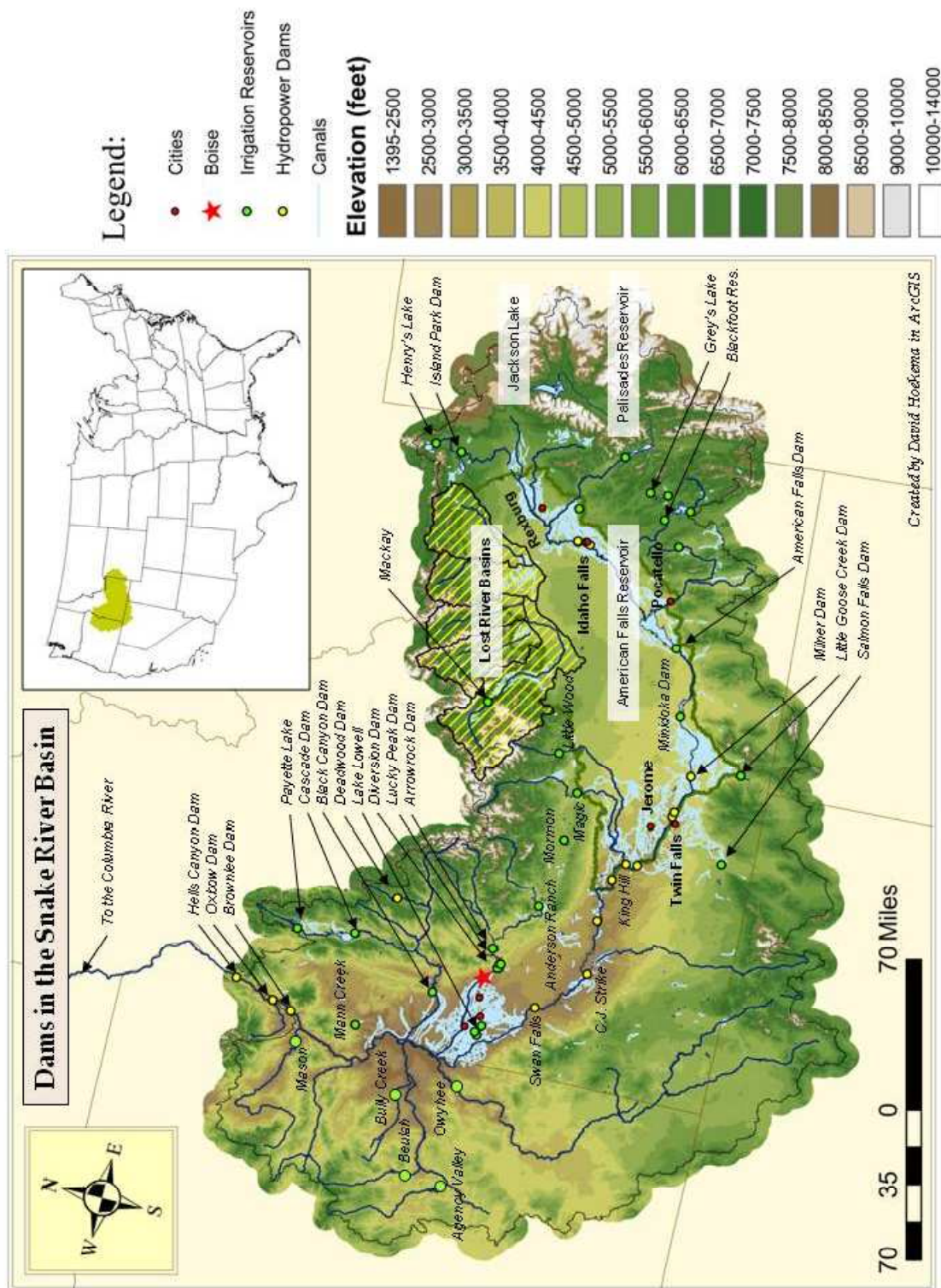


Figure 1.1 Study Area Map of the Snake River Basin Upstream of Hells Canyon Dam Showing Hydropower Dams and Irrigation Reservoirs

and oceanic circulation patterns, that scientists were able to prove with some degree of certainty that human activities can, and are, warming the Earth's atmosphere through greenhouse gas emissions (Weart, 2008; Bates et al., 2008). The proof is based on historic climate simulations using GCMs, developed by multiple institutions around the world. These GCMs can only replicate the historic increase in global temperatures under greenhouse emission forcings (Weart, 2008). These models are nearly unanimous in predicting a global increase in temperature of 0.2°C/decade through 2030, twice the rate of the 19th century warming trend regardless of which emission scenario is used to drive the model (Bates et al., 2008). While it is difficult to precisely estimate how past and future greenhouse gas emissions will affect the hydrologic processes, the International Panel on Climate Change considers it likely (>90% probability) that there will be significant shifts in the hydrologic process that will make planning water resource management based on historic hydrologic patterns less reliable (Bates et al., 2008).

Although research on climate change impacts to the Columbia River basin have addressed issues of surface water irrigation reliability in the Snake River basin (Hamlet and Lettenmaier, 1999; Payne et al., 2004), no model has been developed at a basin scale to support water resource planning and management decisions in the Snake River basin based on projected flows. The research presented here describes the development of an operational water resource planning model that simulates operation of the system using both historic and projected flows. While the model was developed to provide a full assessment of climate impacts within the Snake River basin, the research presented here compares end-of-month reservoir storage in June and October, as well as annual

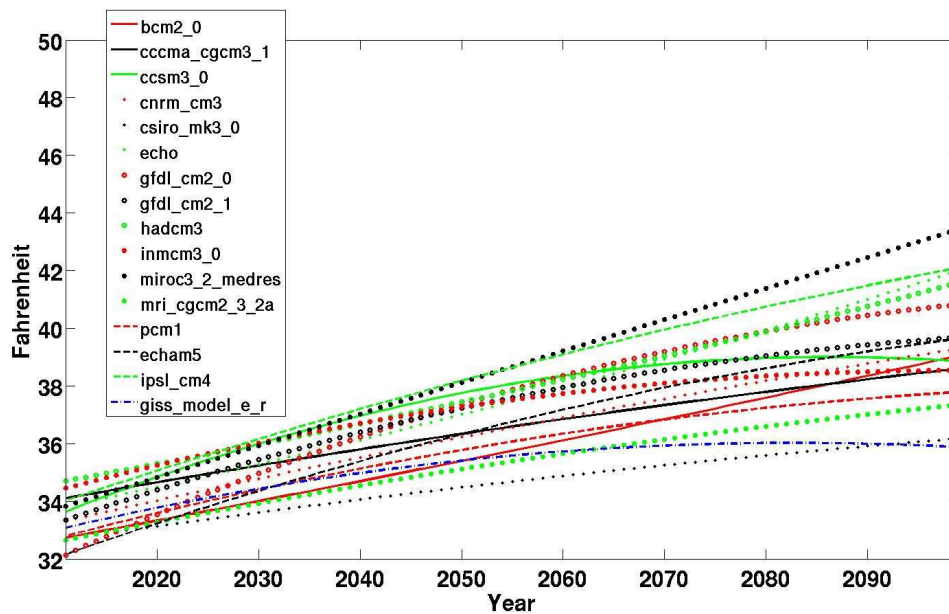


Figure 1.2 Change in Mean Annual Temperature from 2011-2099 based on the 1949-1999 Mean (Jin and Sridhar, in review)

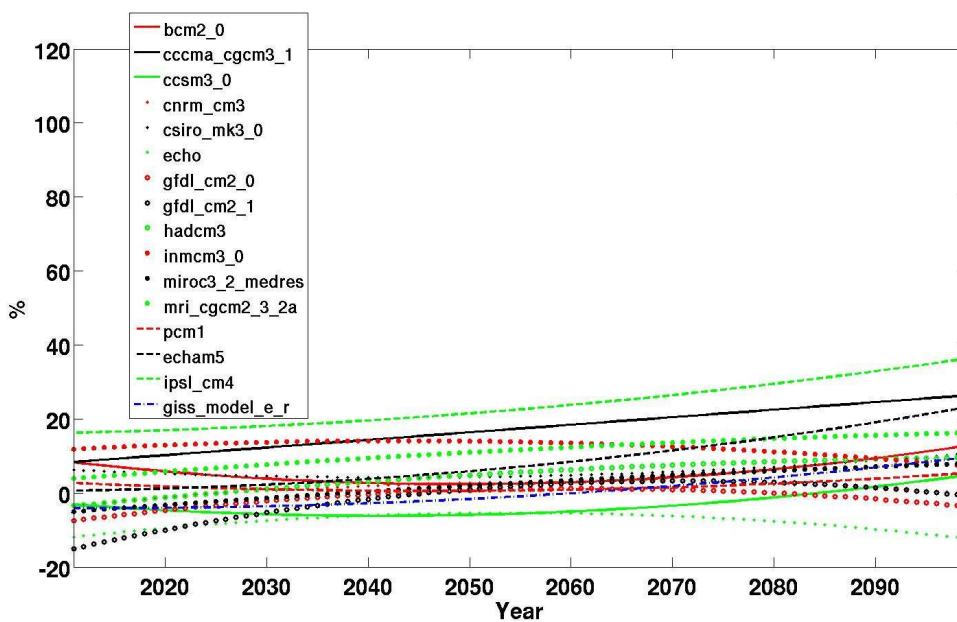


Figure 1.3 Percent Change in Mean Annual Precipitation from 2011-2099 based on the 1949-1999 Mean (Jin and Sridhar, in review)

irrigation shortages over the historic and projected periods. The projected periods are based on three climate scenarios as projected by three GCMs under a mid-range emissions scenario. The first projected scenario is referred to as a cool scenario, the second scenario is referred to as a mild scenario, and the final scenario is referred to as the warm-dry scenario. The cool scenario represents a mild increase in temperature, 5.5°F by 2099, and little change in precipitation. The mild scenario represents a temperature increase of 7°F by 2099 and historic levels of precipitation. The last warm-dry scenario shows a decrease of precipitation by about 10% and a temperature increase of about 10°F by 2099. The three scenarios are used to test the hypothesis that the historic record is not likely to capture the range of variability indicated by projected climate change.

Recent research by Jin and Sridhar (in review) using downscaled data from 16 GCMs predicts an increase in average temperature, based on the 1949-1999 average annual temperature, of around 5.5 to 11°F by 2099 (see Figure 1.2) in the Snake River basin under the A1B emission scenario (Nakićenović et al., 2000). There is less certainty among the models on the direction of precipitation change, which ranges from -15 to 40% increase of the 1949-1999 average precipitation (see Figure 1.3). The abbreviations for the GCMs used in Figure 1.2 and Figure 1.3 are described in Table 1.1. Research by the United States Bureau of Reclamation (USBR) in the Boise River basin indicates that precipitation changes could have a big impact on water resource management in southern Idaho (Stillwater, 2008). While a drier, hotter future projected by one model might portend greater risk of drought and a slightly warmer and significantly wetter future predicted by another model may imply an abundance of water, neither inference may be accurate, because water resource management and infrastructure have been built based on

the historic hydrograph. The question of whether we will be water rich or poor in the future may lie not so much in the amount of water we receive, but in our ability to manage that water.

Table 1.1 Global Climate Model Descriptions (also see, http://gdo-dep.ucllnl.org/downscaled_cmip3_projections/)

GCM	Description
BCCR-BCM2.0	Bergen Climate Model 2.0, Bjerknes Centre for Climate Research (BCCR), Univ. of Bergen, Norway
CGCM3.1 (T47)	Coupled Global Climate Model 3.1, Canadian Centre for Climate Modelling & Analysis, Canada
CNRM-CM3	Centre National de Recherches Meteorologiques Coupled Global Climate Model, France
CSIRO-Mk3.0	CSIRO Mk3 Climate System Model, CSIRO Atmospheric Research, Australia
GFDL-CM2.0	US Dept. of Commerce / NOAA / Geophysical Fluid Dynamics Laboratory Coupled Model 2.0, USA
GFDL-CM2.1	US Dept. of Commerce / NOAA / Geophysical Fluid Dynamics Laboratory Coupled Model 2.1, USA
GISS-ER	Goddard Institute for Space Studies Global Atmosphere-Ocean Model, NASA, USA
INM-CM3.0	Institute for Numerical Mathematics, Russia
IPSL-CM4	Institut Pierre Simon Laplace Climate System Model, France
MIROC3.2 (medres)	K1 Coupled GCM, Japan
ECHO-G	The Hamburg Atmosphere-Ocean Coupled Circulation Model, Germany
ECHAM5/ MPI-OM	Atmosphere and Ocean Model, Max Planck Institute for Meteorology , Germany
MRI-CGCM2.3.2	The Global Coupled Atmosphere-Ocean GCM, Meteorological Research Institute, Japan
CCSM3	The Community Climate System Model Version 3, National Center for Atmospheric Research, USA
PCM	Parallel Climate Model, National Center for Atmospheric Research, USA
UKMO-HadCM3	Hadley Centre coupled model, Hadley Centre for Climate Prediction and Research / Met Office, UK

Two examples of current water resource planning projects that could benefit from the analysis of projected flows are the United States Army Corp of Engineer's (USACE) study on increasing storage capacity in the Boise River for flood control and aquifer management plans (USACE, 2010) and the East Snake Plain Aquifer (ESPA)

comprehensive aquifer management plan (CAMP). Currently Boise, Idaho's capital city and largest population center, is inadequately prepared to handle flood-risk under historic climate conditions (USACE, 2010); the risk may worsen under climate change (Stillwater, 2008). The Idaho Legislature (House Bill 428 and 644) has mandated that the Idaho Department of Water Resources (IDWR) account for climatic change in the development of CAMPs used for conjunctive management of surface and groundwater within the state. The current ESPA CAMP relies on the historic record to determine if recharge of the aquifer can reverse the decline in discharge from springs in the Snake River Canyon below Milner Dam (Scott, 2010).

The rest of the *Chapter 1* provides background information on climate variability in Idaho and the western United States, on the model used by the IDWR to plan water resource management in Idaho, and on the use of a system dynamics model to simulate diversions in the Snake River basin under projected climate conditions.

Historical Development of Irrigated Agriculture in Idaho

The rapid development of farming communities in the Western United States began with the Homestead Act of 1862 that granted up to 160 acres of land to settlers who *improved* the land. Initially agriculture in southern Idaho, like much of the semi-arid West, was severely limited by the need for irrigation and the ability to obtain a consistent source of water (Slaughter, 2004). The United States Congress passed the Desert Land Act of 1877 to encourage individuals to settle in the semi-arid West. Settlers could obtain 640 acres if they could successfully irrigate the land. However, an individual's ability to finance irrigation projects was usually limited to land within the river valleys and by 1889 only 217,000 acres had been brought under irrigation in the Boise and Snake

River valleys (Slaughter, 2004). In order to irrigate the fertile land above the river valleys, there was a need for greater investment and in 1894 the Carey Act was passed with the hope that the act would provide a mechanism to fund large scale irrigation projects on federal land, with private financing, and state oversight (ISHS, 2004). However, few of these projects succeeded. The successful construction and operation of Milner Dam is one of the rare exceptions (Lovin, 2002; Slaughter, 2004; ISHS, 2004). Many of the projects, like the construction of the New York Canal just upstream of Boise, Idaho on the Boise River, failed due to inadequate finances and speculation (ISHS, 1972). The Reclamation Act of 1902, which led to the creation of the United States Bureau of Reclamation (USBR), opened the door for large scale federally funded water resource projects. Today in Idaho, most of the large dams used to store irrigation water are owned, maintained, and operated through federal oversight by the Bureau of Reclamation (USBR), while the distribution of water, which is owned by the State, is regulated by the IDWR. With the help of these federally funded projects, irrigated agriculture expanded from 217,000 acres in 1889 to 3.3 million acres by 2007 (Slaughter, 2004; USDA, 2007). The three largest federal irrigation projects in Idaho are the Minidoka Project initiated in 1904 (Stene, 1997), the Boise Project initiated in 1905 (Simonds, 1997), and the Palisades Project, which received final authorization in 1950 (Simonds, 1996). These projects were developed to increase irrigation storage, produce electricity, and provide storage space for flood control. Table 1.2 summarizes the major infrastructure and storage capacity based on data from the USBR website (see, [www.usbr.gov/pn /project/index.html](http://www.usbr.gov/pn/project/index.html)).

Table 1.2 Federally Operated Irrigation Projects in Idaho

	Dams	Storage Capacity (kaf)	Hyrdopower (megawatts)	Acres (thousands)
Minidoka Project (1904)	Minidoka	95.2	28	1,100
	Jackson Lake	847		
	American Falls	1,672	*112.4	
	Island Park	135.2		
	Grassy Lake	15.2		
Boise Project (1905)	Anderson	423.2	40	397
	Ranch	286.6	18	
	Arrowrock	4		
	Hubbard	159.4		
	Dearflat	161.9		
	Deadwood	646.5	*14	
	Cascade			
Palisades Project (1950)	Palisades	1,200	176.6	765 supplemental

* hydropower facilities owned by Idaho Power which has 17 hydroelectric facilities along the Snake River and its tributaries (Idaho Power, 2011, www.idahopower.com/AboutUs/OurPowerPlants/Hydroelectric/hydroelectric.cfm)

Climate Variability and Water Conflict

While agricultural expansion was the motivating factor for constructing large irrigation projects across the Western United States, many of the projects and institutions developed to allocate water were motivated at least in part by stress on water supply due to population growth and climatic variability (Slaughter, 2004). The construction of the Minidoka Project with the Jackson Lake Dam and the Boise Project with Arrowrock Dam followed the severe drought of 1901 and 1902 in which portions of the Snake River near Blackfoot, ID went dry for the first time (Fiege, 1999). The construction of the Boise and Minidoka projects during a period of unusually wet conditions known as the 20th century pluvial (Woodhouse et al., 2005) allowed a rapid development of surface water irrigation.

The severe drought in 1919, following this wet period, led to the formation of the Committee of Nine in 1923. This committee was tasked with differentiating between natural flow and stored water (Slaughter, 2004). The last major surface water irrigation project, which developed the second largest reservoir in the system, the Palisades Project, was authorized in response to the failure of the earlier projects to provide adequate supply during the 1930s drought (Simmonds, 1996). Most recently, the decision to manage surface water and groundwater rights conjunctively was caused by the decline in the water table and discharge from the ESPA (Slaughter, 2004), which was due in part to two recent multi-year droughts. Severe drought in the early 1990s corresponded to a dramatic decline in spring discharge, which recovered partially during a wet period in the late 1990s and then collapsed even further during the extremely dry decade of the 2000s (Kjelstrom, 1995; Blew and Bowling, 2009).

Early promoters of irrigation in the Western United States promoted irrigated agriculture as a means to free farmers from their dependence on the rain (Fiege, 1999). These early promoters, and the settlers they inspired to move west, did not realize that while irrigation would free them from relying on summer rains the dependability of their water source would instead rely on their ability to capture and manage runoff from a highly variable snowpack. Figure 1.4 displays the variability of *unregulated*¹ gaged flow by decade on the Boise River near Twin Springs (Clark, 2010) and *naturalized*² flow at Heise on the Snake River. Both of the gages are located upstream of the major surface

¹ The flow in the Boise River near Twin Springs, ID represents gaged flow (USGS gage #13185000) above Arrowrock Dam. The flow is called unregulated because there is little direct human influence upstream of the gage.

² The flow in the Snake River near Heise, ID (USGS gage #130375000) is impacted by two major reservoirs: Palisades and Jackson Lake. The *naturalized* flow at this point represents the quantity of flow that IDWR calculates would have been in the river if the upstream reservoirs allowed all natural flow to pass downstream.

water diversions and respectively represent the annual variability of supply in the western and eastern portions of the Snake River basin. The general trend of increased range of decadal flow in Figure 1.4, at least until the recent multi-year drought of the 2000s, may indicate an intensification of the hydrologic cycle during the instrumental record. Figure 1.5 shows the Palmer Drought Severity Index (PDSI) from 1700 to 2003 over the Snake River basin (Cook et al., 1999). Figure 1.5 is based on a gridded dataset, such that the grid points plotted represent grid point 71 (representing the western plain) located at 115W 40N and grid point 87 (representing the eastern plain) located at 112W 37.5N. While both the decadal variability of streamflow (Figure 1.4) and the PDSI index (Figure 1.5) indicate severe drought during the Dust Bowl decade of the 1930s, Figure 1.5 highlights the two recent multi-year droughts from 1987-1992 and the latest drought, which started in 2000 and according to the Natural Resource Conservation Services' (NRCS) Surface Water Supply Index (SWSI) continued until 2006 in the eastern basin (NRCS, www.id.nrcs.usda.gov/snow/watersupply/swsi-main.html#uppersnake). The PDSI record based on paleoclimate records (i.e., climate records based not on instrumentation, but on natural proxies) using tree ring data indicates that drought was much more frequent during the 1700s and 1800s in comparison with the 1900s (Cook et al., 1999). For example, for a fourteen-year period, 1870 to 1883, thirteen out of fourteen years had less than normal moisture conditions with six of those years being categorized as moderate or severe drought (PDSI < -2). Such extended periods of dryness indicate that the instrumented record (even after 100 years) may not provide an adequate view of climatic variability. Overall, both the 1700s and 1800s experienced more dry years than indicated by the instrumented record of the 1900s. Paleoclimate records based on longer

proxies, though lacking high temporal resolution and accuracy, indicate even greater fluctuations in wet and dry cycles (Cook et al., 1999; Woodhouse et al., 2005).

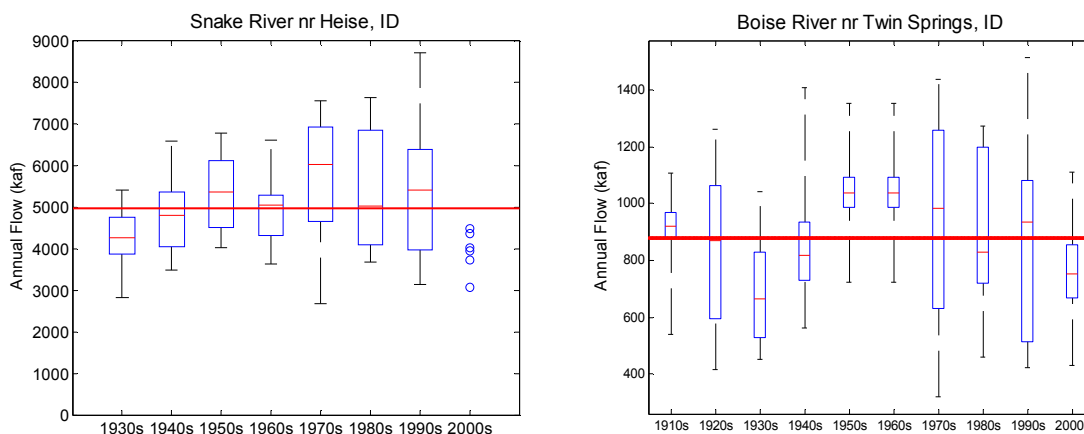


Figure 1.4 Boxplot of Naturalized Flow at Heise, ID (1930-2005) and Unregulated Flow on the Boise River near Twin Springs, ID (1911-2009)

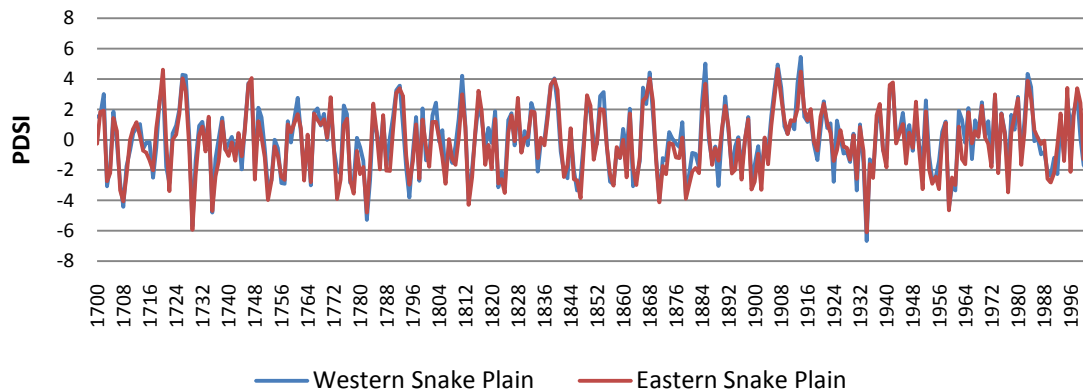


Figure 1.5 Three Hundred Year Reconstruction (1700-2003) of Summer PDSI Based on a Gridded Tree-ring Dataset (Cook et al., 1999)

System Dynamics Modeling

Today when water managers are faced with the challenge of addressing climate change, some may prefer to wait for a consensus from researchers on how climate change will impact the hydrograph. However, even a cursory review of climate change research

indicates that the science of climate change is fraught with uncertainty. It is difficult to know which emission scenario and GCM is most likely to represent the future. There is also debate about the best method for downscaling climate data from GCMs to drive hydrologic models. Waiting for consensus on future climate predictions is likely to continue the historic process of waiting to change management until a crisis strikes. As Slaughter (2004) points out, Idahoans have been able to adapt fairly well in the past. Part of this adaptability may have been due to a common public interest to expand water usage for agriculture and hydropower. However, as the public demand for water use increases and diversifies, the ability to handle crises and adapt institutions may become more difficult. A recent groundwater model produced by IDWR and the University of Idaho which was produced with heavy stakeholder involvement, has come under attack because inevitably a model designed to resolve a dispute based on historic conditions will have some *losers* and some *winners* (Cosgrove et al., 2008). The managers who wait to handle crisis until technical methods improve may face increasing difficulty in finding a resolution.

The question then lies in how to plan for a highly uncertain future. A possible solution to this problem that is explored in this thesis is the use of a system dynamics model to plan management decisions. The basic thought behind system dynamics modeling is that when there is a large degree of uncertainty regarding the inputs into a system, then it is unwise to focus on predicting the inputs precisely. Rather, the focus should be on developing a robust system that will perform well given widely varying inputs (Radzicki and Taylor, 1997). A wide array of inputs is common in climate modeling where ensemble predictions are increasingly popular. This type of modeling

principle seems ideally suited to modeling water resources in the highly uncertain environment of climate change. The downscaled GCM data provides a wide range of inputs while the modeling focuses on correctly analyzing how the stocks, flows, and feedbacks within the system interact. The goal of the research in this thesis was to develop a system dynamics model of water management in the Snake River basin that contains critical physical and user-related feedback loops. As such, this thesis focuses on developing a framework for analyzing climate impacts on agricultural surface water diversions and does not seek to provide a full analysis of climate change scenarios. To accomplish this goal, I chose to model future climate impacts using three GCMs and the A1B emission scenario. (For details on the establishment of projected emission scenarios used to drive GCMs, see Nakićenović et al., 2000.) The GCMs used are the ECHO model (Legutke and Voss, 1999) developed at the Max-Planck-Institute for Meteorology, the Community Climate System Model (CCSM3) model developed by the National Center for Atmospheric Research (NCAR, <http://www.cesm.ucar.edu/index.html>) in the United States, and the Parallel Climate Model (PCM1) developed jointly by the Los Alamos National Laboratory, the Naval Postgraduate School, the U.S. Army Corps of Engineers' Cold Regions Research and Engineering Lab, and NCAR (<http://www.cgd.ucar.edu/pcm/>).

The basic interaction of surface water diversions, reservoir content, and minimum flows is based on IDWR's Snake River Planning Model (SRPM). In addition to modeling reservoir content, natural flow, irrigation calls, and diversions, the model includes the impacts of evapotranspiration (ET), precipitation, and diversions on aquifer recharge and thus groundwater/surface water interactions with the ESPA. While the

focus of this model is on surface water diversions, the basic platform could be modified in the future to include the analysis of hydropower, flow augmentation, and irrigation impacts from both surface and groundwater sources on water resource management. To my knowledge, this is the first time a water management model has been developed for the Snake River basin that seeks to dynamically represent projected flows in the basin with a level of detail consistent to the current historic flow models used for water planning and management in the State of Idaho.

CHAPTER TWO: PHYSICAL DESCRIPTION OF THE SNAKE RIVER BASIN

Climate, Geology, and Irrigation within the Snake River Basin

The Snake River Plain is a broad plain formed by the passage of the North American tectonic plate over the Yellowstone hotspot (Mabey, 1982; Smith, 2004). Most of the surface of the central portion of the eastern Snake River Plain is covered by deep layers of volcanic rock (Kjelstrom, 1995). These layers were formed by multiple small lava flows. The boundary layers, or rubble zones, between the lava flows are highly permeable and frequently interconnected (Welhan and Reed, 1997). An axial ridge that runs east-west through the center of the plain prevents rivers flowing from the mountains north of the eastern Snake River Plain from reaching the Snake River (Smith, 2004), which flows westward along the southern edge of the plain. These rivers flowing out of the northern mountains are often referred to as the *lost* rivers, because they disappear into the highly permeable lava fields. The location of the lost river basins are shown in Figure 2.1. There are pockets of agriculture on the northern side of plain where fluvial deposits from mountain streams have accumulated over the volcanic rock. Agriculture in these regions is supported by diversions from the lost rivers, and groundwater pumped from the aquifer.

The bulk of Idaho's surface water irrigated agriculture is located in five regions along the southern fringe of the plain adjacent to the Snake River, as shown in Figure 2.1 with rivers in blue and canals in light blue. The first agricultural region, in the far eastern portion of the plain, is supplied by irrigation water from Henrys Fork, Falls River, and

Teton River. The second agricultural region is located mainly on the southside of a large bend in the Snake River between Heise and Idaho Falls. Surface water irrigation for this region is mainly diverted from Willow Creek and the Heise to Lorenzo reach of the Snake River. The third agricultural region, to the east and north of American Falls Reservoir, is supplied by diversions from the Lorenzo to Blackfoot reach of the Snake River and the Blackfoot River. The fourth region is located mainly between Rupert and King Hill. Irrigation for the fourth region is diverted from the Blackfoot to Milner reach of the Snake River. Discharge from the East Snake Plain Aquifer through natural springs located beneath American Falls Reservoir provides an additional 2500 cfs (ft³/s) to this reach of the river (Kjelstrom, 1995). The fifth and western most agricultural region diverts its surface water supply mainly from the Boise and Payette rivers.

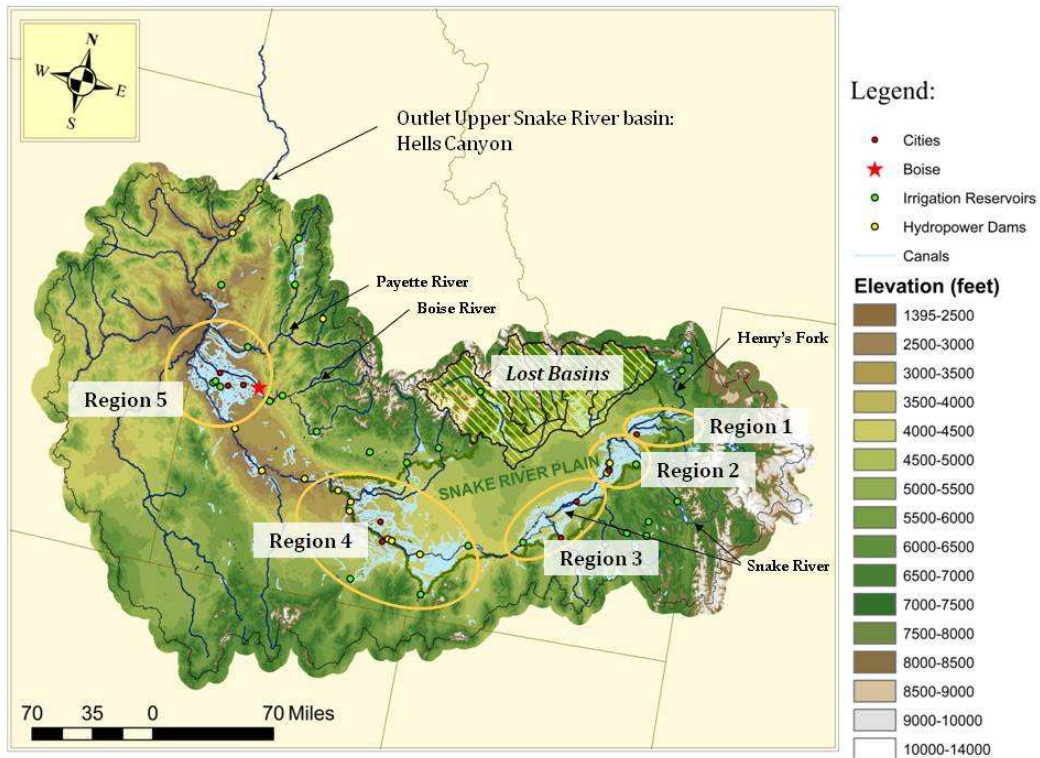


Figure 2.1 Map Showing Five Major Surface Water Irrigation Regions in Southern Idaho

Elevations in the plain vary from about 2,000 ft in the west to around 6,000 ft in the east. The climate is semi-arid with most portions of the plain receiving between 6 and 12 inches of rain annually. Precipitation in the plain follows a general east-west gradient with the east receiving more moisture. Natural vegetation is composed mostly of bunchgrass and sagebrush, with willows and cottonwoods growing along stream channels. The local atmospheric interactions caused by dense agricultural clusters in the midst of a vast semi-arid plain are not well understood. Alfaro et al. (2005) suggests that a spring soil moisture feedback exists in the Snake River Plain, in which low spring soil moisture translates to hotter, drier summer conditions with increased groundwater pumping. Since irrigated agriculture maintains relatively consistent soil moisture during the irrigation season, the feedback must be based on the advection of dry air from the non-irrigated regions over the irrigated fields, resulting in an increased vapor pressure deficit along the atmosphere/plant/soil interface, resulting in increased transpiration.

Without irrigation, agriculture would be very limited as precipitation during the growing season is inadequate to support the crop water requirements. Most of the precipitation comes during the winter months in the western portion of the plain, while precipitation peaks during the spring in the eastern plain.

For both geologic and water management purposes, the Snake River Plain can be divided into eastern and western regions. The division occurs geologically near King Hill and for water management purposes at Milner Dam on the Snake River roughly 90 miles upstream of King Hill. Nearly 40% of natural flow within the Snake River basin originates in the western basin, 40% originates in the eastern basin, and the remaining 20% enters the Snake River from the East Snake Plain Aquifer (ESPA) between Milner

Dam and King Hill (as calculated from the reach gain file provided by IDWR with SRPM). The source of natural flow within the Snake River basin is primarily from the accumulation and melt of snow-pack in the mountains surrounding the basin where precipitation increases significantly with elevation (Kjelstrom, 1995).

For water resource management purposes, the Snake River is divided into east and west at Milner Dam. At the time Milner Dam was constructed, the promoters of the project acquired water rights for almost all the unallocated flow upstream of Milner (Slaughter, 2004). Under current management, nearly all of the flow of the Snake River is diverted at Milner Dam during the growing season for irrigation. Although the river is nearly dry below Milner Dam, the flow in the Snake River in the Milner Dam to King Hill reach of the Snake River increases substantially due to springs discharging water from the ESPA. The western portion of the Snake River Plain extends from King Hill to the beginning of Hells Canyon. Flows within this stretch of the Snake River are mostly used for non-consumptive purposes, including hydropower production and aquaculture. The Snake River Canyon below Milner dam supports several trout farms that produce 75 percent of the United States commercial rainbow trout (DEQ, 2005). Idaho Power operates 8 power plants within or downstream of the Thousand Springs reach (Idaho Power, 2011). Almost all surface water irrigation below Milner Dam is diverted from the Boise and Payette rivers, the two largest tributaries of the Snake River. Surface water/groundwater interactions within this portion of the basin are less profound than in the eastern plain. The agricultural portions of western plain are mostly underlain by Quaternary and Tertiary sedimentary rocks with much lower hydraulic conductivity than the lava flows in the eastern plain (Kjelstrom, 1995).

Surface Water Diversion Infrastructure and Institutions in the Snake River Basin

The following section describes a brief history of the some of water resource infrastructure and institutions that govern water distribution in the Snake River basin. These structures and institutions are key factors in modeling water resource distribution in the Snake River basin. For a more detailed history of water rights distribution in Idaho, the reader is invited to read *Irrigated Eden: the Making of an Agricultural Landscape in the American West* (Fiege, 1999), which provides a detailed history of irrigation in the Snake River Plain.

Out of Priority Delivery in the Eastern Snake River Basin

One key factor in modeling surface water diversions in Idaho is that water is not delivered entirely by the priority of water rights. The fundamental law, established by the Idaho State Constitution governing water distribution in Idaho, is based on the Priority Doctrine, often referred to as “first in time first in right” (Slaughter, 2004). However, the enforcement of priority has often proven difficult to enforce and has led to costly litigation. To counter the time-consuming process of enforcing priority during water crisis, numerous extra-legal institutions have been developed to allow users with senior water rights to loan or rent water to junior water rights holders in times of shortage (Fiege, 1999). The Committee of Nine was established in 1923 to guarantee that water released from storage in reservoirs on the South Fork of the Snake River in Jackson Lake (and later Palisades) makes it past the natural-flow diverters in the Idaho Falls region to the downstream owners of storage rights. The committee is also responsible for negotiating transfers of water from senior users to junior users during dry years (Fiege,

1999). The passage of the Rexburg decree allowed senior users to loan water to downstream users without losing their right to the water (Fiege, 1999). This arrangement was crucial to supply irrigation water to irrigators in the Blackfoot region. The Blackfoot diversions are located below a losing reach of the Snake River. During the drought of 1901-02, water users upstream of Idaho Falls had dried up the Snake River, even diverting water into unplanted desert land rather than risk losing the priority of their water right to downstream water users with junior rights (Fiege, 1999). The Rental Pool established on the Snake River in 1979 also provided for water delivery out of priority (Slaughter, 2004).

These out-of-priority water deliveries lead to some contention on how demand and shortages should be modeled. *Chapter Three* addresses the issue of calculating demand and shortages more fully in the absence of strict priority deliveries.

Out of Priority Delivery in the Western Snake River Basin

In 1905, recognizing that administering water rights by priority in the Boise Valley would not be equitable, a decree was issued by the courts in 1906 that when priority could not be met because of declining flows all diversions should be cut to 75% of their deliverable right. If priority could not be met with a 75% cut in deliveries, all canals would then be forced to cut deliveries to 60% of their recognized right. Only when priority could not be met with a 60% cut in deliveries could priority be enforced (Murphy, 1935). As in the eastern Snake River basin, rental pools were later established to further facilitate out-of-priority deliveries on the Boise basin in 1988 and in the Payette basin in 1990 (Slaughter, 2004).

Interbasin Transfers

Another key factor in modeling water resource diversions in the Snake River basin is to include interbasin transfers between subbasins. The Teton River irrigators below St. Anthony can call water from the Island Park Reservoir, located on the Henry's Fork of the Snake River. The water is transferred through the Crosscut Canal. The Eagle Rock Canal located below Heise delivers water to provide supplemental water for surface water diversions from Willow Creek. Clark's Out Canal transfers water from Grays Lake in the upper reaches of the Willow Creek basin to the Blackfoot Reservoir on the Blackfoot River. The Blackfoot River also receives supplemental irrigation from the Snake River via the Reservation Canal.

Groundwater/Surface Water Interactions in the Boise and Payette River Basins

The relatively low permeability of the Quaternary and Tertiary sedimentary rocks in the Boise and Payette River basins has resulted in a significant rise of the groundwater table along the Boise and Payette rivers. Busbee et al. (2009) record that the water table in land irrigated by the New York Canal, which diverts from the Boise River, has risen by over 100 feet. This increase in groundwater levels caused the lower reaches of the Boise and Payette rivers to become gaining reaches. Drainage districts were developed to prevent farmland along the Boise and Payette rivers from becoming water logged due to the elevated water tables (Fiege, 1999). Prior to surface water irrigation, both the Boise and Payette river basins are thought to have had losing reaches upon entering the Snake River Plain (Shurtleff, 2010; Schmidt et al., 2009). The raising of the water table and return flows from surface water irrigation have caused many historically intermittent streams to become perennial. The switch from losing to gaining reaches at the bottom of

these river basins has resulted in a phenomenon in which upstream users face water shortages during drought while downstream users have an abundance of water. The result is that downstream users can rely on natural flow to supply diversions while upstream users rely on both natural flow and storage rights.

Goundwater/Surface Water Interactions in the Eastern Snake River Basin

While surface water deliveries have significantly raised the water table and transformed the hydrogeology of the western basins, a similar transformation took place with groundwater/surface water interactions between the Snake River and the ESPA on the eastern side of the Snake River basin. Prior to the 1950s, the continuously expanding network of surface water diversion canals caused recharge and consequently discharge from the highly permeable ESPA to increase significantly. The most notable increases were seen in spring discharge in the Snake River Canyon between Milner Dam and King Hill. Spring discharge at the Thousand Springs reach, near Hagerman, ID, reached a peak discharge of about 6800 cfs in the 1950s. A major expansion of groundwater pumping beginning in the 1950s, along with improved irrigation conservation by surface water users (Johnson et al., 1999a), and severe droughts in the 1990s and 2000s have reduced flows to the current rate of 5000 cfs (Blew and Bowling³, 2009), just slightly higher than the 1915 flow of 4800 cfs (Kjelstrom, 1995). Since water rights developed at the springs during the period of increasing discharge are senior to those of the groundwater users, several attempts by the spring users have been made to curtail the

³ David Blew and Jon Bowling of Idaho Power reviewed USGS's calculation of spring discharge and found an error in spring discharge calculations by the USGS starting in 1998. They cite a personal communication from Tom Brennan of the USGS in which he acknowledges the error and corrects the flows. USGS original discharge calculation was 5480 cfs for 2008.

rights of groundwater pumpers. There is currently no resolution to this conflict, although the Idaho Water Resources Board and IDWR hope to resolve the issue through the conjunctive management strategy known as the Comprehensive Aquifer Management Plan (CAMP). Details on the CAMP project and implications of the different CAMP scenarios have been modeled in a system dynamics framework using historic flows (Scott, 2010). While I make no attempt in this thesis to address CAMP scenarios, groundwater/surface water interactions are included in the model presented herein as this issue will no doubt be an important factor in future management of water resources in the Snake River basin.

CHAPTER THREE: RECENT HISTORIC TRENDS IN SURFACE WATER DIVERSIONS AND CLIMATE IN THE SNAKE RIVER BASIN

This chapter seeks to identify how climatic attributes such as temperature, precipitation, streamflow, evapotranspiration (ET), and soil moisture have impacted surface water diversions over the last 35 years (1975-2005). The chapter starts by reviewing Clark's (2010) analysis on unregulated streamflow in the study area and then presents an analysis of temperature, precipitation, and diversion trends using the Mann-Kendall non-parametric trend test (Mann, 1945; Kendall, 1975). Diversions were also correlated to the Surface Water Supply Index (SWSI, www.id.nrcs.usda.gov/snow/watersupply/swsi-main.html), Palmer's Drought Severity Index (PDSI), and Palmer's z-index (Palmer, 1965). The research presented in this chapter helped in the creation of a demand file for use in the water resource model in which shortages are determined based on minimum full-supply demand. The chapter also provides some analysis and conclusions on how historic climate change (due both to natural variability and greenhouse gas emissions) has impacted water resources in the Snake River Plain. To my knowledge, this research is the first exploration of climate change impacts on surface water diversions in the Snake River basin.

This chapter contains five sections. The first section reviews the way demand is currently represented in the Snake River Planning Model (SRPM) developed by the Idaho Department of Water Resources (IDWR, Idaho Water Resources Board, 1972), and the reasoning behind creating a new diversion file for use in modeling projected flows. The

second section describes the methods and materials used in the analysis. The third, fourth, and fifth sections present the results, a discussion of the research findings, and some conclusions.

Current Representation of Diversions in Water Resource Planning and Management

Idaho irrigation rights are administered according to Priority Doctrine, in which those with the oldest water rights are given first priority to water during times of shortage (Slaughter, 2004). There are two types of water rights that impact surface water irrigation in Idaho: natural flow and storage rights. Natural flow refers to the water that would be in the river if no water was stored in the reservoirs. Natural flow rights are measured either by flow rate or by both flow rate and volume. Storage rights are measured by volume, and represent water stored in reservoirs. The volume of storage and rate of diversions are described in thousand acre-feet (kaf, kaf = 43,560 ft³) throughout this chapter to be consistent with current management practices.

Idaho farmers generally determine the amount of land and type of crops planted each season based on carry-over storage and the streamflow forecast, made available before the growing season (Pierce et al., 2010). Streamflow forecasts indicate the amount of natural flow that will be available and whether reservoirs will be able to fill. Carry-over refers to storage water not used in the previous irrigation season.

IDWR is responsible for administering water rights within the state. During the irrigation season, IDWR operates a daily accounting model that keeps track of both natural flow and storage rights. In addition to the accounting model, they have also used SRPM to plan water management in the state for over 30 years (Idaho Water Resources

Board, 1972). The purpose of the model is to guarantee that proposed changes in water management do not limit water users' historic access to water. Changes in water management are applied to the model, which is then run over the historic period to see if the proposed change would result in decreased diversions. If the new simulated management results in decreased diversions, the new management strategy must be revised until no new *shortages* occur. A shortage in the SRPM model is thus defined as a loss in a user's historic access to water, or a decline in diversions. In this thesis, this type of shortage will be referred to as a *planning shortage*. It is possible that a planning shortage may not occur even during the worst drought, as long as historic delivery is maintained. In some extreme cases, the historic delivery may have been zero, and therefore no matter what change in management occurs there will never be a planning shortage. For example, during the drought period in 1992, a canal company that relies on natural flow rights may not have been able to divert water late in the irrigation season because their water rights were junior to that of other users. Although the farmers relying on diversions from this canal may have experienced crop failure, they still received their full water right based on the priority of their right and from a water resource allocation perspective no shortage occurred. Since this model was developed to guarantee that historic delivery is maintained, this definition of a planning shortage is perfectly valid, when actual diversions are applied.

However, because diversion practices change over time (due to changes in infrastructure, land-use, regulations, litigation, etc.), IDWR can only realistically guarantee present users historic access to water based on *present* conditions. This means that IDWR must represent the present condition over the historic climate conditions.

Therefore, IDWR calibrates SRPM to present conditions, and then runs the model with historic hydrologic flows using current and proposed conditions. IDWR represents diversions in the SRPM model by actual monthly diversions over the last 15 years (1991-2005) and then represents historic diversions as the average monthly diversion during the 1991-2005 period. This *present conditioning of the past* assumes that climate is stationary. However, it is likely that this average diversion value may be biased to under predict demand because the recent 1991-2005 average occurs during a period in which the Snake River Plain has undergone two extensive multi-year droughts. As measured by SWSI, drought occurred from 1987 to 1994 and from 2000 to 2005 (it should be noted that this drought continued until 2010 in some portions of the basin) in most of the Snake River basin. Because drought would have limited the water available for diversions during the present condition, the average diversion from 1991-2005 may not represent what could have been legally diverted under more favorable hydrologic conditions.

Declining Surface Water Supply Since 1967

A recent study by Clark (2010) on trends in unregulated streamflow in Idaho, western Wyoming, eastern Oregon, and northern Nevada shows that unregulated flow in 10 out of 11 rivers within the Snake River basin have seen a significant decrease in flow. Trends to the north and east of the eastern Snake River Plain are all highly significant based on the Mann-Kendall (Mann, 1945; Kendall, 1975) trend analysis ($P < 0.10$). While not highly significant, a significant ($P < 0.30$) declining trend of streamflow has also been identified in all gaged rivers in the western Snake River Plain, except the Weiser River. The percent decline in annual mean streamflow is shown in Table 3.1.

Table 3.1 Significance of and Percent Decline in Annual Flow from Unregulated Streams in the Snake River Basin from 1967-2007 (Clark, 2010)

Stream	P-value	Rate of Change (%/yr)
Buffalo Fork nr Moran, WY	0.028	-0.78
Cache Creek nr Jackson, WY	0.017	-1.12
Greys River nr Alpine, WY	0.074	-0.75
Big Lost River nr Chilly, ID	0.018	-1.19
Bruneau River at Rowland, ID	0.212	-
Boise River nr Twin Springs, ID	0.257	-
S. F. Boise River nr Featherville, ID	0.135	-
Mores Creek abv Robie Creek, ID	0.212	-
S. F. Payette River at Lowman, ID	0.141	-
L. F. Payette River at McCall, ID	0.189	-
Weiser River nr Weiser, ID	0.522	-

Methods and Materials

The methods used to conduct this research include a nonparametric trend test of monthly diversions, temperature, and precipitation from 62 diversion locations and 10 climate stations within the Snake River basin, as well as a comparison of surface water diversions to SWSI, PDSI, and Palmer's z-index. This section of the chapter contains two subsections describing first the trend analysis and then a comparison of diversions to the three indices.

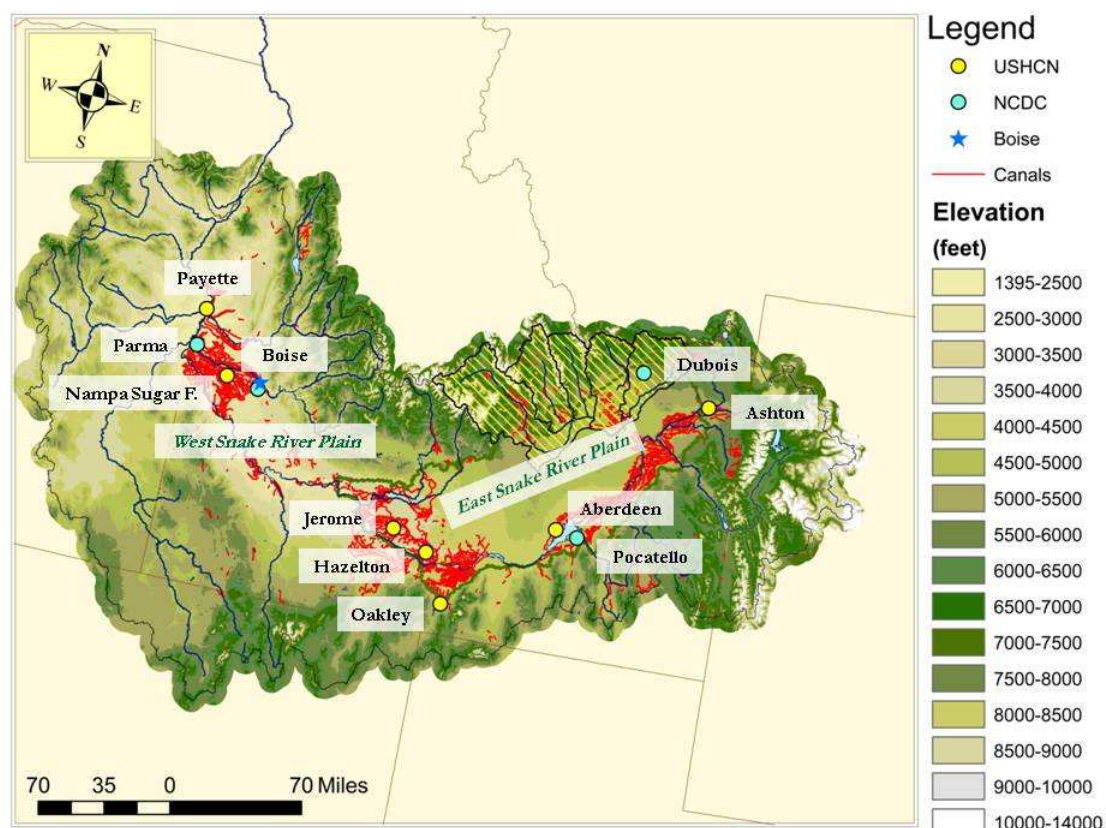
Mann-Kendall Nonparametric Trend Analysis

The detection of trends in canal diversions, precipitation, and temperature were based on the Mann-Kendall non-parametric statistical trend test. The test is based on the null hypothesis that there is no significant increasing or decreasing trend in the data over time. When the probability of the null hypothesis is less than 30% ($p < 0.30$), the trend is considered significant. If the probability of the null hypothesis is less than 10% ($p < 0.10$), the trend is considered highly significant. The choice of significance levels is consistent

with the recent trend analysis for unregulated streamflow in Idaho, western Wyoming, and northern Nevada (Clark, 2010). The data set used for the trend analysis of canal diversions was provided by IDWR, while climate data were downloaded from the National Oceanic and Atmospheric Administration's (NOAA) United States Historical Climatological Network (USHCN, see: www.ncdc.noaa.gov/oa/climate/research/ushcn), and the National Climate Data Center (NCDC) (see, www.ncdc.noaa.gov/oa/climate/stationlocator.html). The choice of the 10 climate stations was based on the completeness of the monthly precipitation and temperature data. Seven climate stations were selected for the analysis from the USHCN database. The location of these stations is shown as yellow dots in Figure 3.1, while location and elevation are listed in Table 3.2. This high quality historic dataset has been corrected for time of observation bias, discontinuities (including urbanization effects), and missing values. More details on the USHCN dataset can be found at the website mentioned above. An additional three Cooperative (COOP) stations (shown in Figure 6 as cyan dots) representing "raw" climate data were also analyzed. These NCDC COOP stations were chosen because they represent the only complete monthly temperature and precipitation records in the Snake River basin over the study period. The USHCN data set contains maximum average daily temperature, average daily temperature, minimum average daily temperature, and total precipitation for each month.

Table 3.2 Location and Elevation of Weather Stations Used in Trend Analysis

Station	Location	Elevation (ft)	Record NCDC
Ashton 1N	44.0N, 111.3W	5212	1948-present
Dubois Exp. Stn.	44.2N, 112.2W	5450	1948-present
Pocatello 2NE	42.9N, 112.4W	4832	1956-present
Aberdeen Exp. Stn.	43.0N, 112.8W	4402	1948-present
Oakley	42.2N, 113.9W	4559	1948-present
Hazelton	42.6N, 114.1W	4060	1948-present
Jerome	42.7N, 114.5W	3740	1948-present
Boise Air Terminal	43.6N, 116.2W	2814	1898-present
Nampa Sugar Factory	43.6N, 116.6W	2470	1976-present
Payette	44.1N, 116.9W	2150	1948-present

**Figure 3.1 Location Map of Weather Stations Used in Study**

Surface Water Supply Index Correlation to Canal Diversions

As mentioned earlier, diversions in Idaho are regulated by natural flow and storage rights. Both annual streamflow and storage are included in SWSI. The streamflow used in the SWSI index represents unregulated flow below the lowest reservoir and above most irrigation diversions. Supply is the sum of the previous month's reservoir storage and the unregulated flow through the remainder of the irrigation season, which ends in September. SWSI values range from -4 for the year with the least supply to 4 for the year with greatest supply. More details on the development and calculation of the SWSI index can be found at: www.id.nrcs.usda.gov/snow/watersupply/swsi-main.html.

In this study, SWSI was recalculated for the Henry's Fork, Snake River below Heise, Boise River, and Payette River for the period between 1971-2005 and then plotted diversions versus SWSI. The recalculation involved re-ranking the years to compare with the diversion data, which ends in 2005. As shown in Figure 3.2, monthly diversions are plotted on the y-axis with SWSI values for each month on the x-axis. A piecewise function is used to correlate supply with diversions during the mid- and late-irrigation season. The first leg of the piecewise function rises along with supply until a breakpoint is reached. After the breakpoint, the slope on the second leg of the piecewise function is zero. During dry years, the amount of water a canal company can divert is limited by the amount of water available in the river and the priority of their water right. As flows increase, the canal company can continue to divert more water until they reach the limit of their need or water right. The piecewise function indicates that surface water irrigation diversions are sometimes limited by supply and sometimes by demand. The objective of

the piecewise function is to minimize the root mean square error (RMSE). An example of this correlation is shown in Figure 3.2 for the month of August on the Burgess Canal, which diverts water from the Heise to Lorenzo reach of the Snake River. The yellow points in Figure 3.2 represent the points that correspond to the rising limb of the piecewise function (supply limited segment) while the blue points represent the zero slope portion of the piecewise function (demand limited segment).

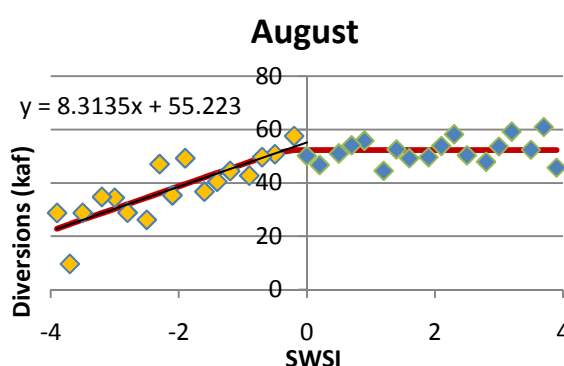


Figure 3.2 1971-2005 Canal Diversion Correlation with SWSI on the Burgess Canal

Palmer Drought Severity Index Correlation to Canal Diversions

In addition to comparing diversions to SWSI, the comparisons of the correlation of diversions to the Palmer Drought Severity Index (PDSI) using the Spearman Rank correlation coefficient (Spearman, 1904) were also performed. PDSI was developed by Palmer (1965) as a means of determining not only the severity of drought but also the beginning and ending of drought. PDSI is calculated using a simple two-layer soil moisture model. Palmer (1965) defines drought as,

...an interval of time, generally on the order of months or years in duration, during which the actual moisture supply at a given place rather consistently falls short of the climatically expected or climatically appropriate supply.

Palmer then goes on to define the severity of drought as "...being a function of both the duration and magnitude of the moisture deficiency." PDSI has been criticized because it lacks a snow algorithm (Dai et al., 2004) and the soil moisture model is fairly crude. For example, evaporation from the soil column occurs at the potential rate, which is calculated empirically using Thornthwaite's method (1948), and all moisture in the first 25 mm (or 1 inch) soil layer must be removed before moisture is lost from the underlying layer, which grossly simplifies soil moisture transfer (Alley, 1984). Despite its weaknesses, Palmer's index has withstood the test of time, and is currently the most widely used method for determining drought (Wang et al., 2009). One of the strengths of the model is its simplicity in that monthly soil moisture can be estimated using only temperature, precipitation, and soil type.

In this thesis, PDSI is used to analyze the correlation between early season soil moisture conditions and diversions at the beginning of the growing season in much the same way SWSI is correlated to diversions. In addition to examining the correlation of spring diversions with PDSI, the z-index value of the Palmer index was also correlated to early season diversions. The z-index, according to Palmer, "expresses on a monthly basis ... the departure of the weather of the month from the average moisture climate of the month." This index is of interest, since it represents only anomalies at the monthly time step and is not affected by long term soil moisture conditions. PDSI cannot take into account the replenishment of soil moisture in the root zone due to irrigation. If soil moisture from the previous irrigation season is carried through the winter by the soil column, PDSI would probably underestimate the springtime soil moisture conditions, reducing the correlation between PDSI and diversions.

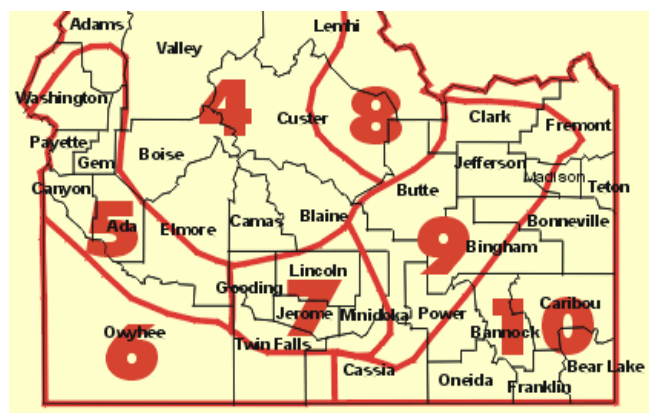


Figure 3.3 Climate Divisions within Southern Idaho
(www.cpc.noaa.gov/monitoring/regional_monitoring/CLIM_DIVS/idaho.gif)

Historic monthly PDSI and z-index data can be downloaded from the NCDC website (www1.ncdc.noaa.gov/pub/data/cirs/), which represents data from 1895 to the present. The data are organized by state and climate division. Climate divisions were established mainly based on drainage basins in the Western United States (Guttman and Quayle, 1996). In this research, both the PDSI and z-index for the 5th, 7th, and 9th climate divisions in Idaho were used. These climate divisions are also referred to as the Western Valleys, Central Plains, and Upper Snake River divisions and are shown in Figure 3.3. The PDSI values are based off temperature and precipitation data weighed equally for all stations within the climate division. In this study, the correlation of the sum of all Boise River diversions (except the New York Canal) were correlated to PDSI values for climate division 5; the sum of all Blackfoot to Milner diversions on the Snake River were compared to PDSI of climate division 7; and the sum of all Heise to Blackfoot diversions on the Snake River were compared to PDSI of climate division 9.

Results

The results of the research are presented in two subsections. First, the results of the trend analysis for temperature, precipitation, and canal diversions, are presented followed by comparison of diversions to SWSI, PDSI, and Palmer's z-index.

Mann-Kendall Trend Analysis

All trend analysis is based on the Mann-Kendall nonparametric statistical trend test as discussed in the *Methods* section. Three levels of trends were identified and are described as follows: a highly significant trend ($P < 0.10$), a significant trend ($P < 0.30$), and no detectible trend ($P > 0.30$).

Temperature Trend Analysis

A review of temperature records from 10 climate stations across the Snake River Plain (see Table 3.3) reveal that all stations have seen a significant ($P < 0.30$) annual temperature increase with a highly significant increase ($P < 0.10$) at 9 of the 10 stations. The average annual temperature increase over this period (1971-2005) is 2.4°F or 0.2°F/decade, based on a linear regression. A review of long-term temperature records in this region indicate that the greatest temperature increase has occurred during this period (1971-2005), as shown in Figure 3.4. Figure 3.4 shows average decadal temperatures at the Nampa and Jerome USHCN climate stations. The last decade of temperature measurement (1996-2005) within this study show an increase of 1.8°F and 2.2°F over the mean annual temperature between 1906-1985.

Table 3.3 Average Monthly, Annual, and Seasonal Temperature Trends from 1971-2005 by Climate Station

Climate Station	Jan	Feb	Mar	Apr	May	Jun	Jul	Aug	Sep	Oct	Nov	Dec	Yr	DJF	MAM	JJA	SON
Significant																	
*Dubois	++	+	++	++			+	+	+				++	++	++	+	+
Ashton	++		++	++	+		+		+			+	++	++	++	++	+
Oakley	++		++	++	++		++	++	++	++			++	+	++	++	++
*Pocatello	+			++	+								+		++		
Aberdeen	+		++	++	++		+	++	++	++			++	+	++	++	++
Hazelton	++		++	++	+		+		+			+	++	++	++	++	+
Jerome	++		++	++			+	++	++	+			++	+	++	++	++
*Boise	+		++	+	+		++	++	++				++	+	++	++	+
Nampa	++		++	+			+	+	++	++		+	++	++	+	+	++
Payette	++		++				++	+	+	++	++	++	++	++	++	++	++
Δ (°F)																	
*Dubois	6.7	2.7	5.5	4.3			2.2	2.2	1.5				2.9	4.3	3.9	1.5	1.8
Ashton	5.9		5.3	4.7	2.7		1.4		2.3			4.0	2.5	4.0	4.2	1.1	1.1
Oakley	5.3		5.0	3.7	3.0		3.6	4.1	4.5	2.9			3.0	2.0	3.9	2.8	3.0
*Pocatello	4.9			2.1	1.6								1.1		2.3		
Aberdeen	6.5		3.8	3.4	3.3		2.6	2.8	4.1	2.6			2.8	3.0	3.5	1.9	2.8
Hazelton	5.7		4.8	3.0	2.6		3.5		4.1			2.0	2.8	3.0	3.5	2.8	2.4
Jerome	5.8		2.8	3.2			2.4	2.8	3.3	2.5			2.3	3.0	3.0	1.6	2.2
*Boise	2.9		2.1	1.5	1.3		2.2	2.2	2.5				1.5	1.6	1.6	1.7	1.2
Nampa	6.9		4.0	2.0			1.4	2.2	3.8	3.1		4.0	2.5	4.0	2.1	1.1	2.8
Payette	6.8		3.6				2.4	3.4	3.2	3.2	2.3	4.0	2.8	4.0	1.8	2.0	3.0
Avg. T (°F)																	
*Dubois	19.9	23.9	32.4	42.7	51.7	60.3	68.6	67.5	57.7	45.6	30.2	20.9	43.6	21.5	45.9	67.2	51.7
Ashton	18.9	22.9	31.1	40.8	50.0	57.5	64.1	62.7	53.9	43.1	29.1	19.9	41.2	20.5	40.6	61.5	42.0
Oakley	28.6	32.9	39.7	45.6	53.5	61.7	69.1	68.3	59.6	49.3	36.8	29.3	47.9	30.2	46.3	66.4	48.6
*Pocatello	24.0	29.0	38.0	45.7	53.9	62.4	70.1	68.9	59.1	47.7	34.4	25.4	46.7	26.0	45.9	67.2	47.1
Aberdeen	22.4	26.9	36.7	44.5	52.9	60.9	67.8	66.3	56.5	45.9	33.0	23.6	44.8	24.2	44.7	65.0	7.3
Hazelton	27.0	31.8	40.2	46.8	54.9	63.7	71.3	69.5	59.5	48.8	35.9	27.8	48.1	28.8	47.3	68.2	48.1
Jerome	27.9	32.8	41.3	48.4	56.4	65.1	73.1	72.0	61.9	51.0	37.3	28.6	49.7	29.6	48.7	70.2	50.1
*Boise	29.9	36.1	43.6	50.0	58.1	66.6	74.4	73.4	63.6	52.2	39.2	30.6	51.6	32.1	50.6	71.5	51.7
Nampa	29.4	36.0	44.5	51.1	59.4	67.5	74.9	73.0	62.8	51.4	38.6	30.3	51.6	31.8	51.7	71.9	51.0
Payette	28.3	35.4	44.7	51.1	59.3	67.1	74.4	72.7	63.0	51.5	38.7	29.8	51.3	31.0	51.7	71.5	51.1

++ represents a highly significant increase in diversions ($p < 0.10$), + a significant increase in diversions ($p < 0.30$), N no significant trend, - a significant decrease in diversions ($p < 0.30$), -- a highly significant decrease in diversions ($p < 0.10$)

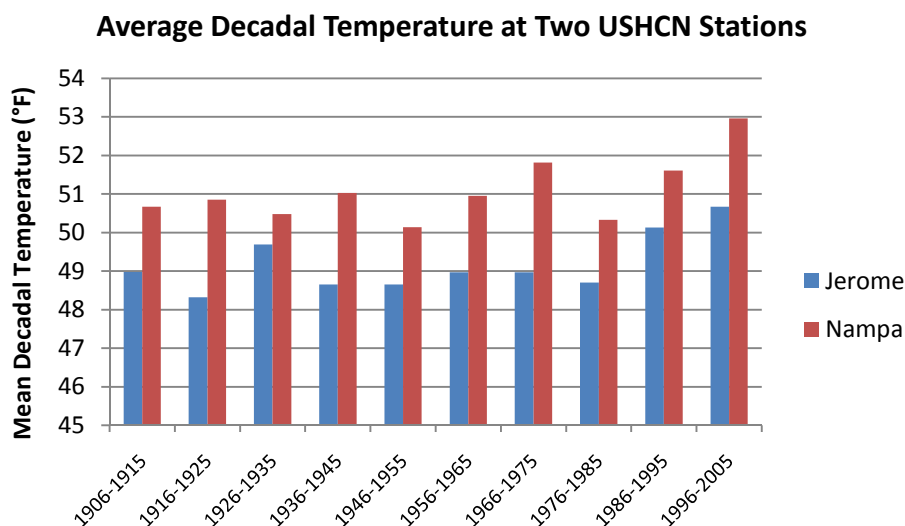


Figure 3.4 Average Decadal Temperature at Nampa and Jerome USHCN Stations

As shown in Table 3.3, all monthly temperature trends are positive or neutral, with the month of January having the greatest temperature increase (on average 5.7°F). The month with the most significant temperature increase was March where all stations, except Pocatello, had a highly significant trend. It should be noted, however, that Pocatello was the station that showed the least temperature increase. Also, Pocatello was one of the three stations where trends were based on raw station data not part of the USHCN climate network. The other two “raw” data stations where trends were analyzed matched more closely with their nearest neighbors (compare Dubois with Ashton, and Boise with Nampa). Interestingly, some months like February, June, and November had almost no significant temperature trends. A review of seasonal temperatures indicate that the season with the most significant temperature increase was the spring season (March, April, and May, or MAM) followed by summer (June, July, and August, or JJA).

Since January is the coldest month of the year, it is a critical month for snow accumulation in the plain. Thirty-five years ago, in the western portion of the Snake

River Plain at the Boise, Nampa, and Parma climate stations, maximum winter temperature hovered around freezing. Now daily average temperatures are beginning to regularly exceed the freezing point. Between 1994 and 2005, the average daily temperature exceeded 32°F in 9 out of 12 years at the Parma Experiment Station⁴, as shown in Figure 3.5. This temperature rise might have contributed to an increase in rainfall and a decrease in the amount of snowfall accumulation in the western Snake River Plain. At the Parma weather station, the amount of days with snowfall greater than 1 inch fell from an average of 17.6 days (1971-1993) to 5.2 days (1994-2005) in January and from 7 days (1971-1993) to 2 days (1994-2005) in February. This is despite the fact that the second period (1994-2005) included the very wet years of the late 1990s. Total snowfall and maximum monthly depth of snow accumulation also fell significantly at the Parma weather station.

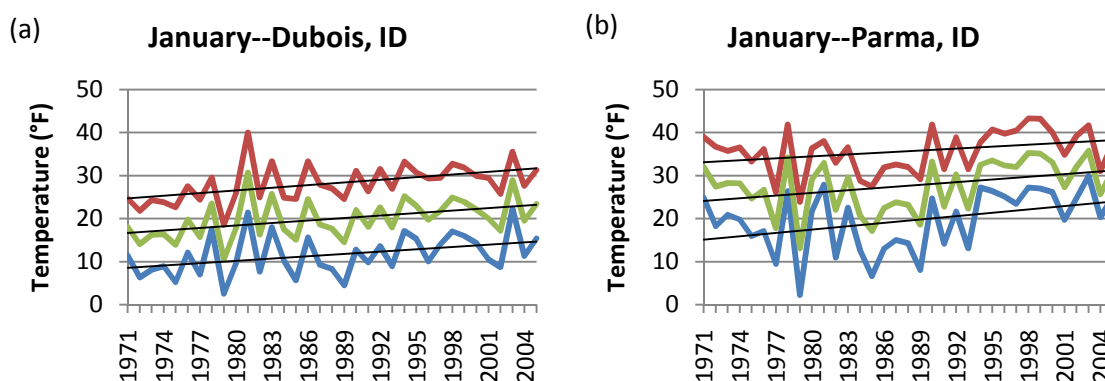


Figure 3.5 January Monthly Temperature Trends for Daily Average Temperature (green), Maximum Average Daily Temperature (red), and Minimum Average Daily Temperature (blue) at the (a) Dubois and (b) Parma Weather Stations from 1971-2005

⁴ The consideration of the Parma snow record, versus that of the USHCN stations, was due to the incompleteness of snow records for the Nampa and Payette stations. Parma was not included in the temperature trend analysis because of incomplete temperature records.

In the eastern Snake River Plain, represented by weather stations at Dubois and Pocatello, where maximum winter temperatures were still mostly below the freezing point in January and February, there was no marked change in the number of days with snow greater than 1 inch, total monthly snow accumulation, or total monthly snowfall. Figure 5 shows the average monthly minimum daily temperature and maximum daily, as well as the average daily temperature from 1971-2005. A study of climate change by Salathé et al. (2008) that modeled local responses to climate change in the Northwest showed that the most significant increases in winter temperatures in the Northwest have occurred, and will continue to occur, in areas like the Snake River Plain, where the number of days with snow cover is declining.

The highly significant spring temperature trends in the months of March and April indicate a potential lengthening of the growing season as identified by Christidis et al. (2007). A trend test on the minimum daily average temperature for the months of April and May are highly significant at 4 of the 5 highest stations (Pocatello being the exception). At these stations, the April minimum daily temperature is regularly beginning to exceed the freezing point. This warming in spring has important implications for surface water irrigation at the beginning of the season.

Precipitation Trend Analysis

Interannual monthly precipitation variability is high across the Snake River basin, making the detection of precipitation trends difficult. The Mann-Kendall trend test revealed that there were few significant precipitation trends at either the annual or monthly scales. In months where trends did exist, April and May were always positive, while the rest of the months were negative. These trends showed no regional bias. The

only consistent seasonal trend at almost all stations was a significant decline in fall (September, October, and November, or SON) precipitation.

Canal Diversions Trend Analysis

Not surprisingly, the decline in historic annual diversions is highly significant for most canals in the Snake River Plain. The decline in natural flow during this period adversely impacted the filling up of the reservoirs, as indicated by a review of the IDWR's monthly reservoir storage records (not shown here). The decline in annual diversions was an obvious result of declines in storage and natural flow, the two main sources of surface water irrigation. However, not all of the decline in diversions is necessarily related to declining supply, as seen by the larger than usual decline in surface water diversions from the Teton River, after the collapse of the Teton Dam in 1976 (Stene, 1997). What is surprising is the consistent increase in springtime diversions shown in Table 3.4 and Table 3.5 in both the eastern and western portions of the Snake River basin, respectively.

Table 3.4 and Table 3.5 show the significance of positive and negative diversion trends for each month during the irrigation season (April-September), as well as the annual trends in the far-right column. Along with the annual trend in the right-hand column is the average annual diversion for that canal during the period from 1971-2005. The canals are listed by number according to the IDWR's numbering system in the SRPM model. As mentioned earlier, some of these canals represent an aggregation of smaller canals; Appendix A lists each canal represented numerically in Tables 3.4 and 3.5.

Table 3.4 Trend Analysis of Canal Diversions in the Eastern Snake River Basin above Milner Dam, Average Annual Diversions (kaf) from 1971-2005 are Shown in Brackets after the Annual Trend, Diversion Codes are Described in Appendix A

River	April	May	June	July	August	September	Annual
Falls River							
010		N	--	--	--	--	--(35.7)
015		N	+	+	N	N	+(4.2)
020	N	N	--	N	-	-	-(24.1)
030	-	--	--	--	-	++	N(27.4)
035	+	N					--(65.7)
040	++	N	--	--	--	--	--(34.1)
Henry's Fork							
045	+	-	--	--	--	-	--(37.1)
050	--	--	--	--	--	-	--(30.1)
060	N	N	--	-	--	N	--(156.6)
070	-	--	--	--	-	++	--(255.4)
080	+	N	--	N	-	-	-(92.3)
Teton River							
090	--	-	--	--	--	-	--(29.7)
100	--	--	--	--	--	-	--(53.5)
110	-	-	--	--	--	--	--(3.0)
120	N	+	--	--	--	--	--(64.1)
Snake River (Heise-Lorenzo)							
135	+	N	--	--	--	--	--(105.9)
137	N	N	--	-	-	N	-(15.0)
140	+	N	-	--	--	-	--(252.8)
145	-	N	--	--	--	--	--(327.8)
150	++	N	--	--	--	--	--(580.8)
160	N	N	--	--	--	--	--(207.3)
Snake River (Lorenzo-Blackfoot)							
170	++	N	--	--	--	--	--(88.6)
175	N	++	+	N	--	N	-(15.0)
180	+	N	-	--	--	--	--(355.7)
190	++	+	-	--	--	--	--(339.2)
200	++	-	--	--	--	--	--(214.4)
220	+	-	--	--	--	--	--(185.2)
230	++	--	--	--	-	-	--(248.6)
240	++	N	--	--	--	--	--(41.7)
242	++	+	-	--	--	-	--(386.2)
Blackfoot River							
248	N	-	N	-	N	--	--(186.9)
249	++	N	--	--	--	--	--(87.3)
Snake River (Blackfoot-Milner)							
253	+	++	++	--	N	-	++(41.7)
260	+	--	--	--	--	--	--(372.7)
270	N	--	--	--	--	--	--(434.8)
280	N	--	-	--	--	N	-(1314)
290	N	--	--	--	--	--	--(960.9)
300	N	--	--	--	--	--	--(1283)

++ represents a highly significant increase in diversions ($p < 0.10$)

+ represents a significant increase in diversions ($p < 0.30$)

N represent no significant trend

- represents a significant decrease in diversions ($p < 0.30$)

-- represents a highly significant decrease in diversions ($p < 0.10$)

Table 3.5 Trend Analysis of Canal Diversions in the Western Snake River Basin from the Boise River and Payette River, Average Annual Diversions (kaf) from 1971-2005 are Shown in Brackets after the Annual Trend

River	April	May	June	July	August	September	Annual
Boise River							
505	N	--	--	--	--	N	-(2.3)
515	N	--	--	--	--	--	--(298.4)
520	N	--	--	--	--	N	--(377.0)
525	-	--	--	--	--	-	--(49.0)
530	N	--	--	--	--	-	--(272.4)
535	++	--	--	--	--	--	--(189.0)
540	++	--	--	--	--	--	--(203.8)
545	++	--	--	--	--	--	--(57.0)
550	+	--	--	--	--	N	--(10.7)
555	+	--	--	--	--	--	--(76.2)
560	N	--	--	--	--	N	--(95.6)
562	++	N	N	--	--	--	--(12.8)
564	++	-	N	--	--	N	N(155.5)
568	+	-	-	--	--	--	N(26.5)
570	++	N	N	--	--	--	--(18.6)
574	N	--	--	-	N	--	N(99.0)
576	N	--	--	--	--	--	--(115.5)
580	N	--	+	N	--	N	+(64.5)
585	N	--	--	--	--	N	--(63.2)
Payette River							
620	+	-	-	-	N	-	-(131.7)
625	+	-	N	N	N	N	N(447.3)
640	+	-	-	-	-	-	-(280.9)
655	+	-	-	-	N	N	N(105.6)
670	+	N	-	-	-	-	-(176.1)

++ represents a highly significant increase in diversions ($p < 0.10$)

+ represents a significant increase in diversions ($p < 0.30$)

N represent no significant trend

- represents a significant decrease in diversions ($p < 0.30$)

-- represents a highly significant decrease in diversions ($p < 0.10$)

To put the declining diversion trends in perspective, both the annual and total decline of diversions were calculated for each of the subsections shown in Tables 3.4 and 3.5 for the 35-year period of study. The total decline in diversions over 35 years in the eastern most irrigation region containing the Henrys Fork, Falls River, and Teton River is about 348 kaf. The middle of the Snake River basin represented by diversions from the main stem of the Snake River has seen surface water diversions decline by roughly 1570

kaf, while the western end of the plain has seen irrigation diversions decline by 210 kaf. It should be noted that complete diversion records were missing on the New York Canal and on the Payette River, so that the decline in diversion from the western portion of the basin are incomplete, and represents only diversions from the Boise River excluding the New York Canal. Except for diversions on the New York Canal that are represented by diversions 515 to 530 and the Payette River, which have incomplete diversion records, the only basin with mixed annual diversion trends is the Falls River. While the months of June, July, and August generally follow the trend of declining annual diversions, April diversions (and May diversions in higher elevation eastern basins) tended to have either a neutral or increasing diversion trend.

Table 3.6 Crop Emergence Dates at Agrimet Stations
(see, www.usbr.gov/pn/agrimet/id_charts.html)

Agrimet Station	Ashton	Aberdeen	Twin Falls	Nampa
Elevation	1615 m	1341 m	1195 m	824 m
Alfalfa	May 1	March 20	March 10	March 5
Spring Grain	May 15	April 15	March 20	March 5
Potatoes	June 10	June 5	May 10	May 1

While annual diversions have fallen sharply, irrigation trends at the beginning of the growing season are rising. In the higher elevation portion of the basin, corresponding to the Dubois and Ashton climate stations (e.g., along the Henry's Fork), the beginning of season irrigation occurs in May. As one moves from east to west, and down in elevation, across the plain, the growing season becomes longer and May diversions switch from positive to neutral below Heise to mostly negative below Blackfoot, while April diversions remain positive. This change in diversion trend is most likely not as related to longitudinal distance from source as to the start of the growing season, which as shown in Table 3.6 varies significantly with elevation. This interpretation seems to be confirmed

by the high correlation found between PDSI and springtime diversions discussed later in the chapter.

April diversions trends have an interesting pattern on the Snake River and Boise River, in that the upstream diversions trends tended to be positive, while downstream diversions trends tended to be neutral. I believe this could be the result of downstream users having a more reliable irrigation supply. The reliance of downstream users on return flows is well documented on the Boise River (Schmidt et al., 2009). A comparison of diversions to SWSI in both the lower Snake River and Boise River indicate that these entities are rarely water short. The reason downstream users are least impacted by water shortages on the Snake is that they rely more on storage, while upstream users on the Snake typically depend more on natural flow (Stene, 1997). This implies that perhaps the more a canal company is prone to shortage the more their users may rely on the early irrigation. I hypothesize that springtime diversion trends may be due either to differences in crops raised based on reliability of supply, or on users ability to apply late season irrigation. (A lack of crop data prevented further study on this topic.) It should be noted that both on the Snake and the Boise rivers the early season (April) diversions, even if neutral contrast to the highly significant decline of diversions in other months. The difference in sign of early season diversions compared to annual diversions has important implications in understanding how increasing temperature impacts irrigation diversions within the Snake River basin and will be shown by the correlation of SWSI and PDSI with diversions discussed below.

Diversion Comparison with Supply and Soil Moisture Indices

The results of comparing diversions to surface water supply represented by SWSI and soil moisture represented by PDSI are shown below. From the analysis, it appears that surface water supply is demand driven in the springtime, and supply driven during the remainder of the irrigation season. Peak runoff from the mountain snowpack occurs during the late spring and early summer, providing ample surface water supply at the beginning of the irrigation season. During the later part of the irrigation season, supply becomes more limited.

Comparison of Diversions with SWSI

Figure 3.6 shows the trend in annual diversions over the period of study (1971-2005) in the Burgess Canal located on the Heise-Lorenzo reach of the Snake River. Overall, the trend in diversions declined by about 2.6 kaf/yr. The decline of diversions on the Burgess Canal would appear to be mainly the result of the extensive 1988-1993 drought as well as the 2000-2005 droughts, as evidenced by the rebound in diversions during the wet period in the late 1990s. The recent multi-year droughts, as noted earlier, decreased both the natural flow and storage water available for irrigators.

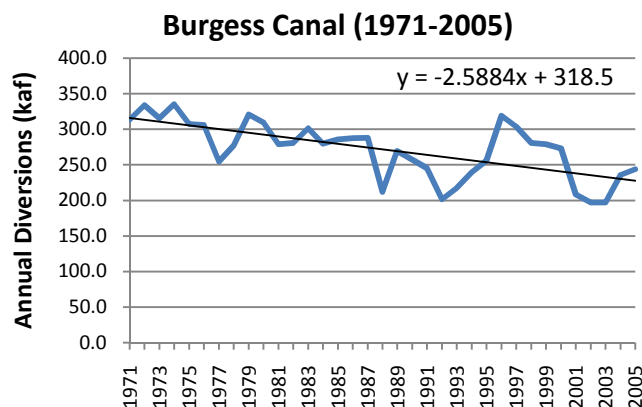


Figure 3.6 Annual Diversions of the Burgess Canal

Figure 3.7 shows a comparison of diversions to SWSI on a monthly basis on the Burgess Canal. The results described here apply to most of the canals in the study. Comparison between diversions and supply, represented by SWSI, did not conform to the piecewise function for the months of April and May. At the beginning of the study period from 1971-1987, there were only three years in which diversions occurred in April on the Burgess Canal. After 1987, diversions occurred in two-thirds of the remaining 18 years. The lack of a clear correlation of SWSI to diversions in April and May is often best represented by a simple declining linear trend with more diversions occurring for years with less supply represented by negative SWSI values than during years with abundant supply represented by positive SWSI values as seen in Figure 3.7b. The increased April diversions may be an indication of the lengthening of the growing season, which in the western United States has occurred mainly in spring (Christidis et al., 2007). The inverse relationship of May diversions to supply indicated that surface water diversion (and thus irrigation) in the early part of the year was driven more by need than supply. Just as Alfaro et al. (2005) found that groundwater irrigation begins earlier in dry years, it appears that surface water irrigation begins earlier in years with less supply, which typically would be drier years. This understanding was verified by investigating the correlation of PDSI and Palmer's z-index to spring diversions as discussed later in the chapter. After May, diversions correlated with supply according to the piecewise function described earlier, indicating that for the remainder of the year diversions were often driven by supply. As would be expected, the rising limb of the piecewise function tended to become progressively steeper between June and September as reservoirs were depleted late in the season during years with low supply.

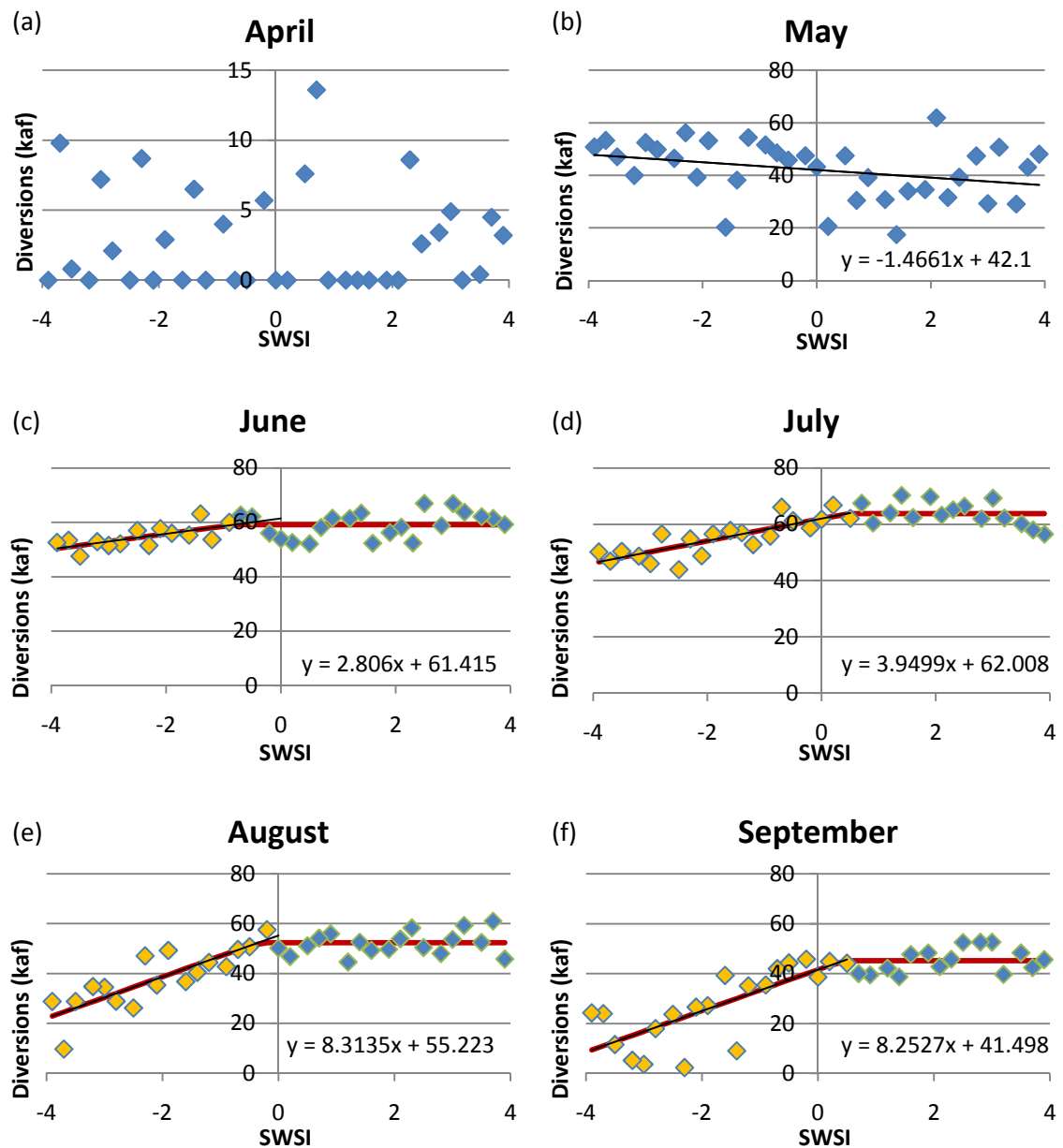


Figure 3.7 Monthly Correlation of Burgess Canal Diversions to SWSI (1971-2005)

Correlation of April Diversions with PDSI and the Z-index

It was found that in a heavily irrigated semi-arid region like the Snake River Plain, where summer precipitation is almost always inadequate to meet the crop water demand, PDSI has almost no correlation (using the Spearman's rank correlation

coefficient) with mid- and late-season surface water diversions. Based on the earlier SWSI correlation, it was found that during the mid- and late-season irrigators tended to keep diversions as high as needed. However, during the first month of irrigation (usually April), both March and April PDSI values, as seen in Table 3.7, provide significant correlation to the first month diversions from the Boise River located in climate division 5 (see Figure 3.3 for climate division locations). The correlation of PDSI to first month diversions indicated that at the beginning of the season, the amount of surface water diversions corresponded to the amount of water needed to restore moisture to the soil column. As expected, during wet years, represented by positive PDSI values, diversions were low; while during drier years, represented by negative PDSI values, diversions were higher since more water was needed to replenish depleted soil moisture.

Table 3.7 The Correlation of PDSI and Palmer's Z-index to Diversions in the Snake River Plain Based on Spearman's Rank Correlation Coefficient

	Boise River	Central Snake	Upper Snake
March PDSI	-0.62	-0.36	-0.48
April PDSI	-0.67	-0.40	-0.54
March z-index	-0.77	-0.65	-0.69
April z-index	-0.60	-0.45	-0.56
March + April z-index	-0.83	-0.67	-0.71

Correlation of March and April PDSI to April diversions was less significant in climate divisions 7 and 9, as compared to division 5. This decline of correlation may be due to PDSI not distinguishing between precipitation as snow vs. rain (Dai et al., 2004). As mentioned earlier, snow covered area in the western plain has nearly disappeared due to winter warming, while in the eastern plain, due to cooler temperatures corresponding with higher elevation, winter snow cover has been less affected by warming. Because temperatures remain below freezing longer in the eastern plain, more moisture may also

be maintained in the soil column from the previous irrigation season. Because of the low correlation of PDSI to diversions in the central and eastern portions of the plain, an analysis to correlate diversions to Palmer's z-index was performed. Palmer's z-index represents the departure of climate from normal conditions at the calculated timestep, in this case monthly.

Table 3.7 shows that Palmer's z-index consistently showed greater correlation to diversions than PDSI. The increased correlation of the z-index to PDSI is likely due to the fact that PDSI represents long-term soil moisture trends, while the z-index represents only monthly anomalies in climate conditions. It also found that greater correlation occurred when the April and March z-indices together were added together (see Table 3.7). The higher correlation of the combined indices is likely due to the fact the spring soil moisture is heavily influenced by climate anomalies in both March and April. If both March and April climates were anomalously dry, one would expect that greater diversions would be needed to bring soil moisture up to field capacity in the springtime than if only one month was unusually dry.

Discussion

In considering the impacts of climate change on surface water diversions in the Snake River Plain during the period (1971-2005), it is important to recognize the difference between interannual climate variability and climate change. Precipitation records, for example, contain very few long-term trends. As Mote and Salathé (2010) point out, the detection of significant changes in precipitation are likely to be difficult, well into the next century, due to climate variability. On the other hand, the temperature record has highly significant trends, at the annual, seasonal, and monthly scales. This

trend would seem to be largely a product of long-term, and most likely human-induced, climate change. The loss in snow-cover in the western portion of the plain, which is likely to migrate eastward (Salathé et al., 2008) as the temperature warms, is mostly a product of the significant increase in January temperatures. The rise in springtime temperatures and corresponding trend of earlier diversions also corresponds to the highly significant increase in springtime temperature, causing a lengthening of the growing season (Christidis et al., 2007). The correlation of PDSI and Palmer's z-index indicates that diversions each spring are a product of the interaction of precipitation and temperature on antecedent soil moisture conditions prior to the irrigation season.

Interestingly, the rise in temperatures during the peak of the growing season has had little discernable impact on surface water diversions. The flat limb on the summertime SWSI versus diversion graphs captures both diversions in the high supply years of the 1970s and late 1990s. Any impact of rising temperatures on summertime surface water diversions is masked by the fact that the amount diverted each month is partially dependent on water right limits. Future studies at the farm scale of application might be able to better capture the impact of rising temperature on crop water demand.

The implications of this research for water resource management in the Snake River basin are that long-term planning for climate change should focus on climate impacts to supply (e.g., snowpack) and the lengthening of the irrigation season. The impact of changes in supply due to climate change should use the flat limb of the SWSI index to indicate the amount of water farmers would like to divert given adequate supply in order to provide canal companies, water resource managers, and irrigators a sense of how climate change may impact the reliability of their surface water supply. Use of

average diversions over the last 15 years is likely to underestimate diversion demand during high supply years. On the annual scale of predicting water demand, this research indicates that Palmer's z-index in March could be used to estimate early season diversions.

I hypothesize that the physical mechanisms for declining soil moisture are as follows. When temperatures remained below freezing in the winter, snow could accumulate above the soil column until the spring thaw, at which point the snow would melt recharging soil moisture. With winter daytime temperatures in the western plain often exceeding the freezing point, the snow melts during the day; meaning that snow can no longer accumulate to previous depths eliminating some of the soil moisture recharge that occurred with the spring thaw. Without the high albedo of snow cover deflecting incoming radiation, the absorption of incoming solar radiation leads to higher latent (soil evaporation) and ground heat fluxes. Direct verification of surface flux trends is not possible for this study area. Availability of soil moisture for evaporation from the soil column and subsequent heating of those soil layers probably warms the ground, creating a positive ground heat flux feedback loop (meaning that soil is heating). Therefore, instead of storing moisture during the winter, the soil column is losing moisture and enters a warmer spring with less moisture. This study establishes a relationship between near surface hydrological response and irrigation diversions due to changing climate conditions.

In order to gain a better understanding of how crop water demand and changes in land-use impact surface water diversions, further research could be done using a water resource management model that accounts for the various land use changes, canal

seepage, irrigation practices, and water rights. Also, the establishment of flux measurement and soil moisture monitoring stations that could confirm results of modeled data would be highly beneficial to the study of climate impacts in the basin. Also, if a dataset of land-use, canal seepage, and irrigation practices at the farm scale could be assembled, these records could help close the water budget and identify how increased efficiency of irrigation may be helping farmers adapt to climatic change.

Conclusions

While one cannot, from the research presented here, differentiate how much of the hydrologic change in the Snake River basin has been forced by anthropogenic sources versus natural climate change, one should be able to detect how climate attributes are changing, and how these changes are influencing surface water demand. The results of this research leads me to believe that the marked decline in irrigation during the last three and a half decades is at least partly the result of a decline in water supply caused by declining natural flow (Clark, 2010). Since this decline is in part the result of drought, it is likely that if the basin enters a period with higher streamflow, we would see a rebound in annual diversions. However, the increase in diversions in the mid- and late-irrigation season would be limited by water resource infrastructure and the limitations imposed by water rights.

While annual diversions have declined, springtime diversions have had a strong increasing trend within low and mid-elevation river reaches in the Snake River basin that are the result of increasing temperature. Warmer spring temperatures result in the earlier timing of irrigation within some parts of the basin. In the lower elevation portions of the basin, wintertime temperatures have passed the freezing point, resulting in loss of snow

cover and earlier snowmelt (Sridhar and Nayak, 2010), which has likely led to greater absorption of solar radiation, which leads to drier spring soil moisture conditions. Although there are some limited trends of increased springtime precipitation, spring precipitation has not been able to offset increasingly dry springtime soil moisture conditions. The trend of drier spring soils is likely to continue under a warming climate and spread to the higher elevation portions of the basin within the next couple decades, should warming continue to occur at the present rate. Both the realization that mid- and late-summer irrigation diversions cannot increase beyond identifiable thresholds and that spring irrigation demand will continue to increase is critical when studying the impacts of climate change on water resources in the Snake River basin.

CHAPTER FOUR: MODEL DESCRIPTION OF THE SYSTEM DYNAMICS – SNAKE RIVER PLANNING MODEL

Existing Models and Model Selection

Idaho water resources management is a complex process involving many public and private interests. Modeling the complex water resource operations in the Snake River basin at a level of detail significant to water resource managers requires a level of knowledge of the basin beyond the scope of this master's thesis. Therefore, considerable effort was made to identify a model that could use and adapted to provide detailed operational level information about how the entire system works. There are three main models used to represent water resource management in the Snake River. The Idaho Department of Water Resources' (IDWR) Snake River Planning Model (SRPM) (Idaho Water Resource Board, 1972), the Bureau of Reclamations (USBR) MODSIM model (Labadie and Larson, 2007) referred to as the Snake River Basin Model (SRBM, USBR, 2000), and the University of Washington's SnakeSim model (VanRheenen et al., 2003). The SPRM model developed in FORTRAN and most recently calibrated in 2005 represents a classic linear programming method. This model requires historic inputs and carries basic assumptions of stationarity. Operations are based on irrigation calls. The focus of the model is on irrigation demand and instream flow requirements. SRPM output includes irrigation shortages and instream flow shortages by month.

The SRBM model of the Snake River, developed for the Bureau of Reclamation as a decision support system, is a highly complex model that includes several reservoirs

in eastern Oregon. MODSIM is a specialized reservoir operations model that requires specialized coding for adaption to individual river basins (Labadie and Larson, 2007). As such, the model lacks the inherent flexibility in the generic framework of system dynamics models. As illustrated by Miller et al. (2003), the model can be dynamically linked to an aquifer through response functions.

The SnakeSim model was developed by the University of Washington with the STELLA system dynamics platform and was designed to handle projected flows and was specifically developed for the study of climate change as a research model. As such, it was not developed for making management decisions and provides output at a coarser resolution than either the SRPM or SRBM models. The output determines the reliability of irrigation flows and hydropower generation.

The eventual choice to use the SRPM as the base model for the research was based on the desire to analyze climate impacts using a modeling framework familiar to water resource managers in the Snake River basin. While SRPM does not contain a hydropower component, it is used by Idaho Power (USGS, 2010), Idaho's largest private hydropower generator, and hydropower components could be added as demonstrated by Scott (2010). Also a significant consideration for using the model was the model's thorough documentation and the willingness of current and former staff at IDWR and Idaho Power to assist in my understanding of the model.

Components of the System Dynamics Model in Powersim Studio 8

Powersim Studio 8, like other system dynamics models, has three major components: stocks, flows, and auxiliaries. Stocks represent a location where real items can be stored. Flows represent how items are transferred between the stocks. Auxiliaries

determine how various stocks and flows interact. In the System Dynamics – Snake River Planning Model (SD-SRPM), stocks represent reservoirs and flows represent rivers or diversion channels. The volume within the reservoir is measured in thousand acre-feet (kaf). This choice of units is based on the original SRPM model. Flows are measured in kaf/month, since the timestep is monthly. There are three types of auxiliaries included in the model. Input auxiliaries transfer data to the model from a spreadsheet. Calculation auxiliaries contain programmed code to direct the flow within the model. A special kind of calculation auxiliary, known as the delay auxiliary, causes a delayed reaction in the transfer of water from one model component to the next.

The Basic Structure of SRPM and SD-SRPM

Before going into the details of how SD-SRPM was created it is necessary to describe operations in the original SRPM model. The following description of SRPM is based largely on two documents, *River Operations Studies for Idaho* (Idaho Water Resource Board, 1972), *Willow Creek – Blackfoot River – Portneuf River Systems* (Idaho Water Resource Board, 1975) and a personal investigation of the model. The three main inputs to the model include a diversion file, a reach gain file, and an indicator file. The reach gain file describes the amount of water gained and lost within 89 reaches of the Snake River system. The diversion file contains actual diversions at 97 locations within the basin from 1991-2005 and the average monthly diversion of the recent period (1991-2005) representing diversions from 1928-1990. The indicator file describes the reservoir characteristics for 23 reservoirs, flood operation rules for 8 flood control reservoirs, assigned flows at numerous reaches, the reservoir call order and return flow factors for all diversions, and special operations for the New York Canal and Lake Lowell.

The basic structure of the model includes three loops. Each loop starts with reach one and then works its way down to the last reach. Appendix B shows schematics of SRPM and SD-SRPM. The first loop accumulates natural flow reach by reach, trying to meet irrigation demand by natural flow. Excess natural flow at the end of the loop (or river branch) is stored in the nearest upstream reservoir. The second loop then seeks to meet instream flow requirements, minimum releases from reservoirs, and diversion demand unmet by natural flow through the release of storage water. The final loop performs flood operations. If flood releases would result in downstream flooding, the loop is repeated with more water released earlier in the year. This looped structure of SRPM was not retained in the SD-SRPM model, as a system dynamics model requires that all calculations for each timestep be carried out in the same timestep. Rather than having a looped system, the SD-SRPM model operates two parallel versions of the river simultaneously: a natural flow river and a regulated flow river. These two parallel rivers will be referred to as the natural flow structure and the regulated flow structure in describing the model.

The natural flow structure is used to calculate calls for storage water. The *natural flow* referred to in the SD-SRPM model is different from *natural flow* in the SRPM model. In SRPM, natural flow refers to the sum of all reach gains upstream of a given location; while in SD-SRPM, natural flow consists of all reach gains below the nearest upstream dam at a given location. The natural flow, as defined in the SD-SRPM *natural flow* river, better represents the real system, where natural flow above the reservoirs has to be *called* for, otherwise it is kept in the reservoirs and becomes storage water. In SD-SRPM, the natural river flow is allowed to go negative as each diversion calls for its full-

supply. The storage call then becomes the most negative flow in that stretch of river. Since the SRPM indicator file indicates that most diversions within the river sections between reservoirs have the same reservoir call order, this method of calculating reservoir calls simplifies calculations. The called for water is then released from the reservoir to meet irrigation demands in the regulated flow structure. The following subsections describe how various model structures within SRPM were incorporated in the system dynamics framework.

Modeling Reservoirs

One of the fundamental modeling concepts included in both SRPM and SD-SRPM is the assignment of pools within reservoirs. There are five pool levels assigned to each reservoir per month in the SRPM model. These five pool levels create four pools within the reservoir as seen in Figure 4.1. Pool level one represents the greatest volume that can be stored within the reservoir during any give month. Pool level five represents the maximum drawdown of the reservoir that can occur in any month. Pool level five cannot be set below a reservoir's dead storage level. If level five is set at zero that means that the reservoir can be completely emptied to meet downstream demand if necessary. When the reservoir fills, the pools fill sequentially from bottom to top. The lowest pool must be full before the next pool can store water. When water is called from the reservoir, the uppermost pool with some content must be completely drained before water can be released from the next pool. When a downstream demand requires storage water, the *call* is met according to the assigned *call order* for that demand. The call order contained in SRPM's indicator file directs that the demand be met from upstream reservoirs in a prescribed order. Based on the call order, the program seeks to release

water from the first pool within the first prescribed reservoir. If there is adequate water in that pool to meet the demand, the water is released from storage and the call ends. If more water is needed, the program goes to the next reservoir in the call order and checks whether any storage is available in the reservoir's first pool. Assuming there is no storage in Pool 1 in the second reservoir and there are only two reservoirs in the call order, the program goes back to reservoir 1 and drafts water from Pool 2. If the demand is still not met, the program proceeds according to the call order pool by pool until the demand is met or both reservoirs' fourth pools are empty. The program cannot draft water to meet downstream demand below Level 5 in any reservoir. Table 4.1 shows call orders within the Snake System.

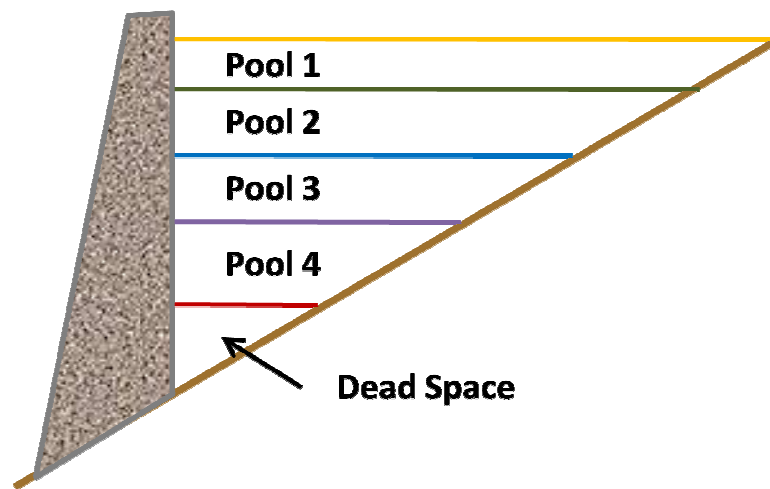


Figure 4.1 Side View of How Pool Levels are Represented in SRPM and SD-SRPM

The pool levels are used to calibrate the SRPM model to the present conditions, based on end of month (EOM) reservoir content and streamflow at specified locations. The calibration is based on the last 25 years of measured data from 1981-2005. An

example of how pool levels in the Palisades Reservoir vary on a monthly basis is shown in Figure 4.2.

Table 4.1 Call Orders in the Snake River Basin as Represented in SD-SRPM

River	Call Order	Reservoirs
Henry's Fork	Call 3	Island Park
	Call 5	Island Park, Henry's Lake
	Call 26	Grassy Lake
Snake River	Call 8	Palisades, Jackson Lake
	Call 14	American Falls, Palisades, Jackson Lake
	Call 27	Lake Walcott, American Falls, Palisades, Jackson Lake
	Call 28	American Falls, Palisades, Jackson Lake, Lake Walcott
Blackfoot River	Call 30	Blackfoot, Palisades, Jackson Lake
Boise River	Call 19	Arrowrock, Anderson Ranch, Lucky Peak
Payette River	Call 23	Cascade, Deadwood

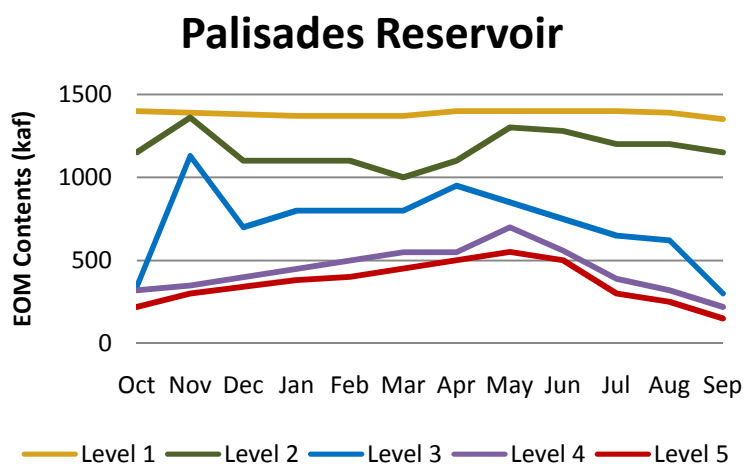


Figure 4.2 Pool Levels within the Palisades Reservoir

Figure 4.3 represents the SD-SRPM model structure by which water is drafted from the Palisades Reservoir and Jackson Lake to meet irrigation demand represented by Reservoir Call Order 8. The red auxiliaries represent pools in the Palisades Reservoir

and the black auxiliaries represent pools in Jackson Lake, starting with pool one at the top and pool 4 at the bottom. The left column contains the calculated volume in each pool. The middle column represents the demand carried to the next pool level, and right column represents the amount drafted from each pool to meet the demand at a given timestep. The code applied to calculate the Jackson Lake Pool 1 auxiliaries are shown below:

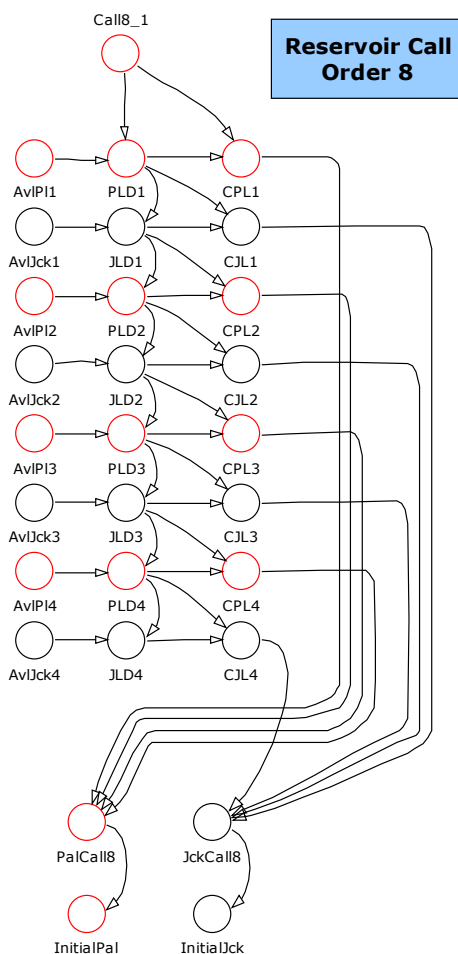


Figure 4.3 Example of Call Order 8 from SD-SRPM

- $AvIjck1 = (\text{Storage available in Jackson Lake Pool 1})$
- $JLD1 = PLD1 - \text{IF}(AvIjck1 > PLD1, PDL1, AvIjck1)$
- $CJL1 = PLD1 - JLD1$

The final amount drafted from each reservoir is the sum of the draft from each pool and is calculated at the bottom of the call order as follows, respectively for Palisades Reservoir and Jackson Lake:

- $PalCall8 = CPL1 + CPL2 + CPL3 + CPL4$
- $JckCall8 = CJL1 + CJL2 + CJL3 + CJL4$

Modeling Diversions

Diversions (D) in the SD-SRPM reservoir operation structure are modeled as a flow out of the main channel of the river. All diversions within a reach have been summed into a composite diversion demand (DD). Each reach that contains a diversion has been broken into an upstream reach and downstream reach. If reach number, N , has a diversion, the upstream reach is labeled *ReachNa* and the downstream reach is labeled *ReachNb*. Based on the reservoir calls made in the natural flow structure, a certain quantity of flow enters reach N (NF). There may also be a reach gain (RGN) within that reach. The diversion demand (DD) is based on model input and is read into the model through input auxiliaries. The diversion is then calculated by the following steps:

- 1) Calculate available flow, AF:

If $RGN > 0$, Then $AF = NF$, (RGN is added to the reach after diversion)

If $RGN < 0$, Then $AF = NF + RGN$, (AF cannot be < 0 kaf/month)

- 2) Calculate the amount diverted (D) from the river:

If $DD \leq AF$ Then $D = DD$

If $DD > AF$ Then $D = AF$

It should be noted that the river is allowed to go dry according to this logic. Historically, rivers in the Upper Snake have gone dry (Fiege, 1999). However, most of the time the river is prevented from drying by minimum flow requirements described in the description of assigned flows. Should the Endangered Species Act (ESA) require a certain flow be maintained in a reach, the diversion could be limited to that minimum flow, however at this stage such a procedure has not been introduced. Once the diversion (D) is calculated, the next step is to calculate the return flow.

Figure 4.4 shows the structure for Reach 31 within SD-SRPM. Reach 31 represents the Snake River between Irwin and Heise, upstream of the Eagle Rock Canal. Diversion 129 (D129_1) represents the sum of pump diversions from Heise to Irwin. The blue flows represent the Snake River, the green flow represents the diversion canal, and the cyan auxillary (RG_31) represents the reach gain. The code for each of the auxillaries is described below:

- $\text{Reach31a} = \text{Reach 29} + \text{IF}(\text{RG_31} < 0 \ll\text{kaf}\gg, \text{RG_31}, 0 \ll\text{kaf}\gg) / 1 \ll\text{month}\gg$
- $\text{Avail31} = \text{IF}(\text{Reach31a} > 0 \ll\text{kaf/month}\gg, \text{Reach31a}, 0 \ll\text{kaf/month}\gg) * 1 \ll\text{month}\gg$
- $\text{DR31_1} = (\text{Demand in Reach 31})$
- $\text{Div 31} = \text{IF}(\text{DR31_1} < \text{Avail31}, \text{DR31_1}, \text{Avail31}) / 1 \ll\text{month}\gg$
- $\text{SR31} = \text{DR31_1} - \text{Div31} * 1 \ll\text{month}\gg = (\text{Shortage in Reach 31})$
- $\text{P30} = \text{IF}(\text{SR31} > 0 \ll\text{kaf}\gg, 1 - (\text{SR31} / \text{DR31_1}), 1) = (\text{Percentage of demand delivered})$

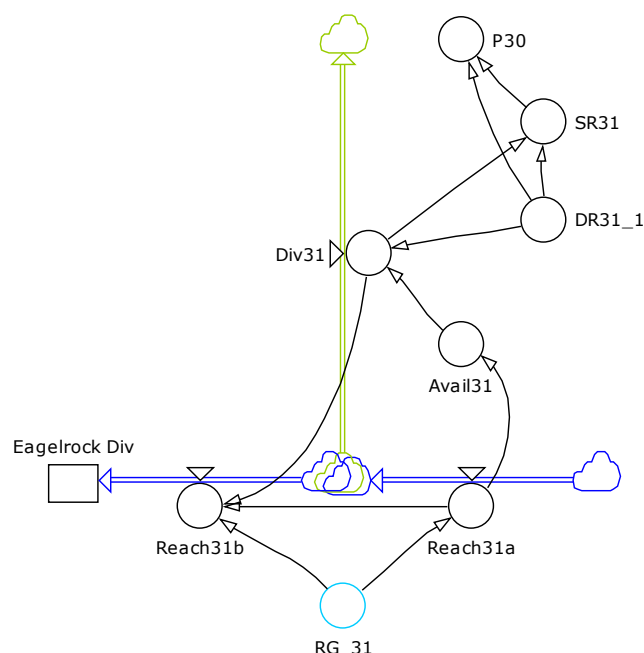


Figure 4.4 SD-SRPM Diversion Calculation Structure

Modeling Return Flow

Return flow (RF) is the quantity of diverted water that returns to the river downstream of the diversion point through drainage canals. Return flow occurs through overland flow during flood irrigation, failure to utilize all water in the main canal system, and because of near surface groundwater seepage into drainage canals or nearby streams from lateral flow in the shallow aquifer. In SRPM, each diversion is provided up to 10 lag factors to calculate the return flow. Although SD-SRPM calculates the amount diverted using a composite of all diversion demand within a reach, SD-SRPM calculates the return flow based on each diversion entity. The first lag factor represents how much of the diversion will return to the river within the month of the diversion. The second lag factor represents how much of the diversion will then return to the river the next month and so forth for the remaining lag factors. In addition to containing lag factors, the

indicator file also directs the return flow from each diversion to a given downstream reach. Return flow may not necessarily return to the same river from which it is diverted. Return flow to a river other than the source usually occurs when two rivers flow parallel to one another for some distance as is the case with the Henry's Fork and Teton rivers, as well as the Blackfoot and Snake rivers. In some cases, SRPM allows water to return to the reach from which it was extracted. At the locations where this occurs, SD-SRPM returns the flow to the next downstream reach, otherwise SD-SRPM has maintained the lag factors and return flow locations included in SRPM.

Div	Return Reach	RF 1	RF 2	RF 3	RF 4	RF 5
81	17	3%	3%	3%	3%	3%
90	21	50%	32%	0	0	0
91	19	3%	3%	3%	3%	3%
100	19	12%	3.60%	1.10%	0.3%	0

$$\text{July Return} = \begin{array}{c} \text{Fac} \\ 0.120 \\ 0.036 \\ 0.011 \\ 0.003 \\ 0.000 \end{array} \begin{array}{c} \text{D100} \\ 120 \\ 110 \\ 50 \\ 15 \\ 0 \end{array} \begin{array}{c} \text{Month} \\ \text{July} \\ \text{June} \\ \text{May} \\ \text{April} \\ \text{March} \end{array} = \begin{array}{c} \text{RF19} \\ 14.40 \\ 3.96 \\ 0.55 \\ 0.05 \\ 0.00 \end{array}$$

Sum 18.96 kaf

Figure 4.5 Calculation Method for Determining Return Flow

The procedure for calculating return flows is as follows. The table at the top of Figure 4.5 represents 5 return flow factors, *RF*, for 4 diversions (81, 90, 91, 100) on the Teton River. The return flow from each diversion is assigned a reach. For example, diversion 81 return flow is directed to reach 17. Below the table in Figure 4.5 is the procedure for calculating the return flow from diversion 100 to reach 19 for some year in the month of July. The five return flow factors are placed in an array starting with return flow factor 1, *RF1*, and ending with return flow factor 5, *RF5*. The return flow array is then multiplied by an array of the previous five months of diversions starting with the

most recent diversion. The sum of the multiplied array is the amount of water that returns to reach 19 in July based on the last five month's diversions.

The model structure for the return flow calculations using delay auxiliaries is shown in Figure 4.6. Figure 4.6 represents Reach 60 and diversion 260, which represents diversions from the Burley Southside Canal. RF260 calculates the return flow in the due to diversions at the current timestep, RF260M1 calculates the return flow from the current timestep that will occur in the coming month, and RF260M2 calculates the return flow from the current diversion that will occur two months later. RF260DM1 and RF260DM2 are delay auxiliaries that delay the RF260M1 and RF260M2 by one and two months, respectively. The nodes below the return flow function that calculate diversions are similar to those described in the previous section for Reach 30:

- $D260_1 = (\text{The demand for diversion entity 129})$
- $Irr260 = D260_1 * P60 = (\text{Demand} * \text{Percentage of demand delivered})$
- $RF260 = Irr260 * 0.07 = (\text{Current diversion} * 7\%)$
- $RF260M1 = Irr260 * 0.02 = (\text{Current diversion} * 2\%)$
- $RF260M2 = Irr260 * 0.02 = (\text{Current diversion} * 2\%)$
- $RF260DM1 = DELAYPPL(RF260M1, 1\langle\langle\text{month}\rangle\rangle, 0\langle\langle\text{kaf}\rangle\rangle)$
- $RF260DM2 = DELAYPPL(RF260M2, 2\langle\langle\text{month}\rangle\rangle, 0\langle\langle\text{kaf}\rangle\rangle)$

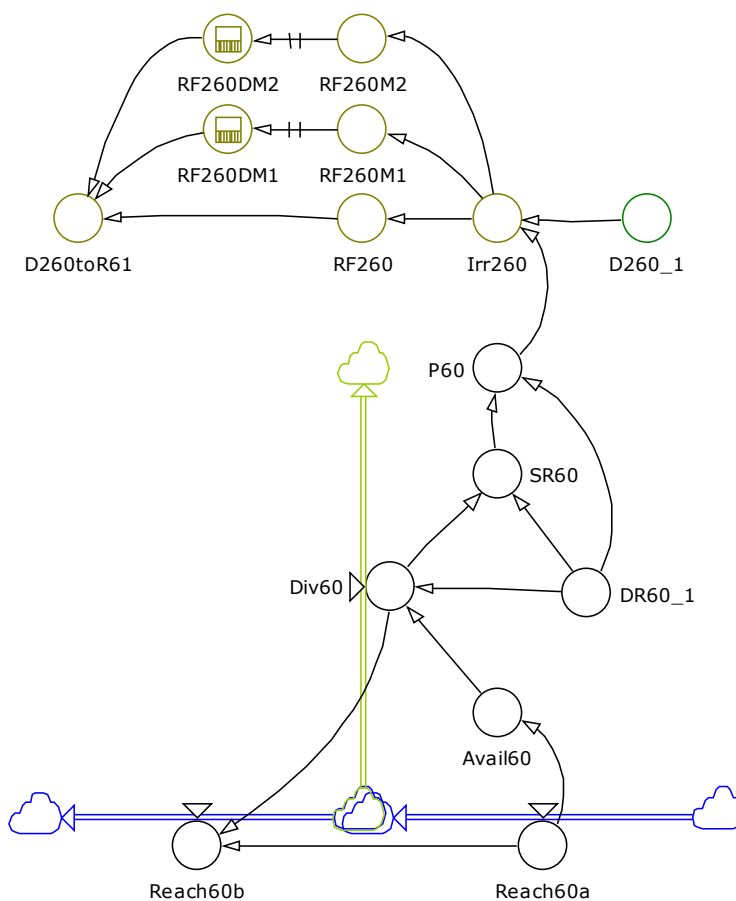


Figure 4.6 SD-SRPM Return Flow Calculation Structure

Modeling Assigned Flows

Assigned flows are placed on river reaches in SRPM so that adequate flow is maintained at those locations to provide for the aesthetic, ecologic, and recreational needs of the river and communities that utilize the river. Not all reaches have an assigned flow, because on many rivers there are critical reaches where managers have found that if they can maintain flow at a prescribed level then the upstream and downstream flow requirements will be met. In SRPM, these critical reaches are assigned four levels of flow corresponding to the four reservoir pools. For example, if storage is available in pool level 2 then storage will be released to meet the level 2 flow requirement. If storage

is not available in pool 2, but is available in pool 3, then water will then be released from the reservoir to meet the flow level 3 requirement. The level of flow assigned to each level must be either equal or progressively smaller from level 1 to level 4. SRPM assigns minimum flows in the second loop such that the highest level of flow possible is released based on available storage. Since the loop structure of SRPM was not maintained in SD-SRPM, it was decided to calculate the minimum flow requirement based the beginning of month pool level. The minimum flow is then added to the reservoir call and released if available.

Figure 4.7 represents the model structure for calculating a minimum flow call for a Level 1 minimum flow requirement based on the level of the Palisades Reservoir at the end of the last month (LevelPal). The same formulas are used for calculating the required flow for the other levels. Although this structure is based on Reach 49, the same calculation could be applied to any other reach with a minimum flow requirement. The blue flow represents reach 49 in the natural flow structure, while the purple auxiliaries calculate the minimum flow requirement. The code within each auxiliary is as follows:

- $1MF49 = (\textit{Minimum flow requirement level 1})$
- $RF40L1 = \text{IF}('1MF49' > \text{Reach49} * 1\langle\langle\text{month}\rangle\rangle, '1MF49' - \text{Reach49} * 1\langle\langle\text{month}\rangle\rangle, 0\langle\langle\text{kaf}\rangle\rangle) = (\textit{Flow needed to meet Level 1})$
- $\text{ReqF49} = \text{IF}(\text{LevelPal} = 1, RF49L1, \text{IF}(\text{LevelPal} = 2, RF49L2, \text{IF}(\text{LevelPal} = 3, RF49L3, RF49L4))) = (\textit{Minimum flow requirement})$

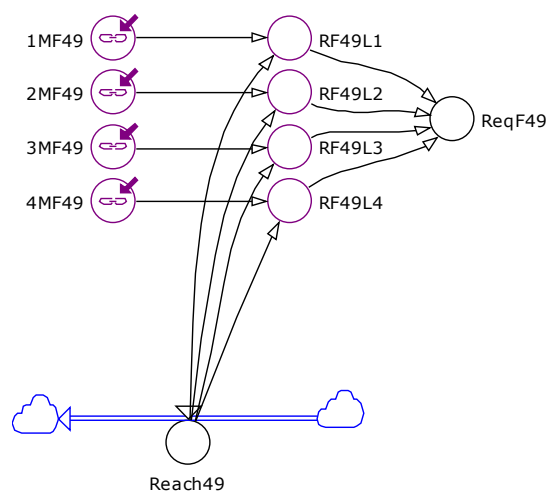


Figure 4.7 SD-SRPM Required Flow Structure

Modeling Flood Control Operations

Flood control is carried out in the third loop of the SRPM model, based on an empirical flood release curve developed by the staff at IDWR. An example of the flood release curves for Palisades Reservoir are shown in Figure 4.8. Historical forecasts are then input into the model through the indicator file and flows released in the appropriate month, based on historical forecasts. In the third loop, SRPM releases the calculated amount and then checks to see if downstream flooding would have occurred. If flooding would have occurred, SRPM then releases flow earlier in the year until maximum release limitations are met. This methodology of redistributing flow does not work in SD-SRPM. Therefore, MODSIM flood operation curves from the SRBM model (provided by USBR) were applied using the hydrologic states developed in the reach gain distribution method discussed in *Chapter 6*. The MODSIM flood operation curves for Palisades using SD-SRPM are shown in Figure 4.9.

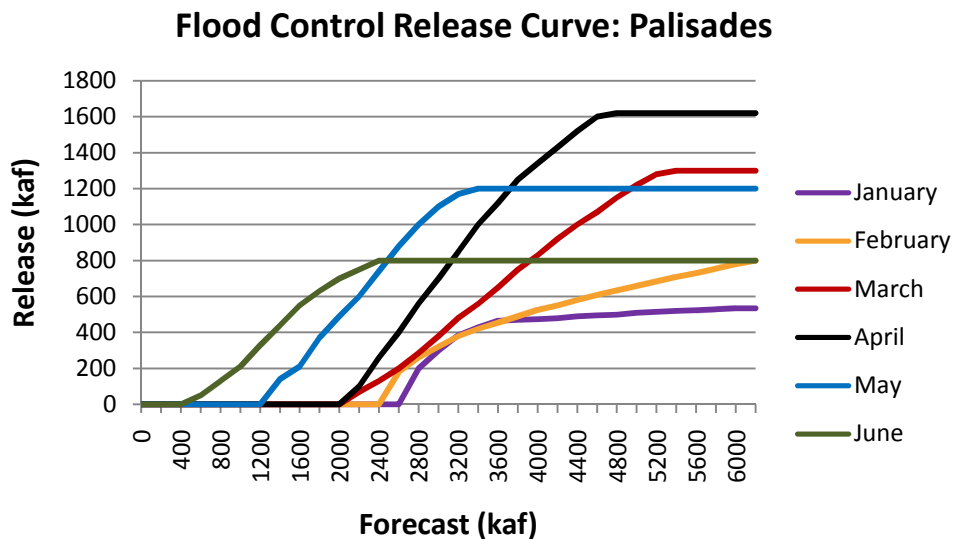


Figure 4.8 Flood Control Release Curve for Palisades Reservoir as Determined by IDWR for SRPM

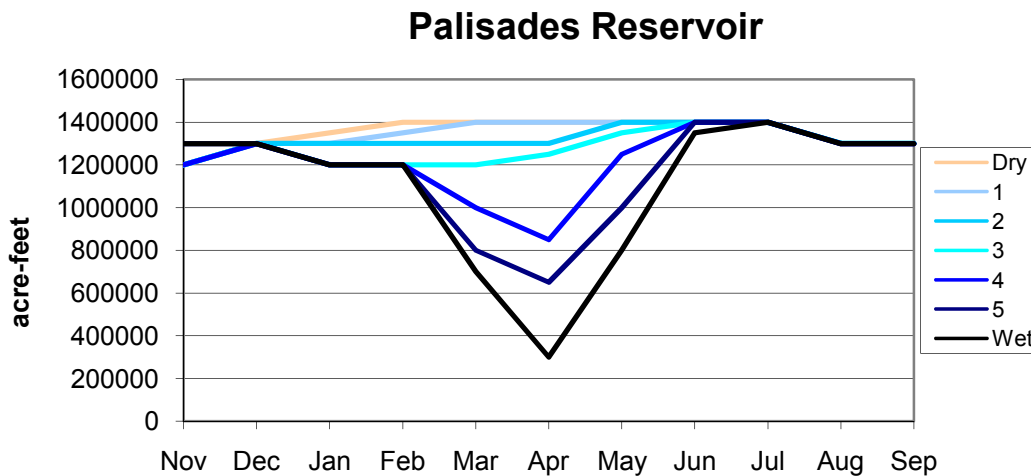


Figure 4.9 SD-SRPM Flood Control Curves

Modeling Reservoir Evaporation

Reservoir evaporation is modeled in SRPM using an empirical relation, based off reservoir historical content. Since this is a small value relative to overall water consumption in the Snake River Plain, and the historic relationship of reservoir pool level

to evaporation rate may change significantly under climate change it was decided not to include a calculation of reservoir evaporation in the first version of SD-SRPM.

Modeling Interbasin Transfers

There are five major canal structures in the SRPM model. Four of these canals (the Crosscut Canal, the Eagle Rock Canal, Clark's Out, and Reservation Canal) transfer flow from one subbasin to the next. The fifth canal, the New York Canal, provides for both irrigation and the filling of Lake Lowell. The New York Canal diverts flow from the Boise River.

Two of the transbasin canals, the Eagle Rock Canal and Clark's Out, are modeled in SRPM as diversions with a return flow factor of 100% in the first month. The Eagle Rock Canal transfers water from the South Fork of the Snake River below Heise to Reach 77 of Willow Creek below Ririe Reservoir. Clark's Out transfers water from Gray's Lake, located in the Willow Creek watershed above Ririe Reservoir, to the Blackfoot Reservoir on the Blackfoot River. Two transbasin canals, the Crosscut and Reservation canals, are modeled dynamically in SRPM so that surface water storage in Island Park Reservoir called by diversions on the Teton River below St. Anthony are routed down the Crosscut Canal, while storage water called from Palisades and Jackson Lake is routed to the Blackfoot River for diversion by the Fort Hall Main Canal and Fort Hall North Canal. In the natural flow structure of SD-SRPM, no water is routed down these transbasin canals since I understand that canals on the Teton River and Blackfoot River do not have natural flow rights in the Snake River. If natural flow within the Teton River and Blackfoot River cannot meet demand, water is called from storage and routed through the

transbasin canals to meet the demand. It should be noted that while New York Canal diversions are modeled, SD-SRPM does not model Lake Lowell operations.

Groundwater Modeling – SRPM

As mentioned in *Chapter 2*, the profound groundwater/surface water interaction between the Snake River and the East Snake Plain Aquifer (ESPA) is the source of Idaho's most recent water resource controversy. The SRPM model originally calculated this interaction using a linear model by reach (Idaho Water Resources Board, 1972). For example, aquifer discharge (or reach gain) to the Snake River in the Buhl to Lower Salmon Falls reach was calculated as:

$$\text{Gain} = 0.301 * x + 2465.5 \quad (\text{units, kaf})$$

where, x = sum of monthly flow in:

- 1) the Big Wood River below Magic Reservoir
- 2) the Little Wood River near Richfield
- 3) the Milner-Gooding Canal
- 4) the Northside Canal

While this method was somewhat crude, it provided a basis for accounting for the surface water irrigation impact on the reach gain. It should be noted that the gain is calculated in a preprocessing step based off historic records. This method of calculating aquifer recharge has been dropped in SD-SRPM for a dynamic simulation of groundwater impacts using response function factors from the Enhanced Snake Plain Aquifer Model (Cosgrove et al., 2006).

Groundwater/surface water interactions have not been modeled dynamically within the western Snake River Plain. The reach gains along the Boise and Payette rivers within the plain are taken directly from the SRPM reach gain file.

Brief History of the East Snake Plain Aquifer Model and Response Functions

In 1974, IDWR developed a groundwater model, which was converted into the USGS groundwater model MODFLOW in 1999 (Johnson et al., 1999b). This groundwater model is referred to as the East Snake Plain Aquifer Model (ESPAM). Later, Cosgrove et al. (2006) updated this model. The new model is called the Enhanced Snake Plain Aquifer Model. This model contains surface/water groundwater interactions along the Snake River. An Excel spreadsheet interface, the East Snake Plain Aquifer Groundwater Rights Transfer Spreadsheet for the Enhanced East Snake Plain Aquifer Model, was developed to evaluate the impact of water rights transfers in the basin (Cosgrove et al., 2007). This spreadsheet can be used to develop response functions that determine how a recharge or extraction of groundwater at any given location in the model will affect groundwater/surface water interactions along eleven reaches in the Snake River (Cosgrove and Johnson, 2005). Dr. Gary Johnson, in 2010, updated this spreadsheet, for purposes of this study, to run on a monthly timestep. The use of response functions calculated from a numerical groundwater model have been found to provide a computationally robust method of modeling the Snake River Aquifer for water resources planning purposes. More detail on the validity of using superposition to evaluate groundwater/surface water interactions in the Snake River Plain can be found in research by Hubbell et al. (1997) and Johnson and Cosgrove (1999). Miller et al. (2003) linked response functions to SRBM in a study on the potential to increase spring

discharge through artificial recharge. Their results compared well to a similar study by IDWR (1999) that used ESPAM to calculate the same interactions.

Linking SD-SRPM Dynamically to the East Snake Plain Aquifer

SD-SRPM was dynamically linked to the East Snake Plain Aquifer (ESPA) through response function. These response functions only represent the changes in groundwater/surface water interactions due to irrigation. At this point, the model does not account for non-agricultural groundwater/surface water interactions such as changes in recharge caused by changes in non-irrigated vegetation and changing precipitation patterns caused by climatic change. The following sections describe the calculation procedures necessary to link SD-SRPM with the ESPA.

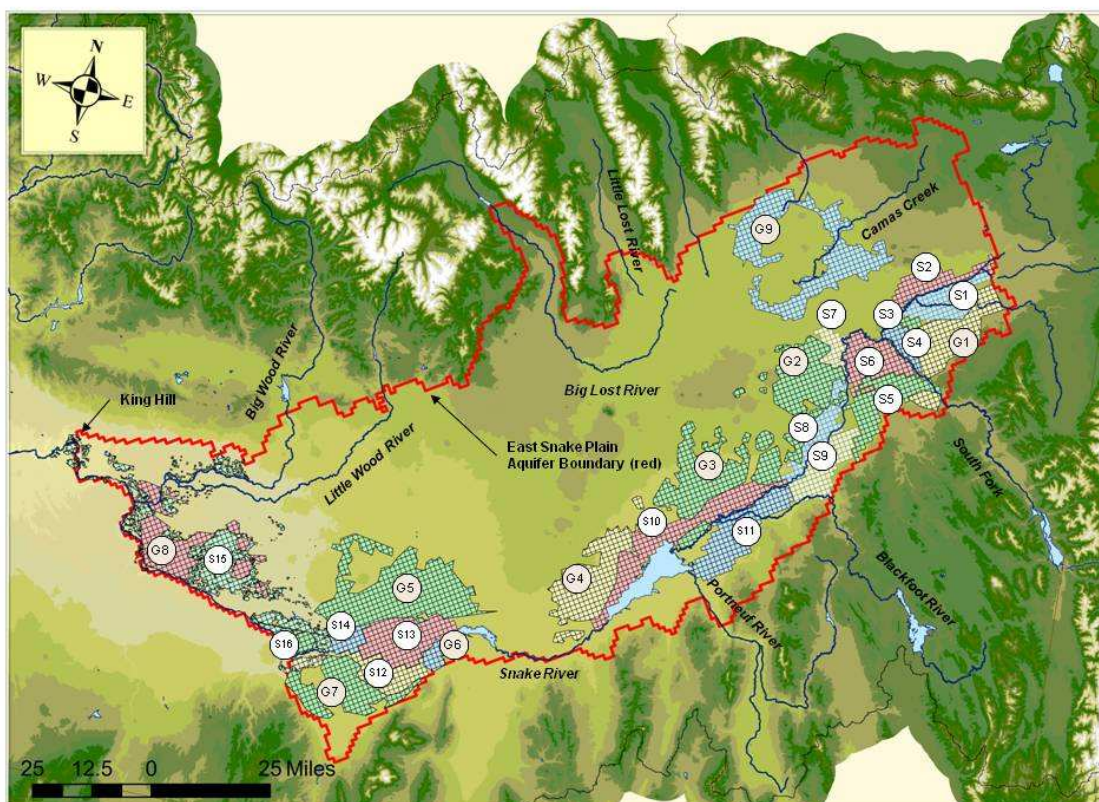


Figure 4.10 Map of Groundwater (G) and Surface Water (S) Irrigation Entities Described in Table 4.2

Modeling Groundwater Recharge in SD-SRPM

The impact of changes in surface water diversion on groundwater recharge is calculated based on response functions calculated from 16 surface water entities representing aggregated diversions. The impact of groundwater pumping within the Snake Plain is represented by 9 groundwater irrigation entities, which are modeled separately from SD-SRPM in a model called GWSIM. Because the amount of water pumped from the aquifer is not currently influenced by surface water availability, there was no need to dynamically link the models. Although the models have not been combined, they could be at a future date, should conjunctive management require groundwater users to reduce pumping in response to surface water availability. Figure 4.10 shows the location and identity number for each irrigation entity for which a response function was calculated. Table 4.2 describes the irrigated region within each irrigation entity and the grid cell at which the response functions were calculated in ESPAM.

A surface water entity represents a regional conglomeration of land served by a group of canal companies. The determination of how to aggregate canal companies was based on the need to include canal companies with significant overlap and water transfer in the same group while maintaining the original diversion groups within SRPM. The aggregation of canal companies was based on two datasets (Gilliland, 2002; Contor, 2010). The amount of surface water irrigated land within each entity was based on a GIS-dataset provided by Contor (2010). Table 4.1 also lists which diversions in the SD-SRPM model are attached to each surface water entity and includes the estimated land area irrigated in each region.

Table 4.2 Irrigation Entities in SD-SRPM and Location of the ESPAM Grid Cells Used to Generate the Response Functions for each Entity

Entity	ESPAM Row	ESPAM Column	Irrigated Area (acres)	% Mixed Source	Diversions
Surface Water Entities					
S1 Henrys Fork	57	189	46,720	0.05	30,35,40,60,80,90,91,100,110
S2 Egin Bench	52	187	27,160	0.30	45,50,51,70
S3 Rexburg	59	180	6,970	0.30	120
S4 Reid	63	178	20,400	0.30	160,165
S5 Harrison	72	169	70,800	0.30	135,175
S6 Burgess	63	170	56,470	0.30	145
S7 Butte & Market	57	163	19,130	0.95	170
S8 New Sweden	72	155	37,500	0.30	175,180
S9 Idaho	80	153	49,370	0.30	190,220
S10 Aberdeen	82	119	42,700	0.70	230,240,242
S11 Blackfoot	87	131	49,760	0.30	248,249,255
S12 Burley	88	51	42,770	0.30	260
S13 Minidoka	82	57	64,050	0.30	270,271
S14 A&B	78	46	24,350	0.95	285
S15 Northside	52	24	240,730	0.3	290,300
S16 Milner	80	36	14,840	0.5	310
Groundwater Entities					
G1 Upper Teton	65	187	67,180		
G2 NW Idaho Falls	62	155	76,620		
G3 Upper Springfield	74	131	109,980		
G4 Upper Aberdeen	85	99	92,010		
G5 Upper Minidoka	72	59	151,560		
G6 Declo	88	63	10,170		
G7 Oakley	86	41	82,450		
G8 Lower Northside	47	21	56,290		
G9 Mud Lake	36	164	127,120		

The calculation of recharge (RG) from surface water entities is critical in correctly determining recharge to the aquifer. There are 6 parameters that affect the quantity of recharge: the quantity of return flow (RF), the quantity of water diverted (D), the depth of precipitation (P), the quantity of canal seepage (CS), the quantity of groundwater pumped in mixed source areas (GP), and the depth of evapotranspiration (ET). Based on ESPAM documentation, canal seepage is only estimated for the Aberdeen diversion (242), Milner-

Gooding diversion (290), and the Northside diversion (300). canal seepage losses of 50%, 30%, and 30% were applied for these canals (Contor, 2004a). It was also assumed that groundwater pumping (GP) occurs only when the surface water application rate falls below ET. Groundwater is then pumped to meet the deficit only within the mixed source portion of the surface water entity. The determination of the fraction of mixed source pumping is based on Contor (2004b) and shown in Table 4.2. The recharge calculation is made in the following steps:

$$SW = ((D-RF)-CS)/A_{sw}, \quad (\text{Equation 4.1})$$

where, A_{sw} = irrigated area within surface water entity

SW = surface water application rate

$$RG_1 = SW+P-ET \quad (\text{Equation 4.2})$$

where, RG_1 = initial recharge calculation

$$\text{If } RG_1 > 0 \text{ then } RG = RG_1 + CS \quad (\text{Equation 4.3a})$$

$$\text{If } RG_1 < 0 \text{ then } RG = CS, \text{ and } GP = RG_1 * GW_f \quad (\text{Equation 4.3b})$$

Where GW_f = proportion of mixed source within the surface water entity

The structure for the recharge calculation for surface water entity 10 (S10, see Figure 4.10) in SD-SRPM is shown in Figure 4.11. In Figure 4.11, auxiliary *SWdepthAber* represents Equation 4.1, auxiliary *RechargeAber* represents Equation 4.2, and auxiliary *AberRecharge* represents Equation 4.3.

To calculate Equation 4.1, which quantifies the depth of surface water applied in the field, the amount of surface water return flow for each diversion entity and the canal seepage for the Aberdeen-Springfield Canal must be removed from the application depth.

The auxiliaries used to calculated Equation 4.1 for S10 are described below:

- $Irr230_1 = Irr230 = \text{percent of demand, } D230, \text{ available for diversion}$
- $Irr240_1 = Irr240 = \text{percent of demand, } D240, \text{ available for diversion}$
- $Irr242_1 = Irr242 = \text{percent of demand, } D242, \text{ available for diversion}$
- $Ap\ 230 = 0.87 = 1 - \text{percent of summed return flow factors}$
- $Ap\ 240 = 0.936 = 1 - \text{percent of summed return flow factors}$
- $Ap\ 242 = 0.944 = 1 - \text{percent of summed return flow factors}$
- $DivAber = (Irr230_1 * Ap230) + (Irr240_1 * Ap240) + (Irr242_1 * Ap242)$
- $CanalLoss242 = Irr242_1 * CLFactorAberdeen = \text{Canal Seepage rate of the Aberdeen-Springfield Canal, which can be adjusted in using the brown slider bar in the upper left of Figure 4.11}$
- $Conversion_10 = 43,560,174 \text{ ft}^3 / 1 \text{ kaf}$
- $IrrigAreaAber = 1,860,237,200 \text{ ft}^2 = \text{area of surface water irrigated land in S11}$
- $SWdepthAber = (((DivAber - CanalLoss242) / 1 \ll \text{kaf} \gg * Conversion_10) / IrrigAreaAber)$

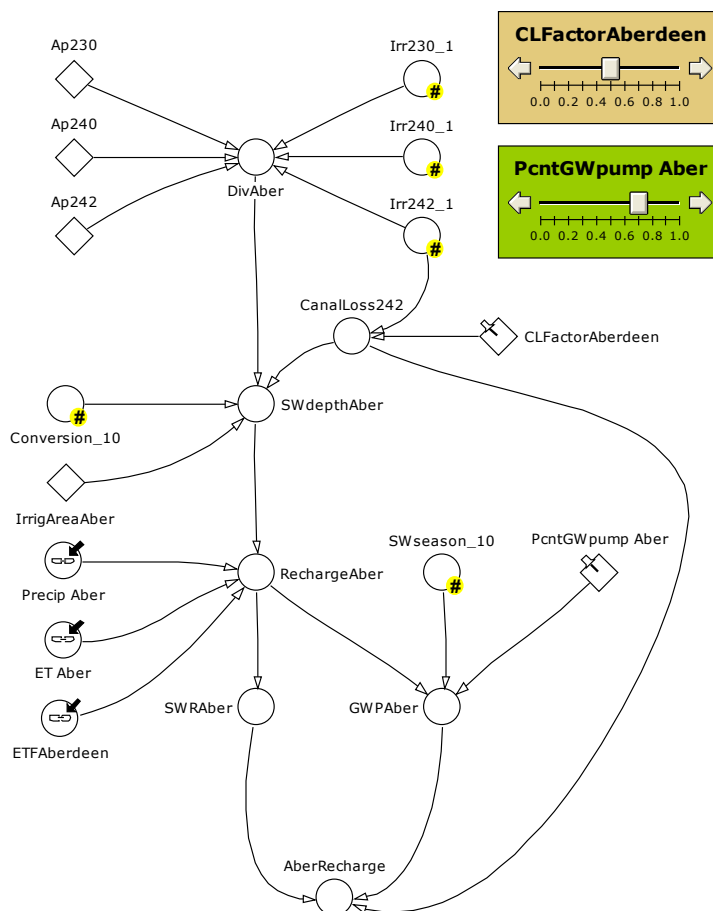


Figure 4.11 SD-SRPM Recharge Calculation Structure for S10 in SD-SRPM

The assumed irrigated area, *IrrigAreaAber*, and the canal seepage rate of 50% are gross approximations. The irrigated area should vary year to year based on forecasted supply (Pierce et al., 2010) and market factors. Also research by Contor (2004a) indicates that the canal seepage varies yearly based on diversion quantity and environmental factors. The uncertainty introduced by canal loss and irrigated area estimates could be quantified by a sensitivity analysis in future research through the use of slider bars.

The calculation of Equation 4.2 represented by *RechargeAber* auxiliary relies on input auxiliaries, as shown in Figure 4.11. The source of the data for these input

auxiliaries is described in the following subsection. The code for RechargeAber is as follows: $SWdepthAber + 'Precip\ Aber' - ('ET\ Aber' * ETFAberdeen)$, in which

- ‘Precip Aber’ = *depth of monthly precipitation within the irrigation entity*
- ‘ET Aber’ = *estimated monthly potential ET within the irrigation entity*
- ‘ETFAberdeen’ = *a reduction factor to estimate actual ET.*

Equation 4.3b indicates that if recharge is inadequate to meet crop water demand, the portion of the irrigation entities with supplemental groundwater pumping are allowed to extract water from the aquifer to meet crop water demand. The estimation of the percent of surface water users with supplemental groundwater supply is a source of uncertainty in the recharge estimates. Irrigation source estimates taken from ESPAM are discussed by Contor (2004b). The code and auxiliaries used to calculate Equation 4.3a and 4.3b are described as follows:

- $SWRAber = IF(RechargeAber > 0\langle\langle mm \rangle\rangle, RechargeAber, 0\langle\langle mm \rangle\rangle) =$
recharge from surface water applied in field
- $GWABer = IF(RechargeAber < 0\langle\langle mm \rangle\rangle AND SWseason_10 = 1,$
 $RechargeAber * 'PcntGWpump\ Aber', 0\langle\langle mm \rangle\rangle)$
- $AberRecharge = ((SWRAber + GWPABer) * IrrigAreaAber /$
 $Conversion_10) * 1\langle\langle kaf \rangle\rangle + CanalLoss242$

PcntGWpump Aber represents the ratio of surface water irrigated land with supplemental groundwater wells to total surface irrigated land in the irrigation entity. The value can be adjusted using the green slider bar in Figure 4.11. The value of *SWseason* is based on an input auxiliary that defines the irrigation system in a monthly binary file, such that groundwater pumping is allowed only during the growing season.

The impact of recharge or pumping from each surface water entity and groundwater entity is then calculated for six reaches within SD-SRPM for each irrigation entity in a manner similar to the return flow calculation, only the arrays multiplied for each response have 600 response factors to represent the accumulated impact of diversions over the last 50 years. Since the model includes effects from 9 groundwater entities and 16 surface water entities to 6 reaches in the Snake River, there are a total of 150 superimposed groundwater surface water interactions calculated at each timestep. The methodology in system dynamics for multiplying these arrays is referred to as an aging loop. The aging loop structure is shown in Figure 4.12 for the surface water entity 10 (S10, see Figure 4.11), which includes the Aberdeen-Springfield Canal. For the sake of space, Figure 4.12 only includes a calculation of groundwater/surface water interactions between S10 and Reach 23 and Reach 40. In the actual SD-SRPM model, the impacts at the other three reaches are also included. The code for the auxiliaries calculating surface water irrigation impacts from S10 on Reach 23 are as follows:

- $\text{RechargeSW10} = \{\text{AberRecharge}, 0\langle\langle\text{kaf}\rangle\rangle, 0\langle\langle\text{kaf}\rangle\rangle, \dots\} = \text{a } 600 \text{ unit array with current monthly recharge as the first component of array (AberRecharge is shown in Figure 4.11) all other values are } 0 \text{ kaf}$
- $\text{Initial Recharge SW10} = 600 \text{ unit array with values of } 0 \text{ kaf to initialize SW10RechargeHistory}$
- $\text{Aging Loop Aberdeen} = \text{FOR (a} = 1..599 \mid \text{SW10RechargeHistory[a]} * 1\langle\langle 1/\text{month}\rangle\rangle)$
- $\text{RFSW10R23} = \text{XLDATA("} \textit{(location of Excel Sheet with Response Function Factors)} \textit{")}$

- $ControlSW10R23 = ARRSUM(FOR(j = 1..600 | RFSW10R23[j] * (SW10RechargeHistory[j] / 1\langle\langle month \rangle\rangle))) + 'Recharge SW10'[1] * RFSW10R23[1]$ = this function multiplies the history of recharge array with the corresponding response function array for the current timestep
- $ASW10R23 = \{ \dots, 0\langle\langle kaf \rangle\rangle, 0\langle\langle kaf \rangle\rangle, ControlSW10R23 * 1\langle\langle month \rangle\rangle \} / 1\langle\langle month \rangle\rangle$ = a 600 unit array of 0 kaf, with ControlSW10R23 as final value
- $SW10R23 = ARRSUM(ASW10R23)$ = groundwater/surface water interaction between Surface Water entity 10 and Reach 23 for a given timestep

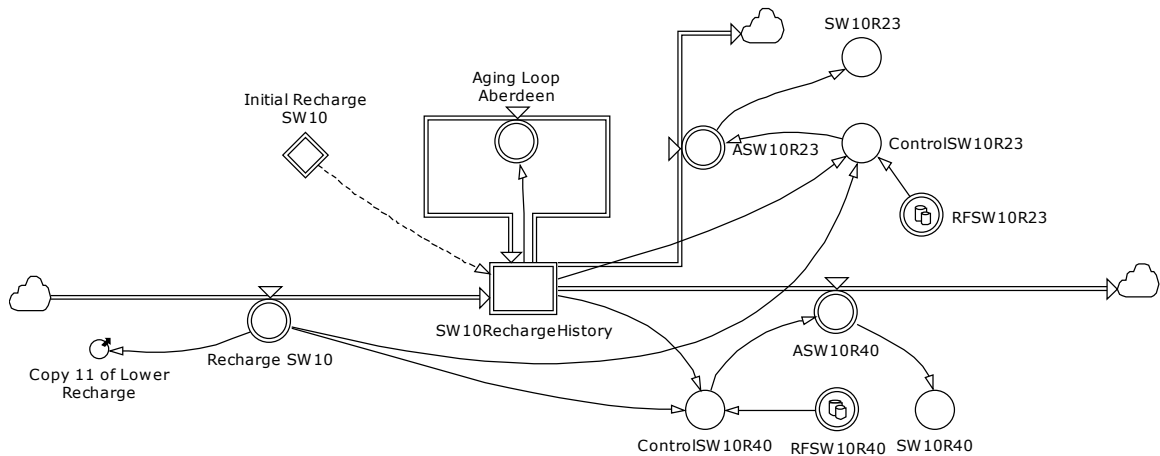


Figure 4.12 Aging Loop Structure Used in SD-SRPM to Calculate Groundwater/Surface Water Interactions for S10

In order to avoid a lagged aquifer response when calculating the present condition over the historic period, a wrapped sequence simulation was performed as suggested by Miller et al. (2003). The wrapped sequence simulation runs over a period of 104 years in which the first 52 years of data from 1928-1979 are simulated back-to-back, before

proceeding to finish simulation of the historic period ending in 2005. Flows from a projected period can then be run from the end of the historic simulation.

Determining the Parameters for the Recharge Calculation

In order to calculate irrigation recharge over the historic period, historic precipitation (P) and ET were needed. The historic P comes from the Hamlet and Lettenmier's (2005) 1/8th degree gridded dataset of precipitation and temperature developed from the NCDC Cooperative Observer network. Monthly potential evaporation from (PE) for bare soil from 2000 was extracted from an historic VIC run of the Variable Infiltration Capacity (VIC) hydrologic model (Liang et al., 1994) based on the same gridded dataset. The VIC model was calibrated to the Snake River basin by Jin and Sridhar (2010, unpublished). VIC PE is calculated using the Arno formulation Franchini and Pacciani (1991). The PE and P applied to each surface water entity was based on an average value of the gridded data points falling in each surface water entity.

An actual monthly ET (AET) dataset for 2000 was then provided by IDWR. The actual ET measurements were based on satellite imagery using METRIC analysis (Allen et al., 2007a, 2007b). Monthly ET reduction factors (ET_{rf}) were then calculated such that, $ET_{rf} = AET/PE$ for the year 2000. This reduction factor was then applied to VIC modeled PE over the historic period, to estimate AET. The AET dataset had a 30 meter pixel resolution. The average depth of AET within an entity was then applied to each irrigation entity.

Determining Non-modeled Groundwater Contributions from the ESPA to Six Reaches

One of the underlying assumptions of the SD-SRPM model, when considering groundwater/surface water interactions and climate change, is that only changes in recharge from surface water and groundwater from irrigation entities impact the aquifer. While the analysis covers most of the surface water irrigation in the plain, the impacts of surface water diversions near Mud Lake, within the closed basins to the north of the plain, from the Big and Little Wood rivers, and from the minor southern tributaries like the Portneuf River and Canyon Creek are not included. Also 20% of the groundwater irrigated areas within the basin are not included, some of this groundwater irrigated region is associated with the surface diversions missed, and/or small agriculture clusters. Also recharge due to precipitation from non-irrigated portions of the basin and seepage from tributary streams are not included within SD-SRPM currently. In order to estimate contributions to groundwater/surface water interactions not modeled, the average reach gain for the five reaches in the SRPM model that interact with the aquifer were calculated and subtracted from SRPM estimated contributions over the 1981-1990 period. The average monthly reach gain were then calculated over this period and became the base reach gain applied at all timesteps (see Table 4.3 for values). Future improvements to the model could be made by seeking to add all recharge contributions to the aquifer to SD-SRPM.

Table 4.3 Base Reach Gains (kaf) in Snake River along the East Snake Plain Aquifer

Month	Reach 23	Reach 40	Reach 49	Reach 57	Reach 59	blw Milner
October	-62.10	-51.05	-56.36	124.57	12.21	447.16
November	-54.61	-80.35	-58.93	126.31	8.45	400.62
December	-42.56	-90.88	-56.75	121.66	8.34	394.46
January	-35.14	-93.13	-52.26	118.87	8.37	390.09
February	-33.26	-85.87	-46.87	102.79	7.79	347.37
March	-35.16	-89.88	-47.44	117.42	5.15	389.84
April	-36.31	-98.44	-52.21	115.42	-4.41	375.87
May	-35.34	-111.24	-57.29	115.04	-11.75	380.68
June	-34.36	-80.85	-60.26	125.79	-33.90	361.53
July	-51.93	-81.75	-66.37	101.81	-5.73	362.74
August	-58.69	-68.60	-64.80	121.19	1.62	384.11
September	-62.46	-63.24	-61.29	118.41	9.96	418.56

CHAPTER FIVE: MODEL VALIDATION AND HISTORIC SHORTAGE ANALYSIS

There were three goals in constructing the SD-SRPM model: (1) replicate operations of the SRPM model, (2) dynamically link the model to the East Snake Plain Aquifer (ESPA), (3) develop a better means to quantify shortages in a climate impact analysis. In the first section of this chapter, SD-SRPM's capacity to replicate SRPM is validated. For this validation SD-SRPM was not linked to the ESPA through response functions. The second section shows that inclusion of response functions does not significantly alter the models performance. The third section then compares how changing demand from the SRPM's *planning shortage demand* to the *minimum full-supply demand* changes the estimation of shortages in the basin. As discussed in *Chapter 3*, the planning shortage demand assumes shortages occur when the average diversion between 1991-2005 cannot be met. A minimum full-supply demand shortage occurs when full-supply demand cannot be met. Full-supply demand was calculated based on the flat limb of the piecewise function in the diversion versus Surface Water Supply Index (SWSI) analysis of 1971-2005 diversions discussed in *Chapter 3*.

Model Validation

Since SRPM represents actual diversions between 1991 and 2005, the validation focuses on model comparison over this period. Validation is based on a comparison of SRPM and SD-SRPM end-of-month (EOM) reservoir content and monthly streamflow using the squared Pearson product moment correlation coefficient (r^2) calculated in Excel. Mean bias is also compared between SRPM and SD-SRPM. Mean bias is

calculated as the modeled (M) data minus the observed (O) data at each timestep (represented by SRPM results), divided by the number of timesteps (n), such that:

$$\text{mean bias} = \frac{\sum_{i=1}^n (M_i - O_i)}{n} \quad \text{Equation (5.1)}$$

In order for the reader to understand the accuracy of the model, SD-SRPM output is compared to observed values where available. Observed streamflow was downloaded from the USGS website (<http://waterdata.usgs.gov/id/nwis/rt>) and EOM was downloaded from the USBR website (<http://www.usbr.gov/pn/hydromet/arcread.html>). The location of key streamflow points referenced in the validation below are described in Table 5.1. It should be noted that SD-SRPM was not calibrated to match observed flows.

Table 5.1 Description of Streamflow Gages Used in Validation of SD-SRPM

USGS Gage Location	Gage #	Reach #	Elevation (ft)	Period of Record
Henry's Fork nr Rexburg	13056500	24	4,806	1909-2010*
South Fork nr Irwin	13032500	30	5,353	1935-2010
Snake River below Milner Dam	13087995	63	4,063	1992-2010*
Boise River near Parma	13213000	98	2,196	1971-2010*
Payette River near Horseshoe Bend	13247500	114	2,626	1906-2010
Payette River near Payette	13251000	119	2,138	1935-2010
Snake River near Weiser	13269000	120	2,086	1910-2009

* denotes incomplete 1991-2005 record

Table 5.2 compares EOM for all major reservoirs in the SRPM and SD-SRPM model above Brownlee Reservoir, and indicates a high level of agreement between the two models with almost all r^2 values greater than 0.80. Table 5.2 also compares modeled versus observed r^2 values for both SRPM and SD-SRPM. While r^2 values of modeled versus observed values, understandably, decline with SD-SRPM as compared to SRPM, SD-SRPM still provides a high level of correlation to historic observations. The decline of modeled versus observed r^2 values between the original SRPM and the new SD-SRPM model are shown in column 4 of Table 5.2. A negative value indicates an increase in

correlation from SRPM to SD-SRPM. The two points where correlation to observations improved significantly in SD-SRPM is flow at Milner Dam and flow into Brownlee Reservoir. Note that graphs of EOM and streamflow for all points in Table 5.2 are provided in Appendix C.

Table 5.2 Statistical Validation that SD-SRPM Replicates SRPM Operations over the Period from 1991-2005 where Mean Bias is Expressed in kaf

	SRPM vs. Observed r^2	SD-SRPM vs. SRPM r^2	SD-SRPM vs. Observed r^2	Decline in r^2	SD-SRPM vs. SRPM mean bias
Henry's Lake EOM	0.44	0.68	0.33	0.11	-0.49
Island Park EOM	0.88	0.74	0.71	0.17	5.22
Grassy Lake EOM	0.01	0.99	0.01	0	0.06
Reach 24	0.95	0.90	0.95	0	21.96
Jackson Lake EOM	0.90	0.83	0.88	0.02	-37.74
Palisades EOM	0.94	0.93	0.87	0.07	6.89
Reach 30	0.97	0.91	0.92	0.05	11.64
Ririe		0.78			-11.91
Blackfoot		0.82			-32.38
American Falls	0.94	0.77	0.81	0.13	251.08
Walcott	0.84	0.82	0.74	0.10	3.86
Reach 63	0.34	0.39	0.58	-0.24	
Anderson Ranch EOM	0.80	0.95	0.81	-0.01	-1.50
Arrowrock EOM	0.34	0.81	0.39	-0.05	-2.19
Lucky Peak EOM	0.57	0.82	0.50	0.07	-14.44
Lucky Peak out		0.92			4.80
Reach 98	0.96	0.86	0.92	0.04	-3.45
Lake Cascade EOM	0.84	0.85	0.73	0.11	-33.41
Deadwood EOM	0.87	0.92	0.81	0.06	-1.17
Reach 114	0.98	0.92	0.93	0.05	-8.23
Reach 119	0.98	0.93	0.93	0.05	3.01
Brownlee In	0.64	0.65	0.87	-0.23	-186.42

Figure 5.1 provides a graphical representation of how both SD-SRPM and SRPM compared to observed EOM and end of system flow for the largest reservoirs on the South Fork of the Snake River, the Henry's Fork of the Snake River, the Boise River, and the Payette River. Appendix C contains a comparison of SD-SRPM and SRPM EOM content at American Falls, the largest reservoir on the mainstem of the Snake River.

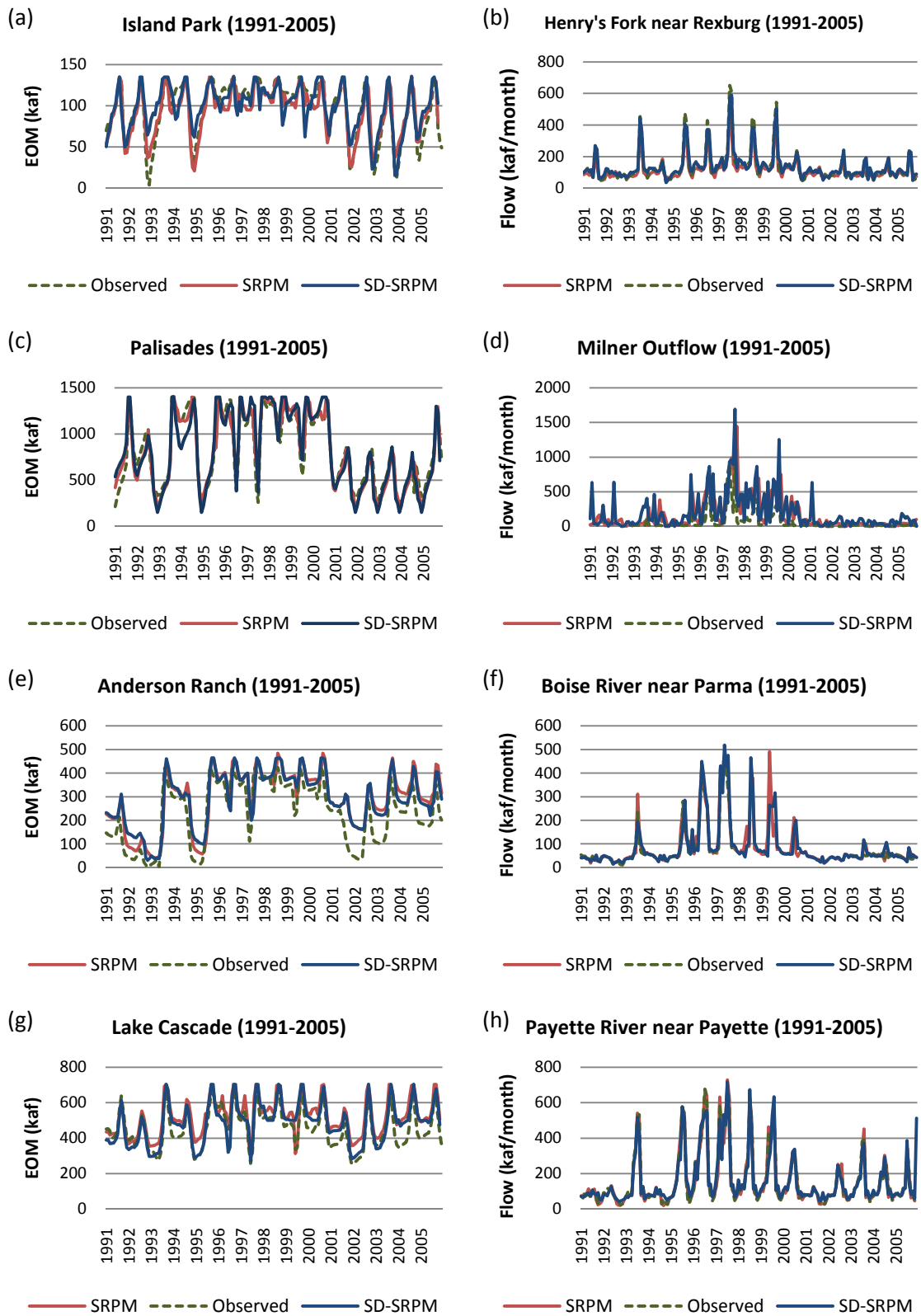


Figure 5.1 Comparison of SD-SRPM, SRPM, and Observed Values

The most significant difference between SD-SRPM and SRPM is the way minimum flow requirements are modeled. In SRPM, minimum flow demands are met reach by reach after natural flow meets irrigation demand. In SD-SRPM, natural flow above the reservoirs is released with storage water and minimum flows in the same timestep based on the previous month's EOM. In general, this may cause excess water to be released from storage, which may be the reason for the large positive bias in American Falls when comparing SRPM with SD-SRPM in Table 5.2. A careful calibration of minimum flow levels in SD-SRPM would probably improve SRPM and SD-SRPM correlation.

Validation of SD-SRPM Being Linked to the East Snake Plain Aquifer through the Use of Response Functions

When the SD-SRPM model is linked to the aquifer with response functions from the groundwater and surface water irrigated regions (which for comparison in this section of the chapter will be referred to as SD-SRPM-GW), very little change in the overall performance of the model is observed (see Table 5.3). Typical declines in r^2 correlation are about 0.01. Note, however, that performance of the model improves at Brownlee. Since there is almost no change in reservoir operations above Milner, it must be that the variance in the significant groundwater interaction below Milner Dam is captured better in SD-SRPM when it is linked with the aquifer. By linking SD-SRPM dynamically to the aquifer, this model can now be used to study issues related to conjunctive management. For example, the model could be used to study how changes in recharge from surface water irrigation, groundwater pumping, or managed recharge, based on CAMP scenarios,

would affect river/aquifer interactions and flows at C.J. Strike and Brownlee reservoirs, which are critical reservoirs for hydropower generation in the basin.

Table 5.3 Statistical Validation of SD-SRPM with Response Functions

	SD-SRPM-GW vs. SRPM r^2	SD-SRPM vs. SRPM r^2	SD-SRPM vs. Observed r^2	SD-SRPM-GW vs. Observed r^2	Decline Observed r^2
Henry's Lake EOM	0.69	0.68	0.33	0.29	0.04
Island Park EOM	0.73	0.74	0.71	0.72	-.01
Grassy Lake EOM	0.99	0.99	0.01	0.01	0
Reach 24	0.90	0.90	0.95	0.95	0
Jackson Lake EOM	0.82	0.83	0.88	0.87	0.01
Palisades EOM	0.91	0.93	0.87	0.86	0.01
Palisades out	0.86	0.91	0.92	0.92	0
Ririe		0.78			
Blackfoot		0.82			
American Falls	0.76	0.77	0.81	0.80	.01
Walcott	0.82	0.82	0.74	0.74	0
Milner	0.28	0.39	0.58	0.57	0.01
Brownlee In	0.59	0.65	0.87	0.91	-.04

Assessing Historic Shortages Based on Minimum Full-Supply Demand

The main objective in creating the SD-SRPM model was to assess the likely impacts of climate change on water supply in the Snake River basin. As such, *Chapter 3* focused on developing a new definition for shortages. SRPM considers that a shortage occurs when the average diversion between 1991-2005 cannot be met. As discussed in *Chapter 3*, a SWSI versus diversion analysis was performed to create a new demand file for SD-SRPM based on minimum full-supply. In this section, the frequency and volume of shortages using both demand files are compared. The frequency of shortages to estimates by the Natural Resource Conservation Service (NRCS) are based on a supply analysis of shortages for the Boise River and Snake River above Milner.

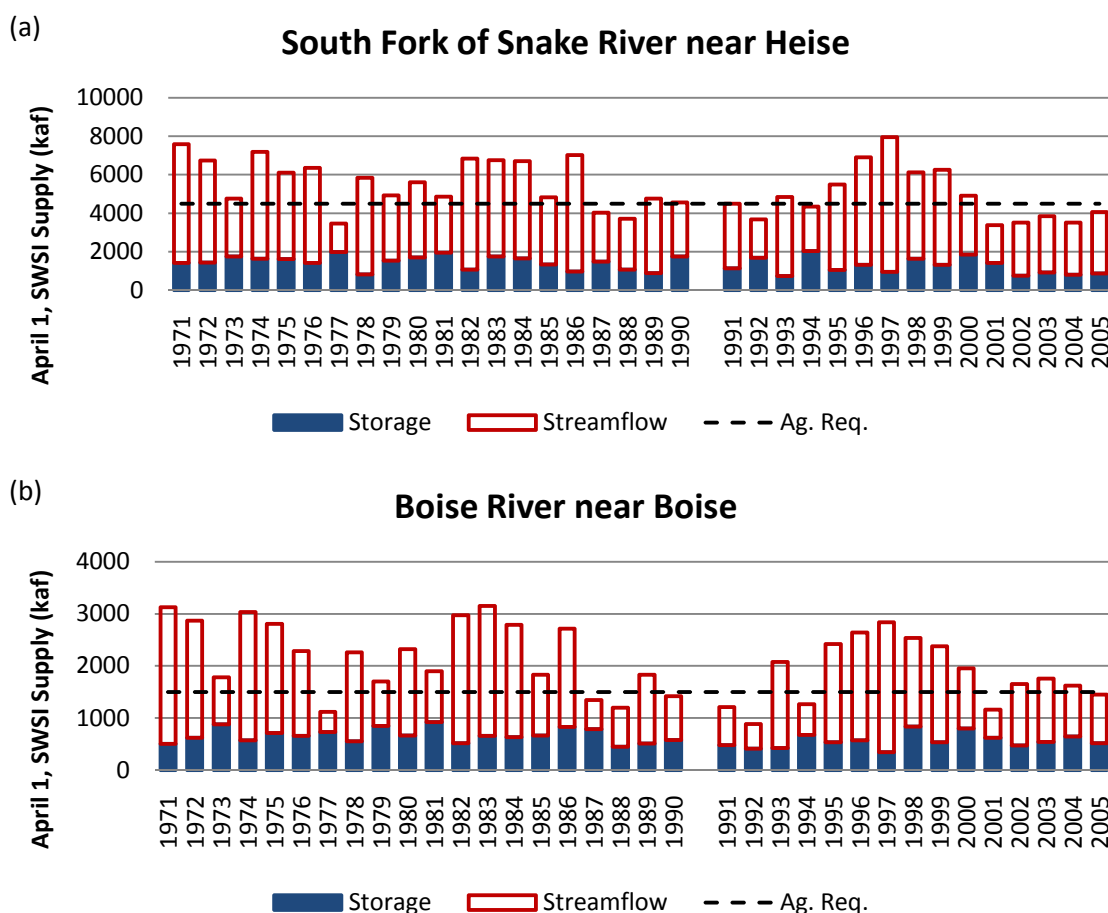


Figure 5.2 SWSI Supply for the (a) Snake River near Heise and the (b) Boise River near Boise

NRCS estimates that shortages may occur when April 1st SWSI values are less than -1.8, corresponding to a supply of 1,500 kaf on the Boise River and to a supply of 4,500 kaf on the Snake River above Heise (NRCS, 2011). These agricultural supply requirements were determined by NRCS with the involvement of stakeholders, and represents a shortage level from the water users' perspective (Abramovich, 2010). Figure 5.2 shows the storage and streamflow components of SWSI on April 1st for the Boise River (Figure 5.2a) and the Snake River (Figure 5.2b). Figure 5.2 indicates that three droughts occurred during the period from 1991-2005. The 1977 drought was a severe single-year event followed by two multi-year droughts, the *end-of-century drought* (ECD,

late 1980s through early 1990s) and the *turn-of-the-century drought* (TCD, which started in 2000, Seager, 2007). As Figure 5.2 indicates, the ECD drought was most severe in the Boise basin, while the TCD was more severe in the Upper Snake River basin. Note that a gap was left in Figure 5.2 to separate the 1991-2005 years analyzed in this chapter within the 1971-2005 record shown.

Table 5.4 Comparison of Shortages in SD-SRPM Based on Average Demand and Minimum Full-Supply Demand

W-YR	Boise River Average Demand	Boise River Minimum Full-Supply	Snake River Average Demand	Snake River Minimum Full-Supply
1991	61.5	377.5	0	41.6
1992	37.7	383.5	56.5	99.3
1993	0	0	0	0
1994	0	182.5	14.9	15.2
1995	0	0	0	0
1996	0	0	0	0
1997	0	0	0	0
1998	0	0	0	0
1999	0	0	0	0
2000	0	0	14.3	0
2001	0	282.4	81.2	11.0
2002	0	93.0	49.4	80.0
2003	0	66.2	49.9	61.7
2004	0	98.1	50.3	19.6
2005	0	106.8	17.9	15.3

A comparison of the frequency and depth of shortages on the Boise and Snake rivers in Table 5.4 indicates that shortages based on minimum full-supply are more realistic in approximating when stakeholders will be water short. The years with historic shortages, as determined by SWSI, are highlighted in Table 5.4. Clearly from a user perspective, the prediction of shortages on the Boise River improves dramatically with the use of minimum full-supply to define shortages. Interestingly, SD-SRPM indicates that farmers experienced shortages throughout the ECD within the Boise River basin,

though not as strongly during 2002-2004 when SWSI indicates adequate supply. Table 5.4 does not indicate much improvement in predicting shortages on the Snake River.

Table 5.5 shows that most of the shortages in the Upper Snake River basin above Milner Dam occur in Region 4 (see *Chapter 2* and Figure 2.1 for a description of the three major surface water irrigation regions within the Snake River basin). This investigation seems to indicate that the SWSI index is geared mostly toward shortages in Region 4, and may be over predicting the occurrence of shortages in Regions 2 and 3.

Table 5.5 Comparison of Shortages in the Snake River Basin by Region under Minimum Full-supply Demand

W-YR	Region 2	Region 3	Region 4	Total
1991	0	0	41.6	41.6
1992	0	76.7	22.6	99.3
1993	0	0	0	0
1994	0	0	15.2	15.2
1995	0	0	0	0
1996	0	0	0	0
1997	0	0	0	0
1998	0	0	0	0
1999	0	0	0	0
2000	0	0	11.0	0
2001	0	57.9	22.1	11.0
2002	0	0	61.7	80.0
2003	0	5.4	19.4	61.7
2004	0	0	19.6	19.6
2005	0	0	15.3	15.3

The apparent improvement of shortage predictions using minimum-fully supply demand on the Boise River interestingly corresponds to a significant increase in SD-SRPM's representation of EOM at all three Boise River reservoirs. EOM at Anderson Ranch, as shown in Table 5.6, improved from an r^2 value of 0.78 to 0.82, while r^2 values at Arrowrock and Lucky Peak, respectively, increased from 0.50 to 0.62 and from 0.34 to 0.50, when using minimum full-supply versus average demand. Table 5.6 also indicates

that when SD-SRPM is run with minimum full-supply demand versus average demand overall representation of river operations is not compromised.

Table 5.6 Statistical Comparison of SD-SRPM Runs Based on Historic Diversions, Average Demand (AD) Diversions, and Minimum Full-Supply (MFS) Diversions

	SD-SRPM vs. SRPM r^2	SD-SRPM (AD) vs. SRPM r^2	SD-SRPM (MFS) vs. SRPM r^2	SD-SRPM (AD) vs. Observed r^2	SD-SRPM (MFS) vs. Observed r^2
Henry's Lake EOM	0.68	0.73	0.58	0.40	0.55
Island Park EOM	0.74	0.69	0.74	0.72	0.78
Grassy Lake EOM	0.99	0.22	0.19	0.13	0.06
Reach 24	0.90	0.90	0.90	0.89	0.89
Jackson Lake EOM	0.83	0.76	0.76	0.81	0.83
Palisades EOM	0.93	0.91	0.89	0.86	0.84
Reach 30	0.91	0.89	0.90	0.89	0.90
Ririe	0.78	0.93	0.93		
Blackfoot	0.82	0.89	0.81		
American Falls	0.77	0.80	0.69	0.78	0.70
Walcott	0.82	0.83	0.83	0.76	0.74
Reach 63	0.39	0.29	0.30	0.49	0.49
Anderson Ranch EOM	0.95	0.94	0.77	0.78	0.82
Arrowrock EOM	0.81	0.82	0.59	0.34	0.50
Lucky Peak EOM	0.82	0.75	0.66	0.50	0.62
Lucky Peak out	0.92				
Reach 98	0.86	0.82	0.90	0.93	0.90
Lake Cascade EOM	0.85	0.82	0.82	0.77	0.76
Deadwood EOM	0.92	0.92	0.92	0.81	0.81
Reach 114	0.92	0.92	0.92	0.93	0.93
Reach 119	0.93	0.92	0.92	0.93	0.93
Brownlee In	0.65	0.59	0.60	0.90	0.90

Conclusions

Based on the SD-SRPM model validation and the historic analysis of shortages, I conclude that SD-SRPM has accurately represented the SRPM reservoir operations model. I also conclude that the use of minimum full-supply demand to define shortages significantly improves the model's ability to predict when stakeholders will be water short without necessarily requiring recalibration of the model. This means that IDWR

could still use SD-SRPM for determining when *planning shortages* would occur under present conditions by using actual diversions, but they could then apply minimum full-supply demand for analyzing shortages under historic and projected climate conditions. The use of minimum full-supply demand provides a tool that will allow stakeholders to consider the sustainability of current agricultural operations under a wide range of hydrologic conditions.

The linkage of SD-SRPM with the ESPA through response functions also provides a dynamic platform for planning conjunctive management in the Snake River basin. Scott (2010) created a similar model in Powersim Studio 8 to assess CAMP scenarios impact on hydropower production in the basin. A future update of the SD-SRPM model could include adding hydropower operations to the model.

The biggest weakness in the SD-SRPM model is the poor correlation of modeled EOM at American Falls to observed EOM. Future research should focus on improving the calibration of SD-SRPM for the region below American Falls; however, care should be taken to maintain the improved correlation of SD-SRPM over SRPM for flow below Milner Dam in Reach 63 and flow entering Brownlee Reservoir downstream of Weiser.

CHAPTER SIX: CLIMATE CHANGE IMPACT ANALYSIS USING SD-SRPM

Having validated SD-SRPM over the historic period, the next step was to test SD-SRPM's usefulness in climate impacts research through a limited climate impact analysis. The goal of this limited climate impact analysis was to test the hypothesis that historic streamflow records do not provide adequate variability to plan future water resource management in the basin. While the results are not conclusive due to the limited scope of the research, the results highlight the need for a thorough study of how climate change may impact future surface water diversions and aquifer discharge in the Snake River basin. The limited climate impact analysis presented here is based on a single emission scenario and that was used to drive three global climate models (GCM). Emission scenarios' represent what future CO₂ emissions might be given general assumptions on population growth, international cooperation in dealing with emissions, and industrial growth, changes in living standards, etc. The A1B emission scenario is considered a mid-range emission scenario (Nakićenović et al., 2000).

In this research, the possible impacts of climate change under the A1B emission scenario were estimated by the ECHO model (Legutke and Voss, 1999) developed at the Max-Planck-Institute for Meteorology, the Community Climate System Model (CCSM3) model developed by the National Center for Atmospheric Research (NCAR, <http://www.cesm.ucar.edu/index.html>) in the United States, and the Parallel Climate Model (PCM1) developed jointly by the Los Alamos National Laboratory, the Naval Postgraduate School, the U.S. Army Corps of Engineers' Cold Regions Research and

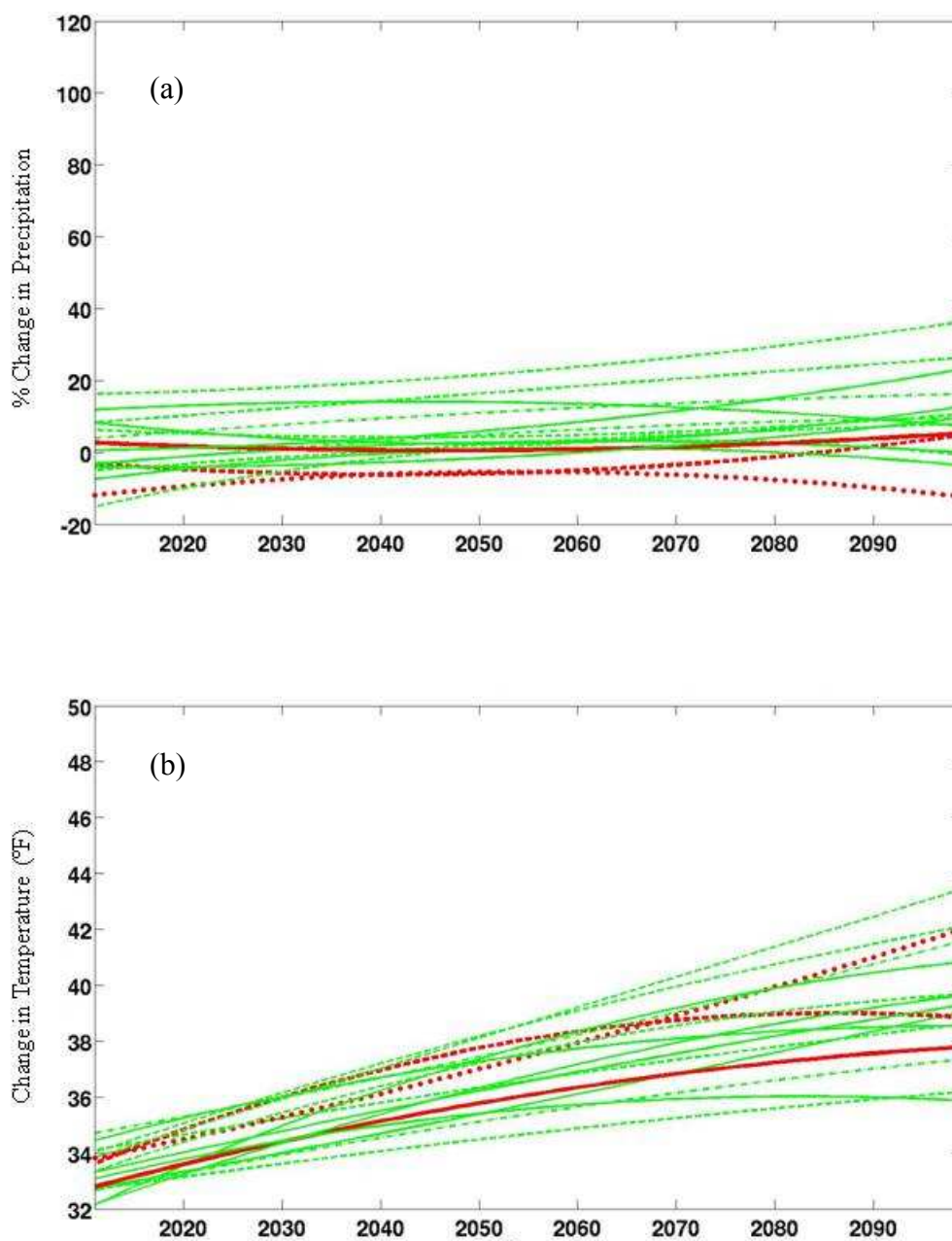


Figure 6.1 A Comparison of GCM Projected (a) Precipitation and (b) Temperature Changes Used in this Study (ECHO-red dotted, CCSM3-red dashed, and PCM1-red solid) versus 13 other GCM Trends

Engineering Lab, and NCAR (<http://www.cgd.ucar.edu/pcm/>). The ECHO model represents a scenario in which precipitation in the Snake River basin declines by 10% from the historic average and temperature increases by about 10°F by 2099. The CCSM3 model represents a milder increase in temperature (about 7°F by 2099) and precipitation within the historic range. The PCM1 model is slightly wetter and cooler than CCSM3 with a temperature rise of about 5.5°F. The choice of these models represented in this climate impact analysis represents the full range of temperature variability, but only captures the moderate to dry precipitation scenarios represented by the 16 downscaled climate scenarios shown in Figure 6.1. Since the purpose of this research was to determine whether or not projected flows are likely to vary within the range represented by the instrumented record of the 1900s, this climate analysis only considers changes in streamflow and ET within the irrigated regions. A more detailed climate change impact analysis of the entire basin awaits further research.

Monthly temperature and precipitation data from the three GCM's mentioned above was downscaled by Jin and Sridhar (2010, in review). The downscaled data were used to drive the Variable Infiltration Capacity (VIC, Liang et al., 1994) hydrologic model in order to obtain potential evapotranspiration, precipitation, and runoff data needed to drive the SD-SRPM model. VIC was calibrated based on historic streamflow by Jin and Sridhar (2010, unpublished). Runoff from the VIC model was routed using the Lohmann routing method (Lohmann et al., 1998a; Lohmann et al., 1998b) to seven locations within the Snake River basin: the Henry's Fork near Ashton, the Falls River near Squirrel, the Teton River near St. Anthony, the South Fork of the Snake River near Heise, the Boise River at Parma, the Payette River at Payette, and the Snake River at

Oxbow Dam. The routed flow was then bias corrected and redistributed by reach using a reach gain distribution method developed for this research. This chapter starts by providing a brief description of the bias correction of the VIC generated streamflow and the development and validation of the reach gain distribution method, before describing the results of the climate change impact analysis.

Bias Correction of VIC Generated Streamflow using Quantile Mapping

While Jin and Sridhar (2010, unpublished) calibrated the VIC hydrologic model to the Snake River basin at 13 locations, the modeled flow still contained some bias in representing historic flows. Bias correction using quantile mapping provides a means of removing systematic bias from a dataset (Hamlet et al., 2002; Wood et al., 2002; Maidment, 1993). The method was performed as follows. A cumulative distribution function (cdf) was created for monthly flows at the seven unregulated flow locations based on IDWR unregulated flow data between the years 1950 and 2005. A second cdf of historic, VIC generated streamflow using the same time period was then created. The difference in streamflow by quantile was then recorded in a *bias* array. Next, a third cdf of projected flows was created. The historic bias by quantile (quantiles were rounded to an accuracy of 0.001) were then added to the projected flow cdf to generate bias corrected flow. Figure 6.2 shows the method. A correction of annual bias as discussed by Hamlet et al. (2002) was not performed.

In Figure 6.2, the historic bias in the VIC streamflow data is represented by the mismatch of the historic cdf (solid blue) and VIC (dashed blue). As can be seen, VIC under represents flow at the 0.65 (65th) quantile by an amount, Δ . As can be seen, future VIC streamflow as represented by the CCSM3 scenario predicts an increase in

streamflow at the 65th quantile over historic VIC flows. Therefore, the historic bias between observed flow and historic VIC is applied to the predicted flow to generate a bias corrected flow at the 65th quantile. This correction removes bias of underpredicted flow from the VIC projected data.

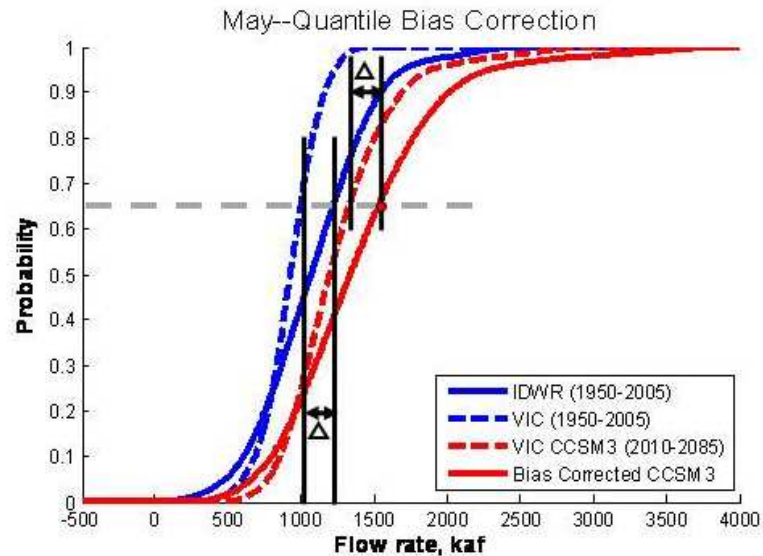


Figure 6.2 Bias Correction of VIC Generated Streamflow

Because VIC cannot represent surface/water groundwater interactions, bias correction cannot accurately correct this non-systematic influence (Hamlet et al., 2002). Therefore, the bias correction of VIC data was only applied where rivers entered the East Snake River Plain. Reach gains along the East Snake Plain Aquifer (ESPA) were modeled as described in *Chapter 4*. Since SD-SRPM was not dynamically linked to the West Snake Plain Aquifer, bias correction occurred where the Boise and Payette rivers joined the Snake River. The bias correction of flow at Oxbow Dam was used only for the purpose of predicting streamflow from minor tributaries in the Snake River Plain based on a least squares linear regression.

Reach Gain Distribution Method

A key factor in modeling climate impacts within the basin at a scale relevant to water managers is to correctly model the reach gains. A reach gain is an historic estimate of the amount of water that would have entered or been lost from a river reach had no storage, diversions, or return flows occurred within the reach. The sum of upstream reach gains represents the ⁵*naturalized* flow, or flow that would have been in the river without storage dams and diversions. The amount of water within a reach gain depends on tributary inflow, runoff, and groundwater/surface water interactions. Because groundwater/surface water interactions are included within a reach gain, the naturalized flow includes the historic impacts of irrigation on the water table. Determining where water is lost or gained within the river has a big impact on the availability and administration of water rights for surface water diversions (Olenichak, personal communication, July 27, 2009).

Because VIC generated streamflow represents ⁶*natural* flow, the reach gain for a given reach is simply the natural flow in a given reach minus the natural flow in the next upstream reach. Since the SRPM model includes 89 reach gains, it would be tedious and perhaps unrealistic to extract and bias correct VIC streamflow at all 89 reaches included in the SRPM and SD-SRPM models. Therefore, I chose extract and bias correct VIC generated flow at critical junctions and then use that flow to estimate upstream reach gains. The estimates for reach gains were based on historic contribution of the upstream

⁵ Naturalized flow includes groundwater/surface water impacts caused by irrigation practices, such as an elevated water table caused by surface water diversions, or lowered water table caused by groundwater pumping.

⁶ Natural flow does not include groundwater/surface water interactions that result from irrigation. Natural flow and naturalized flow are nearly the same in non-irrigated regions.

reach gains to flow at the critical junctions. Historic naturalized streamflow at each junction was categorized into 7 hydrologic states (dry, 1, 2, 3, 4, 5, and wet) based on annual, historic, naturalized streamflow from 1928-1995. The years 1996 to 2005 were not included in developing the reach gain distribution method to provide a validation period to confirm the methodology. This redistribution technique was applied at five calibrated flow points: at Ashton on the Henry's Fork, at Squirrel on Falls River, at Heise on the Snake River, at Parma on the Boise River, and at Payette on the Payette River. The annual flow within each hydrologic state for the five redistributed flow locations are described in Table 6.1.

Table 6.1 Monthly Flow Ranges on which Hydrologic States are Based in SD-SRPM

Hydrologic State	Henry's Fork Ashton	Falls R. Squirrel	Snake R. Irwin	Boise R. Parma	Payette R. Payette
Wet	> 1450	> 900	> 6900	> 4050	> 4500
5	1340-1450	820-900	6150-6900	3650-4050	4000-4500
4	1230-1340	740-820	5400-6150	3150-3650	3500-4000
3	1120-1230	660-740	4650-5400	2700-3150	3000-3500
2	1010-1120	580-660	3900-4650	2250-2700	2500-3000
1	900-1010	580-500	3150-3900	1800-2250	2000-2500
Dry	< 900	< 500	< 3150	< 1800	< 2000

* units are in thousand acre feet (kaf)

The reach gain distribution method presented here follows four steps. First calibrated flow at a location, d , is chosen; typically, the lowest reach in a river and or/junction between two major rivers. Then, the annual natural flows are calculated as the sum of upstream reach gains such that:

$$NF_i = \sum_{j=0}^n RG_j = (RG_0 + RG_1 + \dots + RG_n) \quad (\text{Equation 6.1})$$

where,

i = months in water-year (Oct-Sept)

NF_m = monthly natural flow at location d

n = number of reaches upstream of the reach at location d
 RG_j = reach gain in for reach j

where, $j = 0$ represents the reach at location d

$$NF_y = \sum_{i=1}^{12} \sum_{j=0}^n RG_{ij} \quad (\text{Equation 6.2})$$

where,

NF_y = annual natural flow at location d

Historic annual flows are then divided into flow categories (in this case seven categories) with an equal flow distribution. Wet and Dry flow categories may not have an equal flow distribution if outliers exist at either extreme. I tried to maintain a minimum of five years of flow data in any one category. Flow categories were labeled from lowest to highest flow: Dry, 1, 2, 3, 4, 5, and Wet, respectively. Next, the percent monthly contribution, $p_{m,j}$, of each reach to downstream natural flow was calculated on a monthly basis such that:

$$p_{ij} = \frac{RG_{ij}}{NF_i} \quad (\text{Equation 6.3})$$

and then the mean percent contribution by month and flow category was calculated as,

$$pc_{ij} = \frac{\sum_{y=1}^{y_c} p_{ij,y}}{y_c} \quad (\text{Equation 6.4})$$

where,

y_c = number of years within flow category

y = years in a specified flow category

and a table of percent contributions was produced as shown in Table 6.2 for each flow extraction location. By this method, any flow generated by a hydrologic model at an extraction point could be redistributed to simulate the reach gains needed to drive SRPM

and SD-SRPM. It should be noted that although flow is categorized based on annual natural flow, the reach gains are simulated based on the monthly natural flow.

Table 6.2 October and November Reach Gain Distribution Table for Boise River Reaches

Month	Hydrologic State	74	76	82	84	84	95	96	97	98
October	Dry	0.191	0.140	0.050	0.048	0.022	0.077	0.161	0.174	0.137
	1	0.192	0.147	0.055	0.032	0.022	0.077	0.162	0.175	0.138
	2	0.190	0.138	0.047	0.039	0.022	0.079	0.165	0.179	0.140
	3	0.176	0.131	0.046	0.035	0.024	0.082	0.173	0.187	0.147
	4	0.184	0.140	0.035	0.044	0.023	0.080	0.168	0.182	0.143
	5	0.218	0.152	0.055	0.041	0.021	0.072	0.150	0.163	0.128
	Wet	0.160	0.120	0.050	0.042	0.024	0.085	0.177	0.192	0.151
November	Dry	0.244	0.201	0.066	0.076	0.020	0.047	0.131	0.142	0.072
	1	0.248	0.200	0.079	0.059	0.020	0.047	0.132	0.143	0.073
	2	0.262	0.193	0.077	0.066	0.019	0.046	0.128	0.138	0.071
	3	0.237	0.184	0.068	0.057	0.022	0.052	0.144	0.156	0.080
	4	0.267	0.200	0.066	0.069	0.019	0.045	0.126	0.137	0.070
	5	0.286	0.197	0.066	0.070	0.018	0.043	0.121	0.131	0.067
	Wet	0.258	0.192	0.059	0.071	0.020	0.048	0.134	0.144	0.074

Validating the Reach Gain Distribution Method Using Historic Flow

To determine the validity of the reach distribution method, a new reach gain file based on a redistribution of the monthly historic natural flow at each calibrated point was created according to the percentage contribution tables created earlier. The new reach gain file was then used to drive the SD-SRPM model. Figure 6.3 shows a comparison of EOM reservoir content at Jackson Lake and Palisades Reservoir based on observed EOM and modeled EOM using redistributed historic flows. Table 6.3 compares calculated shortages throughout the model based on the historic and redistributed historic flows. In general, shortages based on redistributed flow are somewhat less than the historic shortages. This may be due to the redistribution method smoothing out flow anomalies that would tend to result in shortages. The under prediction of shortages on the Boise

River should be kept in consideration when looking at the impacts of climate change using projected flow.

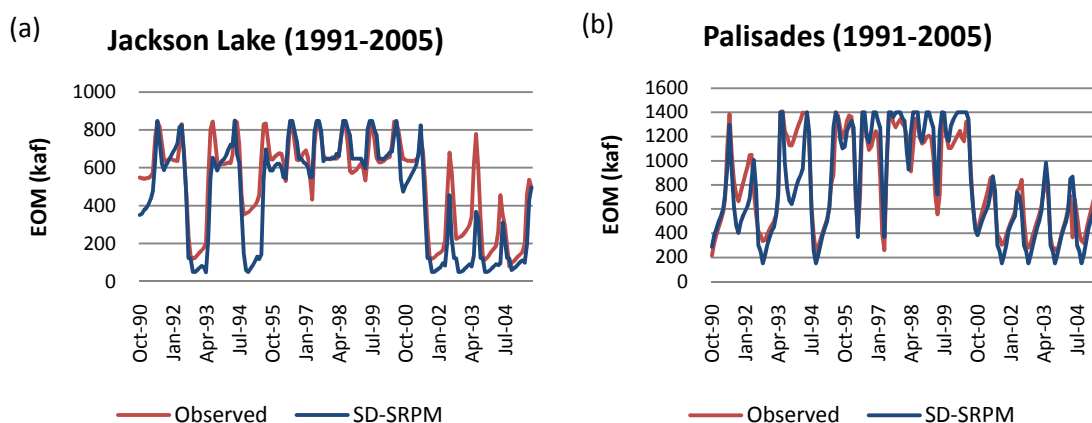


Figure 6.3 SD-SRPM Modeled and Observed EOM at (a) Jackson Lake, $r^2 = 0.82$ and (b) Palisades Reservoir, $r^2 = 0.81$ Using Historic, Redistributed Flow

Table 6.3 Shortages (kaf) by Decade Based on Actual and Redistributed Flow

	1930s	1940s	1950s	1960s	1970s	1980s	1990s
Redistributed Flow							
Falls River	19.9	32.8	9.2	10.8	14.6	25.8	25.4
Teton River	0	0	0	0	0	0	0
Henry's Fork	53.2	46.5	11.4	52.2	8.6	46.3	79.2
Snake abv Shelley	0	0	0	0	0	0	0
Snake abv Blackfoot	143.9	0	0.9	0.8	42.5	0	90.3
Snake abv. Milner	243.7	56.5	325.1	263.7	22.8	37.4	165.2
Blackfoot River	93.1	110.6	189.1	126.2	121.7	22.5	163.5
Willow Creek	25.5	8.7	2.1	1.3	2.2	1.7	4.3
Boise River	266.3	0	0	0	156.5	228.8	906.6
Payette River	4.0	0	0	0	4.8	4.3	13.4
Historic Flow							
Falls River	61.8	15.5	0	10.8	14.6	25.8	25.4
Teton River	0	0	0	0	0	0	0
Henry's Fork	253.8	59.0	0	53.5	25.9	47.0	80.3
Snake abv. Shelley	33.5	0	0	0	0	0	0
Snake abv. Blackfoot	377.3	22.9	3.4	5.4	38.3	0	149.8
Snake abv. Milner	380.1	139.7	391.9	196.7	36.3	37.0	101.9
Blackfoot River	116.8	34.0	46.3	54.3	26.8	8.4	34.7
Willow Creek	12.4	9.6	1.0	2.2	1.9	1.6	4.7
Boise River	899.9	0	0	93.0	360.5	496.2	1038.1
Payette River	2.6	0	0	0	4.6	4.6	9.1

Validating the Use of VIC Redistributed Flow

The next step was to validate the use of bias corrected VIC streamflow. While SD-SRPM was still able to provide a reasonable replication of historic EOM using VIC derived streamflow data (see Figure 6.4), the shortages represented by VIC redistributed data did not match historic shortages based on previous historic simulations. The reason for the decline in correlation when using VIC based streamflow data is likely due to the use of VIC calibrated parameters that were calibrated using VIC4.0.6, and then applied to the latest version of VIC (4.1.1). VIC 4.1.1 has slightly different canopy snow storage and flux calculations, as well as, soil temperature profiles than VIC 4.0.6 (<http://www.hydro.washington.edu/Lettenmaier/Models/VIC/Development/CurrentVersion.shtml>, March 1, 2011). This change in model version may have introduced non-systematic bias that could not be removed by quantile mapping. However, the most recent version, VIC 4.1.1, includes significant improvements in estimating baseflow, which reduced significantly the volume of the bias correction. Work is currently being done to calibrate VIC 4.1.1 to the Snake River basin.

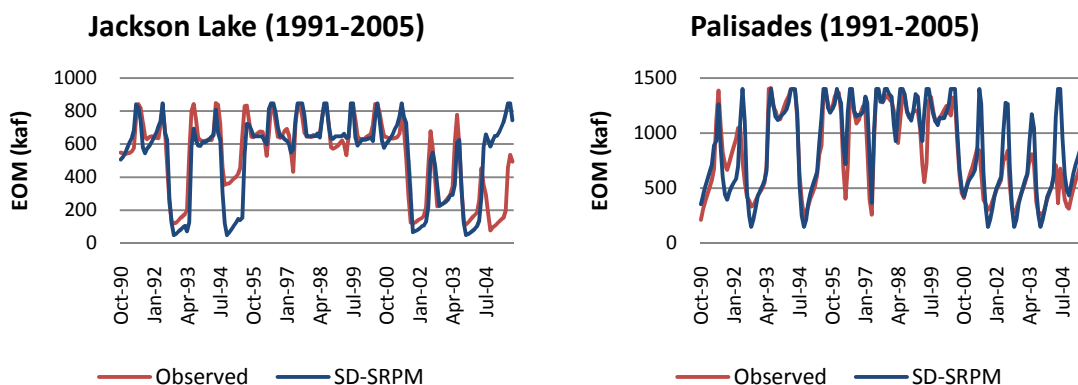


Figure 6.4 SD-SRPM Modeled and Observed EOM at (a) Jackson Lake, $r^2 = 0.55$ and (b) Palisades Reservoir, $r^2 = 0.75$ Using VIC Generated Historic, Redistributed Flow

Climate Change Impact Analysis

The climate impact analysis presented here was performed to test the null hypothesis that the instrumental record of the 1900s provides adequate climatic variability for planning water resource management under future hydrologic conditions in a warming climate. This analysis considers changes to the average unregulated flow hydrograph, reservoir storage, and groundwater/surface water interactions based on two 30-year historic periods (1931-1960 and 1976-2005) and three projected periods (2011-2040, 2041-2070, and 2071-2099). In particular, the reservoir storage analysis focuses on changes in June end-of-month reservoir storage (EOM) and October EOM. Current reservoir operations seek to maximize storage in the reservoirs by the end of June, a decline in June EOM represents a loss of storage capacity within the system. October EOM represents storage in the reservoirs at the end of the irrigation season. The null hypothesis is rejected if more than one of the three GCMs indicate a greater than 10% departure from historic June and October EOM in the two periods 1930-1960 and 1976-2005 versus EOM in the three projected time periods 2011-2040, 2041-2070, and 2071-2099. Finally, the climate impact analysis looks at the implications of flood risk in the regulated flow output. While SD-SRPM is not a flood analysis model, the monthly regulated flow data gives an indication of the potential flood risk. Historically, months with the highest flows correspond to periods of flooding.

Climate Change Impacts on Unregulated Flow

The following analysis compares the average unregulated flow hydrograph for VIC bias corrected flows for two historic and three future time periods. Figure 6.5

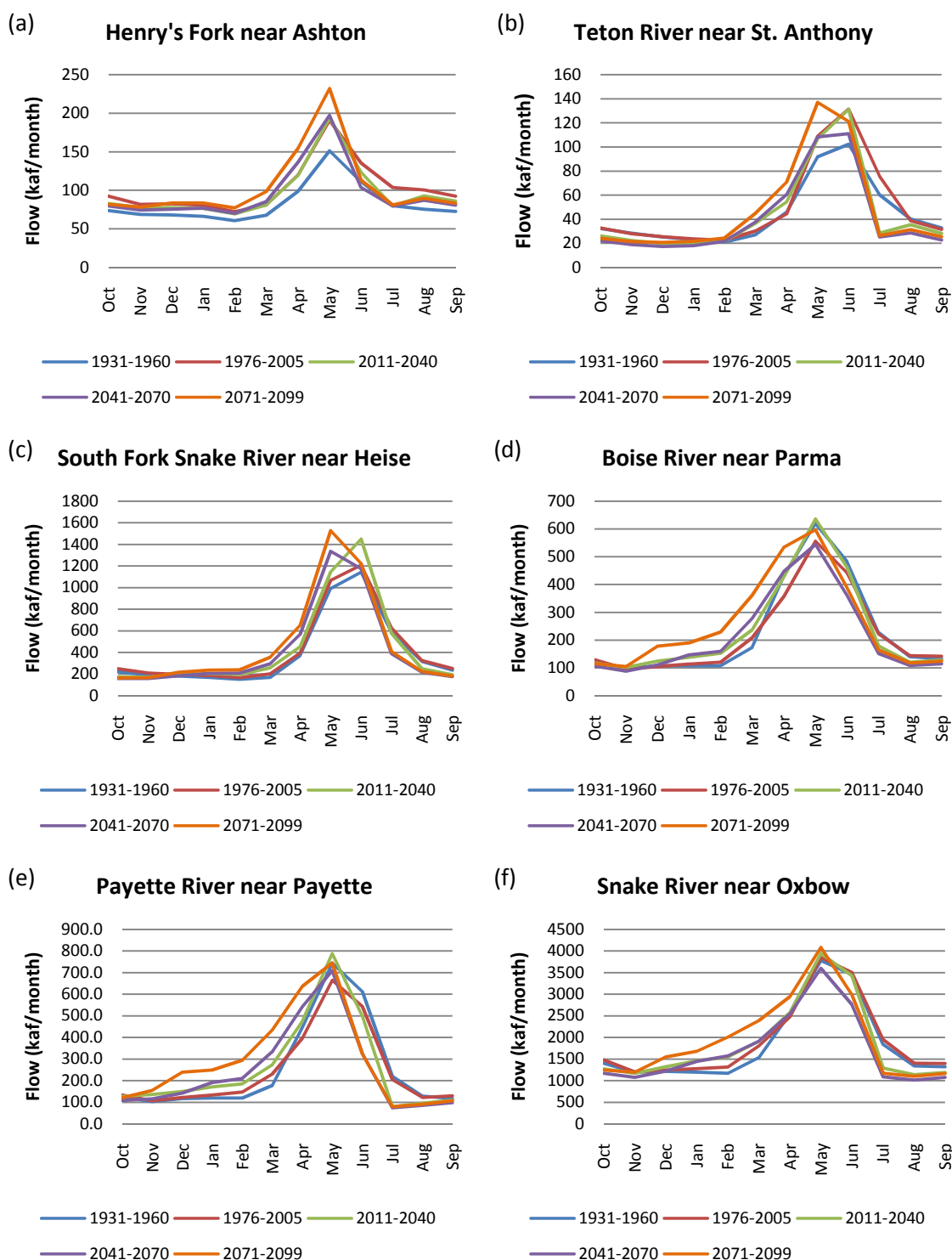


Figure 6.5 Monthly, Bias Corrected, Mean Natural Flow Generated by the VIC Hydrologic Model for the (a) Henry’s Fork, (b) Teton River, (c) Snake River at Heise, (d) Boise River, (e) Payette River, (f) and the Snake River Near Oxbow Dam based on the CCSM3, A1B Climate Scenario

shows the unregulated average flow hydrographs for the two 30-year historic periods and three 30-year projected periods for the Henry's Fork, Falls, Teton, Snake, Boise, and Payette rivers based on the CCSM3 model under the A1B emission scenario. Appendix D contains the average annual hydrographs for all three GCM based climate scenarios using the same time periods. As can be seen in Figure 6.5, there is a profound shift in the hydrograph toward lower summer flows and higher spring flows with peak runoff shifting from June to May as temperatures increase. This trend is not as clear in the cool PCM1 based climate scenario as compared to the other two warmer climate scenarios. The shift in the hydrograph appears to have already begun in some basins and can be identified by comparing the average annual hydrograph of 1931-1960 against the 1967-2005 average annual hydrograph.

Table 6.4 Average Annual Historic and Projected Flow Volumes (kaf)

Time period	Henry's Fork Ashton	Falls River Squirrel	Teton River St. Anthony	Snake River Heise	Boise River Parma	Payette River Payette
Historic						
1931-1960	996.0	640.3	529.6	4749.8	2751.5	3032.9
1967-2005	1233.0	694.6	592.9	5083.3	2637.8	2935.4
ECHO						
2011-2040	1087.7	636.0	444.6	4635.1	2437.2	2680.1
2041-2070	1172.2	690.6	523.6	5395.9	2690.2	2972.6
2071-2099	1192.6	687.5	516.7	5411.0	2627.6	3126.2
CCSM3						
2011-2040	1159.5	688.7	530.4	5281.3	2826.6	3086.7
2041-2070	1148.2	668.3	492.7	5078.9	2620.6	2937.6
2071-2099	1256.2	732.1	569.3	5610.8	3107.3	3476.6
PCM1						
2011-2040	1208.0	710.9	620.8	5427.5	2752.9	2995.5
2041-2070	1237.8	732.2	635.1	5551.2	3053.4	3388.0
2071-2099	1237.1	742.7	632.1	5805.7	3104.3	3449.6

Table 6.4 compares the average annual flow volume for the two historic and three projected flow periods. The historic hydrographs shows slightly declining supply in the western portion of the basin, and significant increases in supply in the eastern portion of

the basin. The period with the least supply is represented by the first projected flow period (2011-2040) as simulated by the ECHO model. In the second projected flow period (2041-2070), the CCSM3 model predicts the driest conditions. By the last projected period (2071-2099), nearly all scenarios show an increase in annual flow. The general indication of the unregulated hydrograph analysis is that more water may be flowing in the rivers as global and regional temperatures continue to rise. This is interesting since none of these models represent a large increase in precipitation. As will be shown in the next section, this increase in streamflow does not necessarily correspond to a decrease in shortages.

Climate Change Impacts on Reservoir Storage and Shortage Calculations

SD-SRPM represents current reservoir operation practices. Current practice tries to maximize storage content in the reservoir by the end of June, while the difference between June EOM and October EOM represents the volume of water drafted to meet agricultural and instream flow requirements. Figure 6.6 shows the decadal average EOM values for both historic and projected periods for each of the three climate change scenarios represented by the dry-hot ECHO model, the moderate CCSM3 model, and the mild PCM1 model for Palisades Reservoir and storage behind the three Boise River dams: Lucky Peak, Arrowrock, and Anderson Ranch. The warmer models coincide with greater draw down in the eastern Snake River basin, but not in the western basin. This is most likely due to a greater shift of the hydrograph in the eastern basin than in the western basin (see Figure 6.5c and 6.5d). As the peak runoff advances earlier into the spring, there appears to be a greater reliance on storage to meet late season irrigation demand. Table 6.5 shows the percent departure of June EOM and October EOM from

the upper and lower bounds of the two historic period (1930-1960 and 1976-2005). Since EOM changes as represented in SD-SRPM using the ECHO scenario and CCSM3 scenario both depart by more than 10% from historic values, I reject the null hypothesis that historic planning provides adequate streamflow variability to plan future water resource management in the Snake River basin.

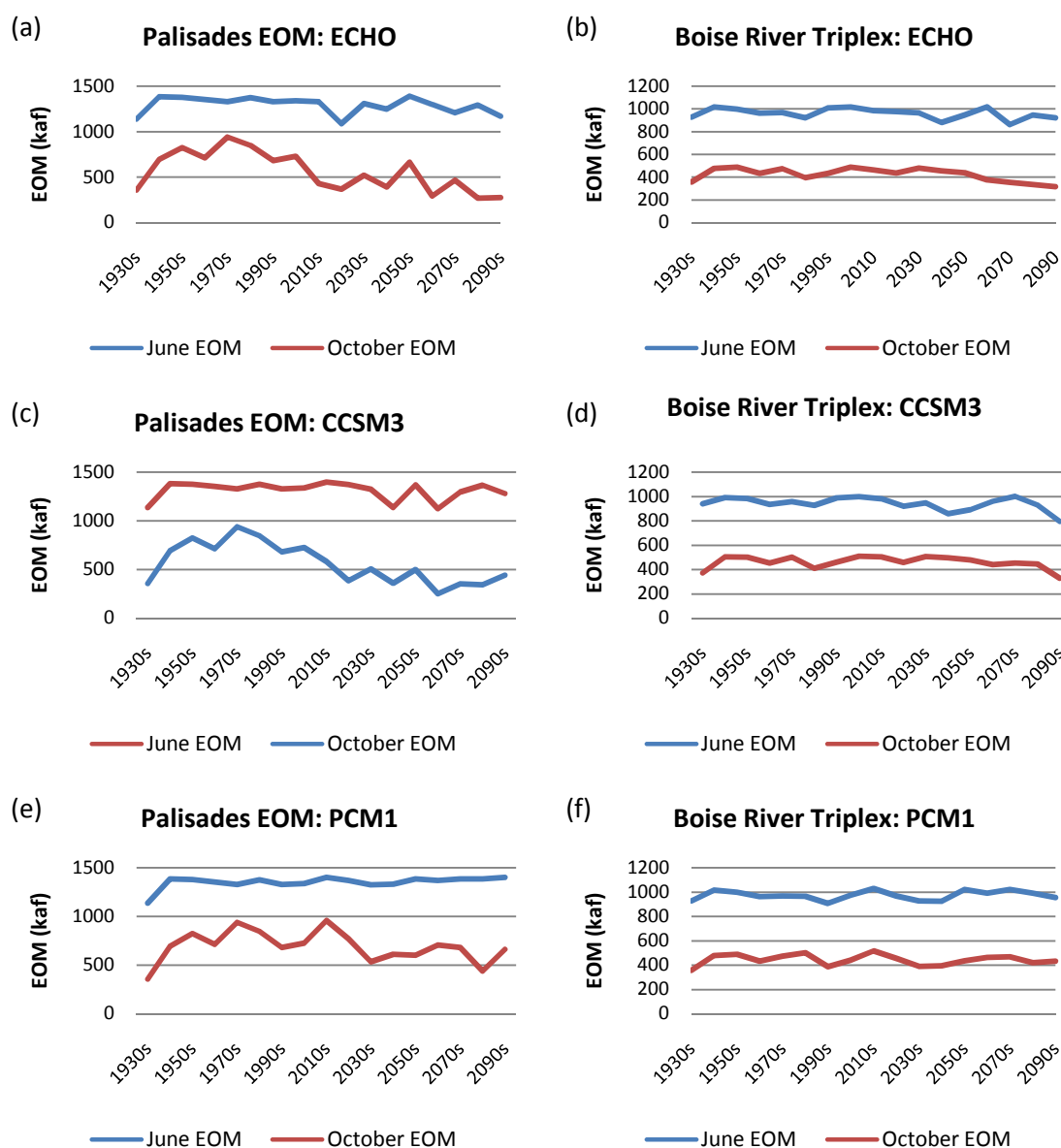


Figure 6.6 June and October Average Decadal EOM for Palisades and the Boise River Storage Triplex Based on the ECHO, CCSM3, and PCM1 Representation of the A1B Emission Scenario

Table 6.5 Average June and October EOM (kaf) for Palisades and the Boise River Storage Triplex

Letter name	Palisades June EOM	Palisades October EOM	Triplex June EOM	Triplex October EOM
Historic (kaf)				
(1931-1960)	1300	626	984	447
(1970-2000)	1322	740	966	433
ECHO				
(% departure)	-4.9	-32.3	w/n	4.8
	-0.1	-15.3	-1.7	-2.7
	-5.1	-45.7	-6.3	-23.6
CCSM3				
(% departure)	3.3	-21.3	-3.0	-9.4
	-8.1	-41.0	-5.5	-5.3
	0.4	-38.5	-6.4	5.9
PCM1				
(% departure)	3.2	w/n	w/n	w/n
	2.9	w/n	w/n	w/n
	5.1	-5.7	w/n	w/n

* w/n means the average projected flow falls within the historic averages

Figure 6.7 shows the annual June and October EOM for Palisades Reservoir and the Boise River Triplex. The Boise River Triplex includes cumulative storage behind Lucky Peak, Arrowrock, and Anderson Ranch Dams. These time series illustrate that not only are GCM trends in temperature and precipitation important, it is also critical to analyze the climate variability (such as drought periods) represented by each GCM. The CCSM3 model represents the longest multi-year drought period 2062-2071 in this study. During this period, Palisades is unable to fill and is completely emptied of storage water 9 times during a 12-year period from 2062 to 2071. A comparison of the 1929-1938 drought period based on June and October EOM, which includes the famous Dust Bowl, to the CCGM3 2062-2071 drought period can be seen in Figure 6.8a. The SD-SRPM estimated shortage for the historic and projected droughts is 952 kaf and 1250 kaf respectively. Table 6.6 compares the location of shortages on three reaches of the Snake below Palisades. Interestingly, there is a significant increase in Lorenzo-Shelly shortages

and a decline in shortages below American Falls. A review of shortages from the SD-SRPM indicates that Lorenzo shortages most frequently occur in the late summer while shortages below American Falls most frequently occur in June. The shift in the hydrograph in this scenario would appear to provide a more reliable supply to downstream irrigators.

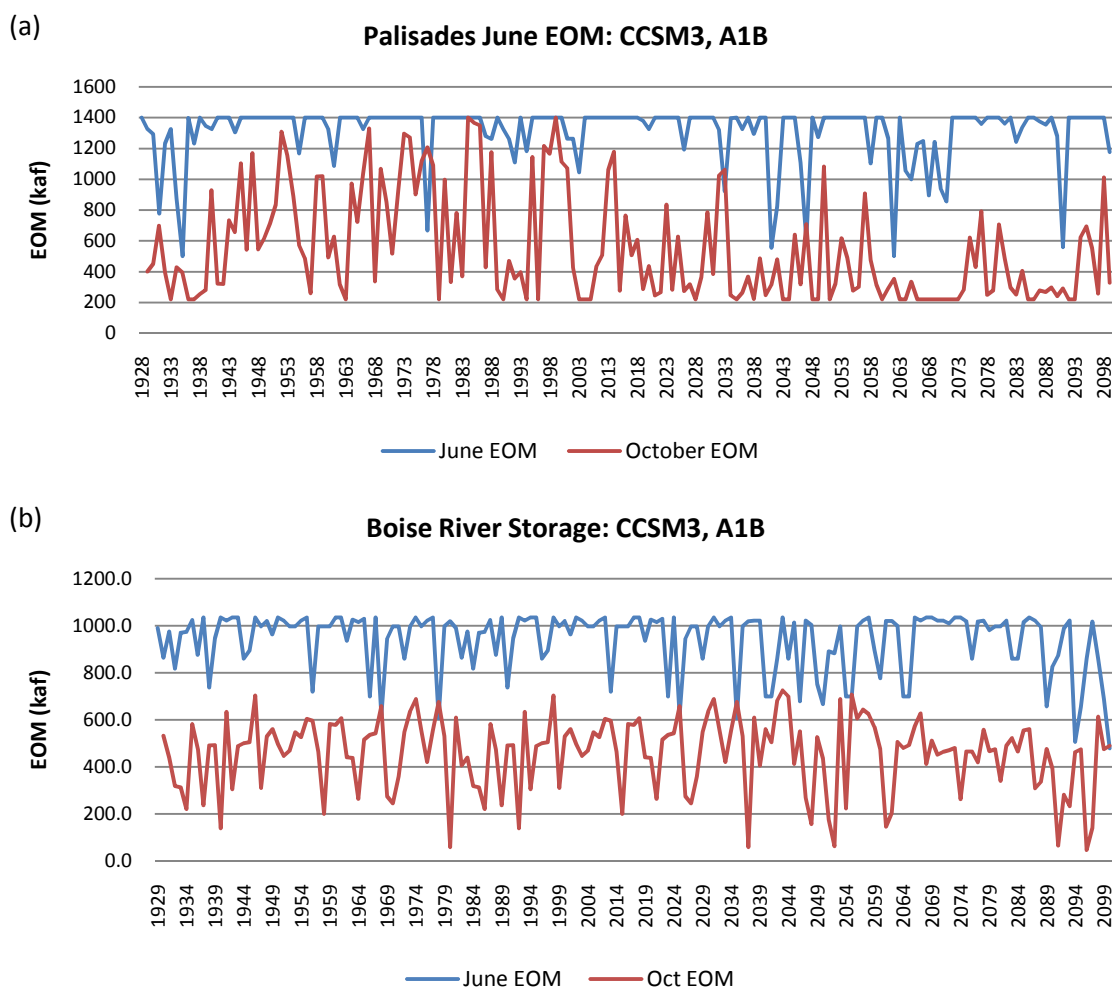


Figure 6.7 June and October EOM from 1929-2099 based on Historic and CCSM3 Climate Scenarios with an A1B Emission Scenario for EOM at (a) Palisades Reservoir and (b) the Boise River Storage Triplex

Table 6.6 Changes in Shortages between Historic Drought and CCSM3 Drought on the Snake River (kaf)

Drought period	Heise to Shelley	Shelly to American Falls	American Falls To Milner
1928-2040	10	357	599
2060-2072	459	711	278

Climate Impacts on Groundwater/Surface Water Interactions

The SD-SRPM model, because of its dynamic link to the East Snake Plain Aquifer (ESPA), through response functions, allows an assessment of how both historic and projected climate would have impacted groundwater/surface water interactions along the Henry's Fork and Snake River down to King Hill given present water infrastructure and demand. Figure 6.8 indicates the fluctuation of total discharge from the ESPA to the Snake River on a decadal basis from the 1930s to 2090 given historic flows and projected flow from CCSM3, A1B climate scenario. Figure 6.8 indicates that had existing water resource infrastructure and practices, including groundwater pumping and surface water diversions been, in place since the 1930s the total discharge from the ESPA would have increased by 25 kaf up to 1999 at which point the CCSM3 scenario indicates a decline in discharge back to the 1930s levels between the 2040s to 2060s after which discharge increases by about 10 kaf by the end of the century.

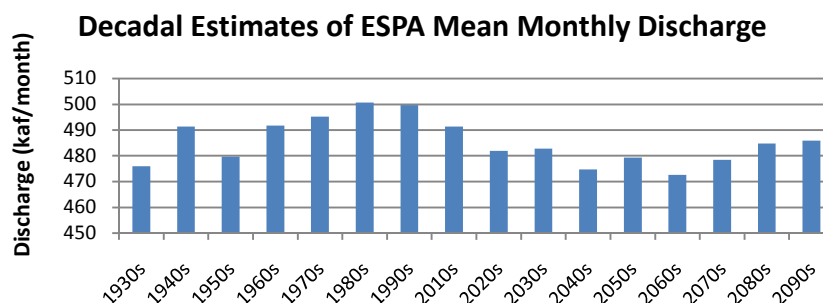


Figure 6.8 Mean Monthly Estimates of Discharge from the ESPA to the Snake River above King Hill by Decade

While it is outside the scope of this thesis to thoroughly analyze the potential impacts of climate change on the ESPA, the 25 kaf fluctuation in ESPA discharge shown in Figure 6.8 provides evidence that SD-SRPM is capturing several critical feedback loops on how climate and agricultural practices impact groundwater/surface water interactions in the Snake River Plain. Changes in precipitation significantly impact the yearly recharge to the ESPA in groundwater regions. Increases in precipitation result in decreased groundwater pumping and decreased precipitation results in increased pumping. In surface water irrigated regions, when low precipitation occurs along with surface water supply shortages, a positive feedback loop is set in motion, which amplifies the occurrence of irrigation shortages. When a shortage occurs because of a surface water supply shortage, less recharge occurs, as a greater percent of the diversion is used to meet crop water demand. The less precipitation that occurs during a period with shortages, the more the diverted water is used to meet crop needs, resulting in less recharge and therefore less discharge from the ESPA to the Snake River. The decline in recharge results in a decline in reach gains and more shortages. The decline in reach gains is then amplified by supplemental pumping by surface water users who rely on a mixed source of surface water and groundwater to meet crop water demand. This groundwater pumping further decreases reach gains and the amount of water that can be diverted. This positive feedback loop results in the aquifer discharge rising and falling in response to available supply and precipitation anomalies. As seen in Figure 6.8, the 1930s and 2060s drought periods, discussed in the previous subsection, correspond to low discharge periods.

This fluctuation in discharge from the ESPA to the Snake River aquifer not only follows decadal trends but also follows annual trends. Figure 6.9 shows an approximately 40 kaf fluctuation in discharge from the ESPA to Snake River during the 15-year period from 1991-2005, closely follows drought as indicated by the comparison of discharge to PDSI in Idaho climate division 9. This fluctuation in aquifer discharge in relation to drought in the Snake River Plain can be identified in the research of Kjelstrom (1995) and Blew and Bowling (2009).

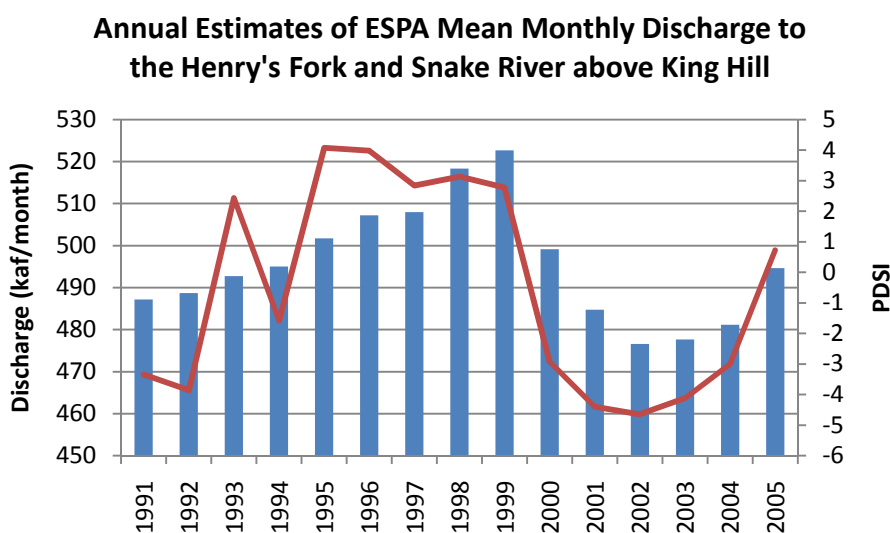


Figure 6.9 A Comparison of ESPA Discharge to the Snake River with PDSI 1991-2005

While there is clearly room to improve the SD-SRPM model through refined calibration and research focused on quantifying recharge more accurately, one of the strong implications of the findings presented here is that long-term plans to conjunctively manage the ESPA should consider the impacts of climate change due to both natural climate variability (Figure 6.9) and long-term trends related to human-induced climate change (Figure 6.8). Otherwise, conjunctive management strategies to enhance aquifer

discharge to the Snake River may simply be offsetting the declining reach gains caused by climate shifts and not reach the sought after increase in reach gains.

Climate Change Impacts on Regulated Flow and Flood Risk

While the SD-SRPM model is not designed for flood risk studies, this section uses the monthly flow volume as a basis for discussing the likelihood of an increase or decrease in flood risk within the basin. Table 6.7 lists the number of events in which monthly flow exceeds the VIC generated historic record monthly flow near Rexburg on the Henry's Fork, near Irwin below Palisades Dam on the Snake River, and below Lucky Peak Dam on the Boise River. Interestingly, the climate scenario with the least shift in peak runoff, the greatest increase in natural flow, and with the least projected shortages, PCM1, also appears to carry the least flood risk. While the hottest and driest precipitation climate scenario, represented by the ECHO model, carries the greatest flood risk based on volume for both the Henry's Fork and Snake River at Irwin. The implication for future research is that flood risk must be assessed based not on general GCM characteristics like the precipitation trend in the basin, but on an event by event basis. Also, this analysis was done on a monthly basis and for flood risk assessment a daily or sub-daily timestep simulation of flows is necessary.

Table 6.7 Peak Historic and Projected Monthly Flows Showing the Frequency and Magnitude (in Brackets) of Monthly, Modeled, Regulated Streamflow

(units in kaf)	Snake River near Irwin	Boise River blw Lucky Peak	Henry's Fork near Rexburg
Historic (1928-2005)	(2102)	(756)	(541)
Projected (2011-2099)			
ECHO	4 (3204)	3 (769)	2 (837)
CCSM3	7 (2577)	4 (1020)	1 (557)
PCM1	2(2320)	3(793)	4 (835)

CHAPTER SEVEN: CONCLUSIONS

Based on the limited climate impact analysis performed in this study, I am able to reject the null hypothesis of the research that assumes the historic instrumented record of the 1900s provides adequate variability to plan water resource management in a warming climate. The three GCMs used to perform this analysis represent a full range of temperature variability but focus on lower precipitation scenario trends. The analysis of climate impacts indicates that the CCSM3 GCM predicts more extensive drought than within the historic record. The analysis of drought indicates a shift in the timing of surface water diversion shortages that favors downstream irrigators on the Snake River. Two of the three models indicate clear shifts in the unregulated hydrograph at a monthly timestep. Based on these findings, it seems imperative that future water resource planning in the Snake River basin include climate impact analysis, even for planning within the 30-year planning window. The rest of this chapter discusses key issues to improve climate impact analysis studies in the basin.

Selection of Model Platform

The use of a system dynamics platform encourages the modeler to think about critical feedback loops that impact system performance. The Powersim Studio 8 platform also provides a powerful user interface that makes the model easier to understand by those outside of the modeling community. While SRPM has provided a powerful tool for the modeling community to study how changes in current management would have impacted historic shortages, it is limited in its capacity to study projected climate

conditions as SRPM cannot directly account for how climate variables such as changes in precipitation or the ET rate would impact diversions and groundwater/surface water interactions. Because the current understanding of climate change impacts within the Snake River basin is limited, models that maintain the historic flexibility of the SRPM model will be highly advantageous.

Modeling Groundwater/Surface Water Interactions

While SD-SRPM includes 80% of the groundwater irrigation within the Snake River basin, a significant shortcoming of this study is a lack of ability to account for changes in flow from the Lost River basins, the Mud Lake surface water irrigation region, and recharge from non-irrigated portions of the basin. Adding recharge calculations and response functions for these additional sources of recharge would provide better understanding of how the portions of the basin without a surface water connection to the Snake River impact groundwater/surface water interactions between the ESPA and the Snake River.

Another limitation of the study is that it does not account for groundwater surface water interactions within the Western Snake Plain Aquifer. While the interactions are less dramatic, the bias correction of VIC flow masks long-term trends in these interactions that may change significantly both as climate and management within the western basin continue to change. These interactions could be accounted for using response functions generated from a groundwater model of the western plain. However, there would need to be a significant amount of work done to link diversions to surface water and groundwater irrigation entities, as was done in the development of the ESPAM model.

Modeling Flood Control Operations

While flood control operations within the SD-SRPM model based on operational curves developed by USBR for MODSIM have performed well in replicating historic reservoir operations, the method does not provide insight into how actual flood control operations are performed. Perhaps a better way to model reservoir operations would be to use historic or VIC generated snow water equivalence (SWE) data to generate a forecast of runoff or select a hydrologic state for food control operations on a monthly basis. The more closely this forecast methodology replicates actual flood control operations, the more likely one will understand how climate change may impact our ability to capture and utilize the available supply. The current methodology hides the existing feedback loops that occur in flood control operations.

Modeling Land-Use Changes and Water Rights

Another feedback loop not included in the SD-SRPM model that could improve the model would be to develop a land-use decision tool. The tool should replicate the decision process by which irrigators determine how much land to irrigate each season based on predicted supply. This decision would be based on several factors including estimated runoff, carry-over storage, possibilities to rent excess water, and expected value of crops. Some basic research is needed to identify the storage rights and natural flow rights of each diversion. Obviously, a user who has a less reliable water supply would be more likely to make land-use decisions based on the forecast than users who are rarely water short.

Modeling Return Flow and Canal Seepage

Another limitation in the current study is the accuracy of the return flow factors being used in the SRPM model, which were transferred to SD-SRPM. Model understanding could be improved by providing documentation on how the return flow factors were derived and the likely precision of those estimates.

Canal seepage estimates on only three canals are included: the Northside Canal, the Milner-Gooding Canal, and the Aberdeen-Springfield Canal. Estimating canal seepage in other surface water entities would greatly improve the understanding of how changes in temperature are likely to impact recharge to the aquifer. Currently, SD-SRPM may be overestimating the application rate of surface water where irrigation water is supplied by supplemental groundwater pumping when diversions are inadequate to meet crop needs.

Research on Historic Impacts of Climate Change

While *Chapter 3* addressed some critical points in how climate impacts diversions within the Snake River basin, there is a need for more extensive research into what causes the variability of historic data within the two portions of the SWSI versus diversion piecewise correlation function. Research should be conducted into how changes in irrigation efficiency may impact the piecewise function. While the piecewise function was used in this research to estimate minimum full-supply demand and user shortages, perhaps a better way to predict planning shortages historically would be to fully utilize both the limbs of the piecewise function to predict diversions, as was done by Scott (2010). Also, PDSI for projected flows should be calculated so that spring diversions can

be set based on antecedent soil moisture conditions as described in *Chapter 3*. This could be done as a preprocessing step outside of the Powersim framework.

Conclusion of Study

The climate impact analysis provided in this research and discussion of future research needs, above, clearly indicates the need for a highly adaptive and user-friendly modeling framework to plan water resource management in a changing climate. While SRPM provided an initial platform from which to develop this model, SRPM was developed based on the principle of stationarity and the SD-SRPM model still contains some of the stationarity assumptions of the original SRPM model. This study shows how important it is that the assumptions based on stationarity be replaced with feedback loops to develop a true system dynamics model of the Snake River basin.

REFERENCES

- Abramovich, R. (2010). Personal Correspondence, June 24, 2010.
- Alfaro, E. J., D. W. Pierce, A. C. Steinemann, and A. Gershunov (2005). "Relationship between the irrigation-pumping electrical loads and local climate in Climate Division 9, Idaho." *Journal of Applied Meteorology*. 44(12):1972-1978.
- Allen, R.G., M. Tasumi, and R. Trezza (2007a). "Satellite-based energy balance for mapping evapotranspiration with internalized calibration (METRIC)—model." *Journal of Irrigation and Drainage Engineering*, ASCE. 133(4): 380-393.
- Allen, R.G., M. Tasumi, and R. Trezza (2007b). "Satellite-based energy balance for mapping evapotranspiration with internalized calibration (METRIC)—applications." *Journal of Irrigation and Drainage Engineering*. 133(4): 395-406.
- Alley, W. M. (1984). "The Palmer Drought Severity Index: limitations and assumptions." *Journal of Applied Meteorology*. 23:1100-1109.
- Arrhenius S. (1896). "On the influence of carbonic acid in the air upon the temperature of the ground." *Philosophical Magazine*. 41(5):237-76.
- Bates, B. C., Z. W. Kundzewicz, S. Wu, J. P. Palutikof, Eds. (2008), Climate Change and Water. Technical Paper of the Intergovernmental Panel on Climate Change, IPCC Secretariat, Geneva.
- Barnett, T. P. , D. W. Pierce, H. G. Hidalgo, C. Bonfils, B. D. Santer, T. Das, G. Bala, A. W. Wood, T. Nozawa, A. A. Mirin, D. R. Cayan, and M. D. Dettinger (2008). "Human-induced changes in the hydrology of the Western United States." *Science*. 319(5866):1080-1083, doi:10.1126/science.1152538.
- Blew, D. and J. Bowling (2009). Spring Discharge Calculation for the Snake River Milner to King Hill Reaches Review of Kjelstrom Methodologies. (www.idwr.idaho.gov/waterboard/MeetingsMinutes/Agenda/IWRB/PDF/8-09/200905SpringDischarge.pdf, January 26, 2010).
- Busbee M. W., B. D. Kocar, S. G. Benner (2009). "Irrigation produces elevated arsenic in the underlying groundwater of a semi-arid basin in Southwestern Idaho." *Applied Geochemistry*, 24:843-859.

- Callendar, G. S. (1938). "The artificial production of carbon dioxide and its influence on temperature." *Quarterly Journal of the Royal Meteorological Society*. 24:223-240, doi: 10.1002/qj.49706427503.
- Christidis, N., P. A. Stott, S. Brown, D. J. Karoly, J. Caesar (2007). "Human contribution to the lengthening of the growing season during 1950-1999." *Journal of Climate*. 20(21):5441-5454, doi: 10.1175/2007JCLI1568.1.
- Clark, G. M. (2010). "Changes in patterns of streamflow from unregulated watersheds in Idaho, western Wyoming, and northern Nevada." *Journal of the American Water Resource Association*. doi: 10.1111/j.1752-1688.2009.00416.x.
- Contor B. A. (2010). Irrigation diversions and returns and surface-water entities for calibration of the Eastern Snake Plain Aquifer Model Version 2, as built. Idaho Water Resources Research Institute Technical Report 201004, Idaho Water Resources Research Institute, University of Idaho, Moscow, ID.
- Contor B. A. (2004a). Irrigation Conveyance Loss. Idaho Water Resource Research Institute Technical Report 04-008. Idaho Water Resource Research Institute, University of Idaho, Moscow, ID.
- Contor B. A. (2004b). Determining Source of Irrigation Water for Recharge Calculation. Idaho Water Resources Research Institute Technical Report 04-010. Idaho Water Resource Research Institute, University of Idaho, Moscow, ID.
- Cook, E. R., R. Seager, M. A. Cane, D. W. Stahle (2007). "North American drought: reconstructions, causes, and consequences." *Earth-Science Reviews*. 81(1-2): 93-134, doi: 10.1016/j.earscirev.2006.12.002.
- Cook, E. R., D. M. Meko, D. W. Stahle, M. K. Cleaveland (1999). "Drought reconstructions for the continental United States." *Journal of Climate*. 12(4):1145-1162.
- Cosgrove D. M., G. S. Johnson, D. R. Tuthill (2008). "The role of uncertainty in the use of ground water models for administration of water rights." *Journal of Contemporary Water Research and Education*. 140(1):30-36, doi: 10.1111/j.1936-704X.2008.00026.x.
- Cosgrove D. M., Contor, B. A., Johnson G. S. (2007). Enhanced Eastern Snake Plain Aquifer Ground-water Rights Transfer Spreadsheet Version 3.1 Users Manual. Idaho Water Resources Research Institute, University of Idaho, Idaho Falls, ID 83402.

- Cosgrove D. M., Contor B. A., Johnson G. S. (2006). Enhanced Snake Plain Aquifer Model Report. Idaho Water Resources Research Institute Technical Report 06-002, Eastern Snake Plain Aquifer Model Enhancement Project Scenario Document Number DDM-019, Idaho Water Resource Research Institute, Idaho Falls, ID 83402.
- Cosgrove D. M. and G. S. Johnson (2005). "Aquifer management zones, based on simulated surface-water response functions." *Journal of Water Resources Planning and Management* 131(2): 89-100, doi: 10.1061/(ASCE)0733-9496(2005)131:2(89).
- Dai, A., K. E. Trenberth, T. T. Qian (2004). "A global dataset of Palmer Drought Severity Index for 1870-2002: Relationship with soil moisture and effects of surface warming." *Journal of Hydrometeorology*. 5(6):1117-1130.
- DEQ (2005), "The Eastern Snake River Plain Aquifer." *State of Idaho Oversight Monitor*, Idaho National Laboratory, Boise, Idaho. (www.deq.idaho.gov/inl-oversight/library/newsletter0505.pdf, February 22, 2011).
- Fiege M. (1999). *Irrigated Eden: The making of an agricultural landscape in the American West*. University of Washington Press, Seattle WA, 98145-5096.
- Franchini, M. and M. Pacciani (1991). Comparative analysis of several conceptual rainfall runoff models. *Journal of Hydrology*. 122:161-219.
- Guttman N. B., R. G. Quayle RG (1996). "A Historical Perspective of U.S. Climate Divisions." *Bulletin of the American Meteorological Society*. 77(2): 293-303.
- Gilliland, B. K. (2002). Aggregation of Surface Water Canal Companies into Surface Water Irrigation Entities. Idaho Water Resources Research Institute Technical Report 04-014, Eastern Snake Plain Aquifer Model Enhancement Project Scenario Document Number DDW-008, Idaho Water Resources Research Institute, University of Idaho, Moscow, ID.
- Hamlet, A.F. and D.P. Lettenmaier (2005). "Production of temporally consistent gridded precipitation and temperature fields for the continental United States." *Journal of Hydrometeorology*. 6(3):330-336.
- Hamlet, A.F., A. Sover, D.P. Lettenmaier (2002). "Climate Change Scenarios for Pacific Northwest Planning Studies: Motivation, Methodologies, and a User's Guide to Applications," Center for Science in Earth System, Department of Civil and Environmental Engineering, University of Washington.
- Hamlet, A. F. and D. P. Lettenmaier (1999). "Effects of climate change on hydrology and water resources in the Columbia River basin." *Journal of the American Water Resources Association*. 35(6):1597-1623.

- Hubbell J. M., C. W. Bishop, G. S. Johnson, J. G. Lucas (1997). "Numerical ground-water flow modeling of the Snake River Plain Aquifer using the superposition technique." *Ground Water* 35(1): 59-66.
- IDWR (1999). Feasibility of large-scale managed recharge of the Eastern Snake Plain Aquifer system. Idaho Department of Water Resource, Boise, ID.
- Idaho Power (2011). Hydroelectric. (<http://www.idahopower.com/pdfs/printPDF.cfm>, Jan. 25, 2011).
- Idaho Water Resources Board (1972). *River Operation Studies for Idaho*.
- Idaho Water Resources Board (1975). *Willow Creek – Blackfoot River – Portneuf River Systems*.
- ISHS (2004). The Carey Act in Idaho (www.history.idaho.gov/Carey_Act.pdf). Idaho State Historical Society, Boise, ID 83702.
- ISHS (1972). "The beginning of the New York Canal" *Idaho State Historical Society Reference Series*, Number 190. Idaho State Historical Society, Boise, ID 83702.
- Jin, X. and V. Sridhar (2010, in review). "Impacts of climate change on hydrology and water resources in the Boise and Spokane River basins." *Journal of the American Water Resources Association*.
- Jin, X. and V. Sridhar (2010, unpublished). "Calibration and water balance analysis of Snake River basin under climate change."
- Johnson G. S. and D. M. Cosgrove (1999a). Application of Steady State Response Ratios to the Snake River Plain Aquifer. Idaho Water Resources Research Institute, Moscow, ID 83843.
- Johnson G. S., D. M. Cosgrove, S. Laney, J. Lindgren (1999b). Conversion of the IDWR/UI Ground Water Flow Model to MODFLOW: The Snake River Plain Aquifer Model (SRPAM). Idaho water Resources Research Institute, Moscow, ID 83843.
- Johnson, G. S., W. H. Sullivan, D. M. Cosgrove, R. D. Schmidt (1999). Recharge of the Snake River Plain aquifer: transitioning from incidental to managed. *Journal of the American Water Resource Association* 35(1): 123-131.
- Kendall, M. G. (1975). *Rank Correlation Methods*. Griffin, London.

- Kjelstrom, L. C. (1995). Streamflow gains and losses in the Snake River and groundwater budgets for the Snake River Plain, Idaho and eastern Oregon, US Geological Survey Water-Resources Investigation Report 03-4244.
- Labadie J. W. and R. Larson (2007). *MODSIM 8.1: River Basin Management Decision Support System: User Manual and Documentation*. Colorado State University, Ft. Collins, CO 80523.
- Legutke, S. and R. Voss, (1999). The Hamburg Atmosphere-Ocean Coupled Circulation Model ECHO-G. Technical report, No. 18, German Climate Computer Centre (DKRZ), Hamburg, 62 pp.
- Lettenmaier D. P. (2008). "Have We Dropped the Ball on Water Resource Research?" *Journal of Water Resource Planning and Management* 134(6): 491-492.
- Liang X., D. P. Lettenmaier, E. F. Wood, and S. J. Burgess (1994). "A simple hydrologically based model of land, surface, water, and energy fluxes for general circulation models." *Journal of Geophysical Research*. 99:14415-14428.
- Lohmann D., E. Raschke, B. Nijssen, D. P. Lettenmaier (1998a). "Regional scale hydrology: I. Formulation of the VIC 2L model coupled to a routing model." *Hydrological Sciences*, 43(1), 131-141.
- Lohmann D., E. Raschke, B. Nijssen, D. P. Lettenmaier (1998b). "Regional scale hydrology: II. Application of the VIC-2L model to the Weser River, Germany." *Hydrological Sciences*, 43(1), 143-158.
- Lovin H. T. (2002). "Dreamers, schemers, and doers of Idaho irrigation." *Agricultural History Society*. 76(2): 232-243.
- Maidment, D. R. (editor in chief) (1993). *Handbook of Hydrology*, McGraw-Hill, Inc, Chapter 18, pp 18-25.
- Mann, H. B. (1945). "Nonparametric tests against trend." *Econometrica*, 13: 245-259.
- Mabey, D. R. (1982). "Geophysics and tectonics of the Snake River Plain, Idaho." *Cenozoic Geology of Idaho*. Bonnicksen, B, R. M. Breckenridge eds., 139-153.
- Meko D. M., C. A. Woodhouse, C. A. Baisan, T. Knight, J. J. Lukas, M. K. Hughes, M. W. Salzer (2007). "Medieval drought in the upper Colorado River basin." *Geophysical Research Letter*. 34:L10705, doi: 10.1029/2007GL029988.
- Miller S. A. , G. S. Johnson, D. M. Cosgrove, R. Larson (2003). "Regional scale modeling of surface and groundwater interactions in the Snake River basin." *Journal of American Water Resources Association*. 39(3): 517-528, doi: 10.1111/j.1752168tb03673.x.

- Milly P. C. D., J. Betancourt, M. Falkenmark, R. M. Hirsch, Z. W. Kundzewicz, D. P. Lettenmaier, R. J. Stouffer (2008). "Stationarity is dead: wither water management?" *Science* 319(5863): 573-574.
- Murphy P. L. (1935). "Early Irrigation in the Boise Valley." *Pacific Northwest Quarterly*. 44: 177-184.
- Mote P. W. and E. P. Salathé (2010). "Future climate in the Pacific Northwest." *Climatic Change*. 102: 29-50, doi: 10.1007/s10584-9848-z.
- Nakićenović N, O. Davidson, G. Davis, A. Grübler, T. Kram, E. L. L. Rovere, B., B. Metz, T. Morita, W. Pepper, H. Pitcher, A. Sankovski, P. Shukla, R. Swart, R. Watson, Z. Dadi (2000). IPCC Special Report: Emissions Scenarios: Summary for Policy Makers. A Special Report of Working Group III of the International Panel on Climate Change. Cambridge University Press, Cambridge, United Kingdom and New York, NY, USA.
- NRCS (2011). Idaho Water Supply Outlook, January 1, 2011. Natural Resource Conservation Service, Boise ID 83709.
- Palmer, W. C. (1965). Meteorological drought, U.S. Weather Bureau Research Paper 45, 3, 19.
- Payne, J. T., A. W. Wood, A. F. Hamlet, R. N. Palmer, D. P. Lettenmaier (2004). "Mitigating the effects of climate change on water resources in the Columbia River basin." *Climatic Change*. 62(1-3): 233-256.
- Pierce J. A. S., M. Bushman, D. Cummings, D. Feichtigher, N. Gollehon, M. Gonella, M. Green, C. Hoefft, S. Mitchell, P. Pasteris, J. Schaefer (2010). A Measure of Snow: Case Studies of the Snow Survey and Water Supply Forecasting Program. United States Department of Agriculture, National Resource Conservation Service, Salt Lake City, UT 84116.
- Radzicki M. J. and R. A. Taylor (1997). Introduction to system dynamics: A systems approach to Understanding Complex Policy Issues. U.S. Department of Energy, Office of Policy and International Affairs, Office of Science and Technology Policy and Cooperation, (www.systemdynamics.org/DL-IntroSysDyn/inside.htm, Jan. 21, 2011).
- Rogers P. (2008). "Coping with global warming and climate change." *Journal of Water Resource Planning and Management*. 134(3): 203-204.
- Salathé, E. P., R. Steed, C. F. Mass, P. H. Zahn (2008). "A high-resolution climate model for the U.S. Pacific Northwest: mesoscale feedbacks and local responses to climate change." *Journal of Climate*. 21(21): 5708-5726, doi: 10.1175/2008/JCLI2090.1.

- Schmidt R. D., L. Stodick, R. G. Taylor (2009). Modeling Spatial Water Allocation and Hydrologic Externalities in the Boise Valley. U.S. Department of Interior Bureau of Reclamation, Pacific Northwest Region, Boise, ID 83706.
- Scott, K (2010). "Modeling Energy Implication of Water Management Decisions on the Eastern Snake River Plain." University of Idaho, Moscow, ID 83844.
- Seager R. (2007). "Turn of the Century North American Drought: Global Context, Dynamics, and Past Analogs." *Journal of Climate*. 20:5527-5552, doi: 10.1175/2007JCLI1529.1.
- Shurtleff, R. (2010). Personal Correspondence, Sept. 24, 2010.
- Simmonds J. (1997). The Boise Project. Bureau of Reclamation, Denver, CO. 80225. (www.usbr.gov/projects/ImageServer?imgName=Doc_1261497242949.pdf, March 1, 2011)
- Simmonds J. (1996). The Palisades Project Bureau of Reclamation, Denver, CO. 80225. (www.usbr.gov/projects/ImageServer?imgName=Doc_1245095449207.pdf, March 1, 2011)
- Slaughter, R. A. (2004). Institutional history of the Snake River 1850-2004. Climate Impacts Group, University of Washington, Seattle, WA 98195-5672.
- Smith, R. P. (2004). "Geologic setting of the Snake River Plain aquifer and vadose zone." *Vadose Zone Journal*. 3(1): 47-58.
- Solomon S., G. Plattner, R. Knutti, P. Friedlingstein (2009). "Irreversible climate change due to carbon emissions." *Proceedings of the National Academy of Sciences*, 106(6): 1704-1709, doi: 10.1073/pnas.0812721106.
- Spearman, C. (1904). "The proof and measurement of association between two things." *American Journal of Psychology*. 15:72-101 (republished (1987) *American Journal of Psychology*. 100:441-471).
- Sridhar, V. and A. Nayak (2010). "Implications of climate-driven variability and trends for the hydrologic assessment of the Reynolds Creek Experimental Watershed, Idaho." *Journal of Hydrometeorology*. 385(1-4): 183-202, doi: 10.1016/j.jhydrol.2010.02.020.
- Stene, E. A. (1997). The Minidoka Project, Bureau of Reclamation, Denver, CO. 80225. (www.usbr.gov/projects/ImageServer?imgName=Doc_1245093434100.pdf, March 1, 2011).
- Stillwater L. (2008). The Effects of Climate Change on the Operation of Boise River Reservoirs, Initial Assessment Report. United State Bureau of Reclamation, Department of the Interior, Boise, Idaho.

- Thornthwaite, C. W. (1948). "An approach toward a rational classification of climate." *Geographical Review*. 38:55-94.
- USACE (2010). Boise River Interim Feasibility Study, Idaho. U.S. Army Corp of Engineers-Walla Walla District – Boise Outreach Office, Boise, ID 83712.
- USBR (2000). River and Reservoir Simulation of the Snake River: Application of MODSIM to the Snake River Basin, United State Bureau of Reclamation, Department of the Interior, Boise, Idaho.
- USDA (2007). 2007 Census of Agriculture, www.agcensus.usda.gov/Publications/2007/Online_Highlights/Farm_and_Ranch_Irrigation_Survey/fris08_1_01.pdf (Jan. 21, 2011).
- USGS (2010). Report as of FY 2009 for 2009ID138B: 'Modeling Energy Implications of Water Management Decisions in the Upper Snake River Basin' (downloaded at <http://water.usgs.gov/wrri/09grants/2009ID138B.html>, Feb. 8, 2011)
- VanRheenen N. T., R. N. Palmer, A. F. Hamlet, D. P. Lettenmaier (2003). "Climate change, fish, agriculture, and power: impacts and implications for future Snake River water resources management." Conference Proceedings Paper, World Water & Environmental Resources Congress, 2003, doi: 10.1061/40685(2003)92.
- Wang, A. H., T. J. Bohn, S. P. Mahanama, R. D. Koster, D. P. Lettenmaier (2009). "Multimodel ensemble reconstruction of drought over the continental United States." *Journal of Climate*. 22(10): 2694-2712, doi: 10.1175/2008JCLI2586.1.
- Weart S. R. (2008). *The Discovery of Global Warming*. Harvard University Press, Cambridge, Mass. (<http://www.aip.org/history/climate>)
- Welhan J. A. and M. F. Reed (1997). "Geostatistical analysis of regional hydraulic variations in the Snake River Plain Aquifer, Eastern Idaho." *Geological Society of America Bulletin*. 109(7): 855-868.
- Wood, A. W., E. P. Maurer, A. Kumar, and D. P. Lettenmaier (2002). "Long range experimental hydrologic forecasting for the eastern U.S.," *Journal of Geophysical Research*. 107(D20), 4429, doi:10.1029/2001JD000659.
- Woodhouse C. A., K. E. Kunkel, D. R. Easterling, E. R. Cook (2005). "The twentieth-century pluvial in the western United States." *Water Resource Research Letters* 32: L07701, doi: 10.1029/2005GL022413.

APPENDIX A

**Source, Diversion Identification, and Canal Companies
for Each Diversion in SRPM and SD-SRPM**

Table A Source, Diversion Identification, and Canals for Each Diversion in SRPM and SD-SRPM

Diversion Source	Diversion	Canals	Data Limitations
Falls River	010	Yellowstone, Marysville	
	015	Misc. diversions Squirrel to Chester	
	020	Farmers Own, McBee, Silkey	
	030	Enterprise	
	035	Fall River	
	040	Chester, Curr	
Henry's Fork	045	Dewey, Last Chance	
	050	St. Anthony Union	
	060	Farmer's Friend, Twin Groves, Salem Union	
	070	Egin Canal, St. Anthony Union Feeder, Independent	
	080	Consolidated Farmers	
Teton River	090	Siddoway, Teton Irrigation, Woodmansee-Johnson	Teton Dam collapse of 1976 may bias trends
	100	Wilford, Pioneer, Stewart	
	110	Pincock-Byington	
	120	City of Rexburg, Rexburg Irrigation	
Snake River (Heise to Lorenzo)	135	Anderson	
	137	Farmers Friend, Enterprise, Salem Union	
	140	Harrison, Boomer & Rudy	
	145	Burgess	
	150	Ross & Reid, Lowder & Jennings, Clark & Edwards, Labelle & Long Island, Parks and Lewisville, North Rigby, White, Bramwell, Ellis, Mattson Craig	
	160	Sunny Dell, Lenroot, Reid, Texas Feeder, Bannock-Jim, Hill-Petinger, Nelson-Corey	
Snake River (Lorenzo to Blackfoot)	170	Butte and Market Lake	
	180	Kennedy, Great Western, Porter, Woodville, Bear Trap	
	190	Idaho	
	200	Snake River Valley	
	220	Blackfoot, Corbett, Nielsen-Hansen	
	230	New Lava	
	240	Peoples	
	242	Aberdeen-Springfield	
Blackfoot River	248	Fort Hall Main	
	249	Fort Hall North	
Snake River (Blackfoot to Milner)	253	Fort Hall Mauchad	
	260	Burley Southside	
	270	Minidoka Northside	
	280	Twin Falls Southside	
	285	Northside Minidoka Pump	
	290	Milner-Gooding	
300	Twin Falls North Side		
Boise River	505	Penitentiary	
	515	New York #2-6	1971-1999
	520	Mora	1971-1999
	525	New York #6-10	1971-1999
	530	Lake Lowell	1971-2003

	535	Ridenbaugh	
	540	Bubb, Rossi Mill, Boise City	
	545	Settlers, Davis	
	550	Thurman Mill	
	555	Farmers Union	
	560	New Dry Creek, Ballentyne, Middleton, Little Pioneer	
	562	Lemp, Warm Springs, Graham-Gilbert, Conway-Hamming, Aiken, Mace-Catlin, Mace-Mace, Hart-Davis, Seven Suckers	
	564	Phyllis	
	568	Canyon County	
	570	Caldwell Highline	
	574	Riverside, Pioneer Dixie	
	576	Sebree, Campell, Siebenberg	
	580	Eureka2, Upper Center Point, Lower Center Point, MacManus & TR	
	585	Bowman & Swisher, Baxter, Andrews, Mammon, Haas, Parma, Island Highline, McConnell	
Payette River	620	Northside Black Canyon	1971-2002
	625	Southside Black Canyon	1971-2002
	640	Last Chance, Farmers Cooperative, Gill Slough, Smith Ditch, Enterprise, Bilbrey, Reed, Kesgard-Tschudy, O'Turley Ditch, Sietz, Woods, Payette River Ranch	1993-2005
	655	Patton-Riggs Ditch, Noble, Rosebury, Stewart, Nichols, Pulley Ditch, Rasmussen, Pump Cooper	1993-2005
	670	Upper Accord, Lower Accord, Nesbitt-McFarland, Barker, Burt, Hendrickson Pump, Pence Pump, Lower Payette Canal, Island Farms Ditch, Johnson Ditch, Simplot Pump, B May Pump	1993-2005

APPENDIX B

Schematics of SRPM and SD-SRPM

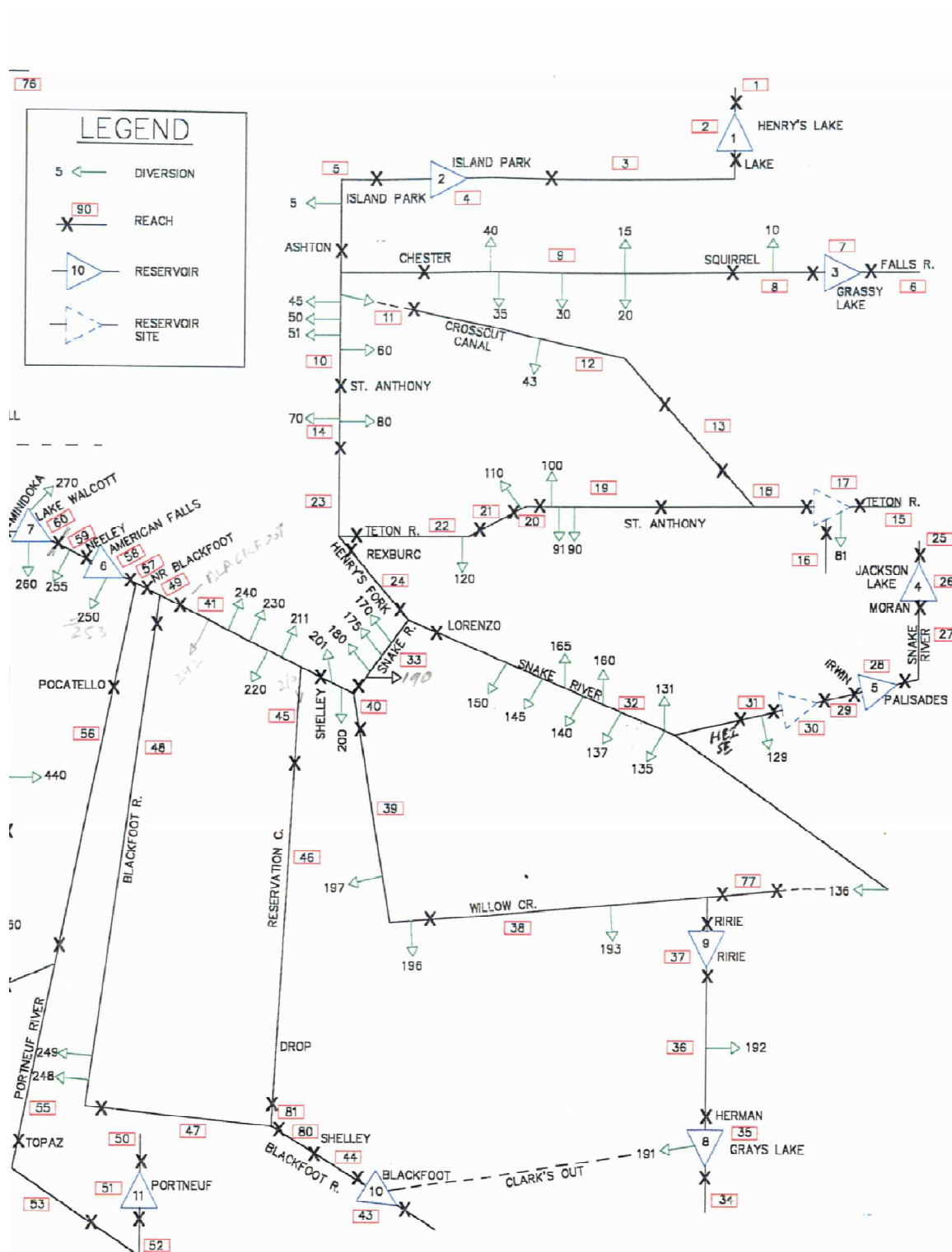


Figure B.1 Schematic of SRPM Provided by Dr. Sudhir Goyal of IDWR Showing the Eastern Snake River Basin

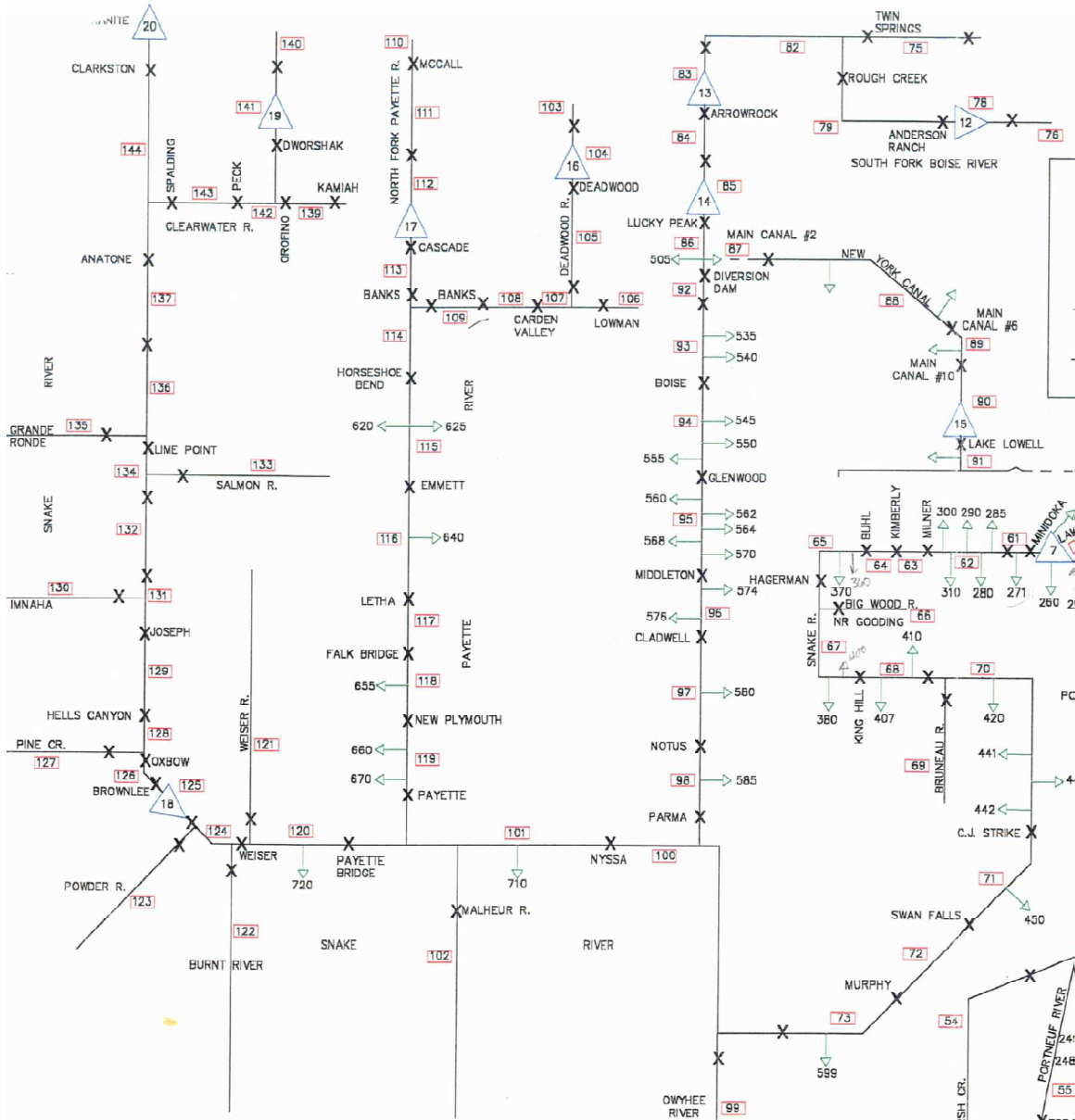


Figure B.2 Schematic of SRPM Provided by Dr. Sudhir Goyal of IDWR Showing the Western Snake River Basin

Figure B.3 Schematic of the Natural Flow Structure in SD-SRPM above Lake Walcott, Excluding Southern Tributaries

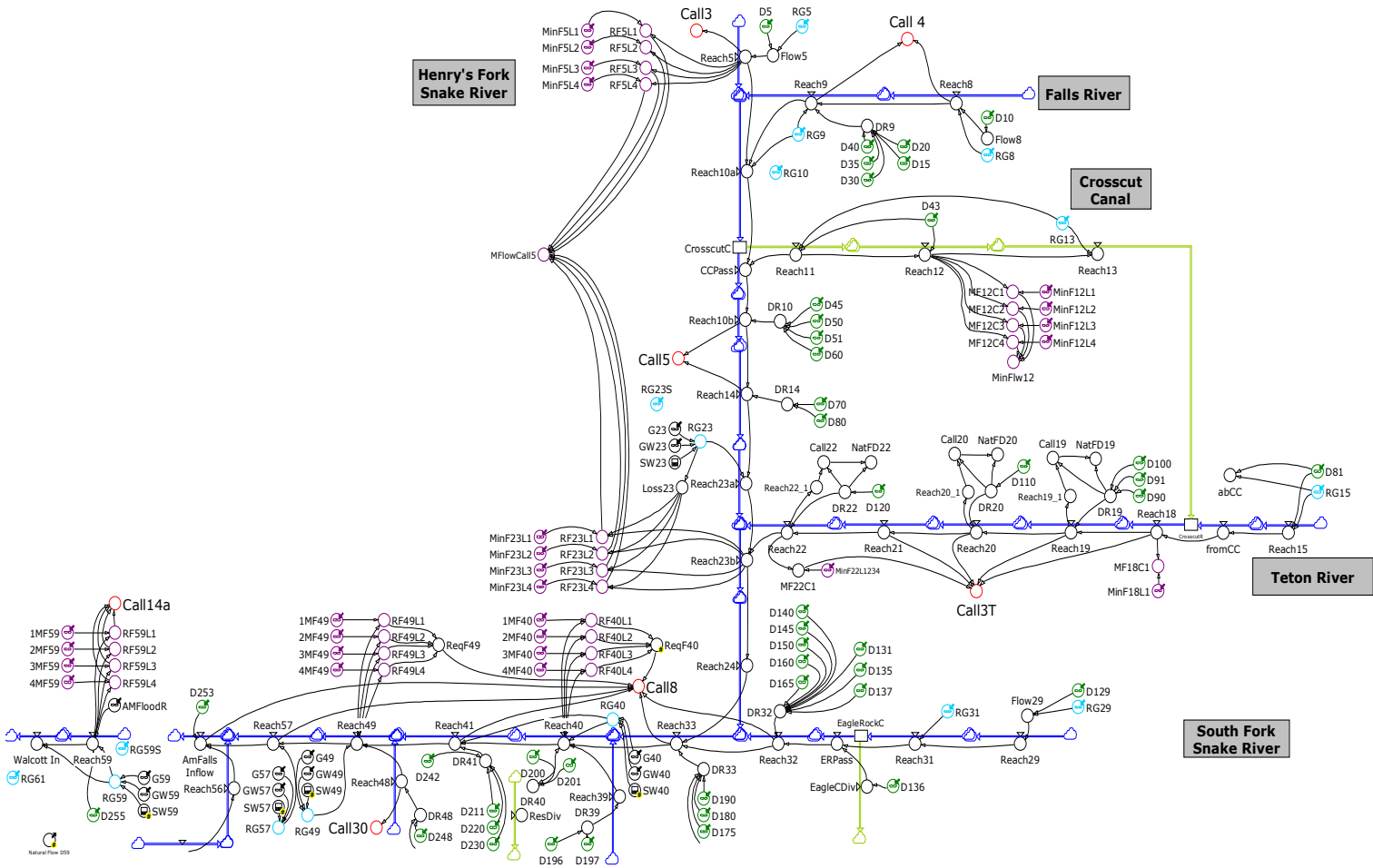
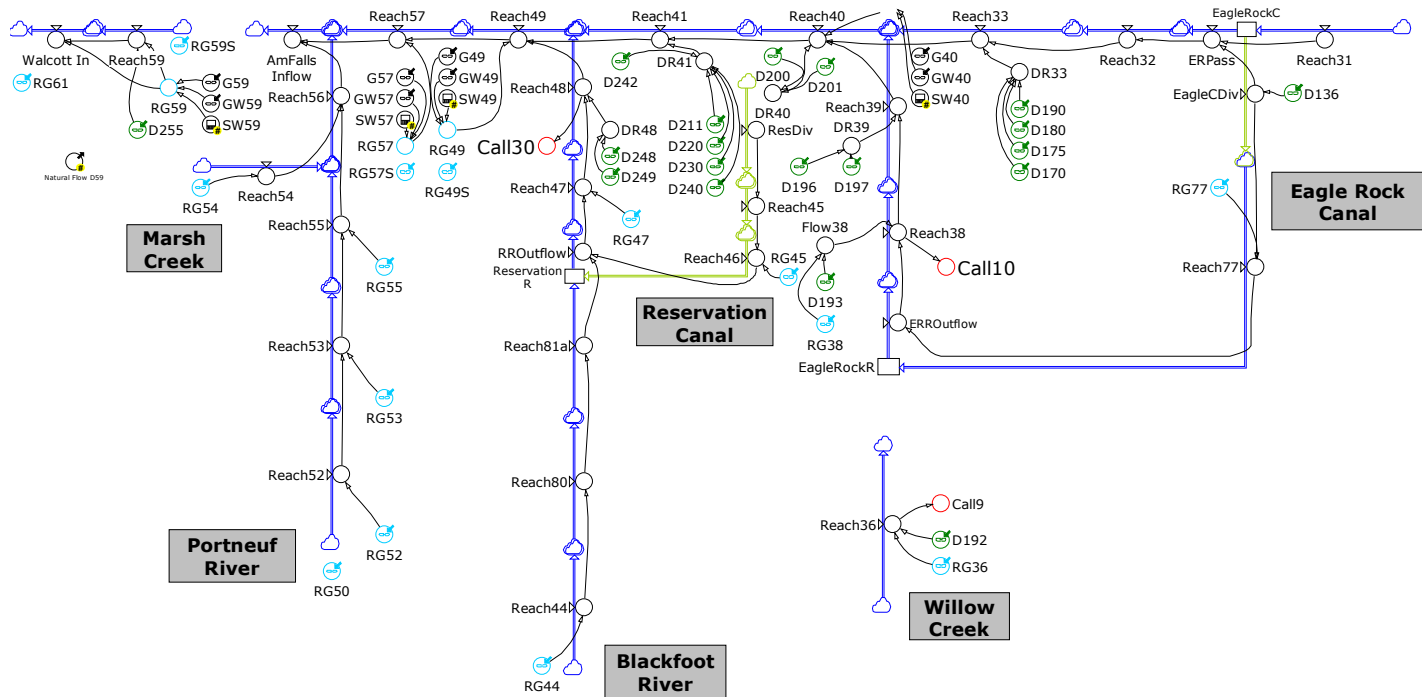


Figure B.4 Schematic of the Natural Flow Structure in SD-SRPM of Southern Tributaries above Lake Walcott



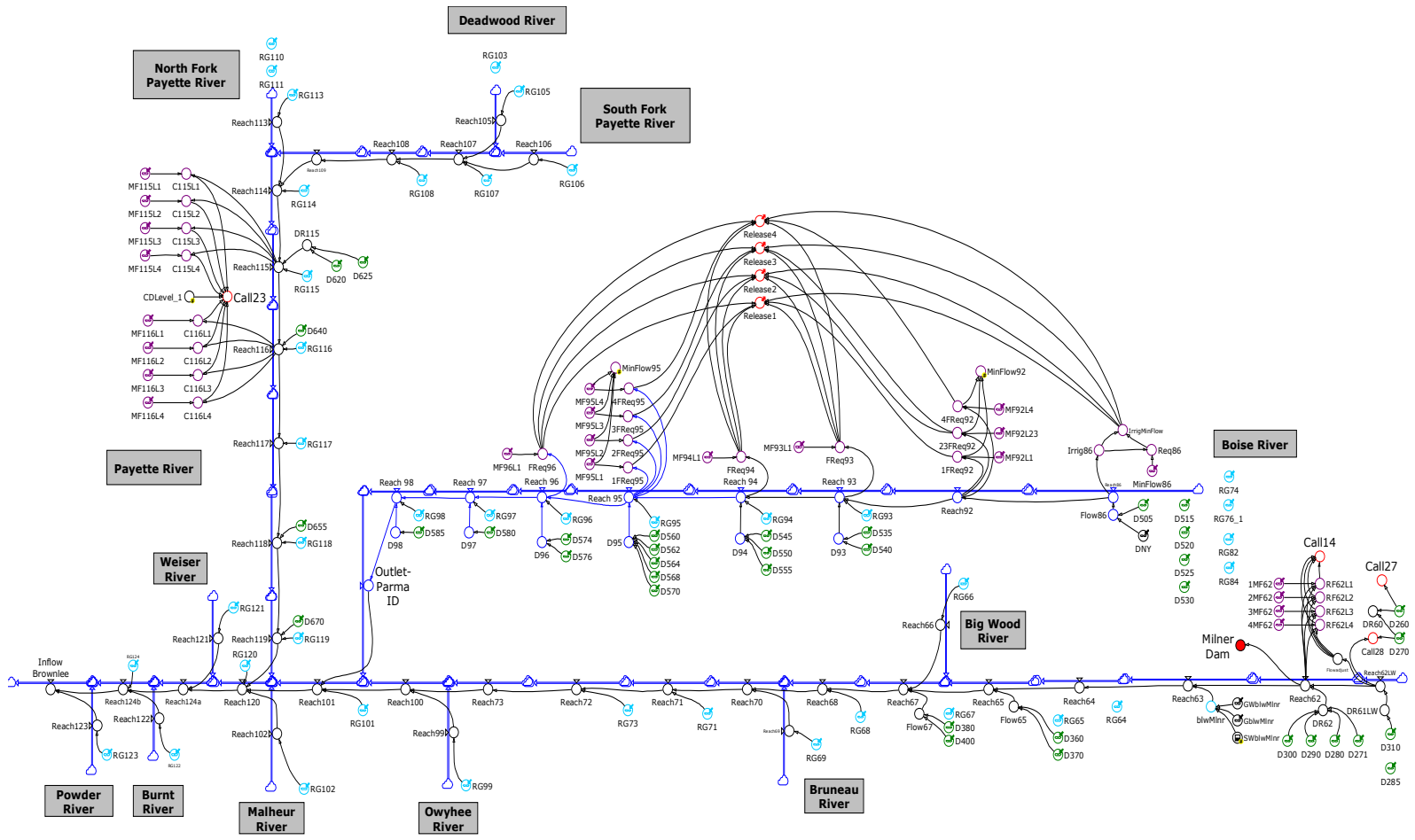


Figure B.5 Schematic of the Natural Flow Structure in SD-SRPM below Lake Walcott

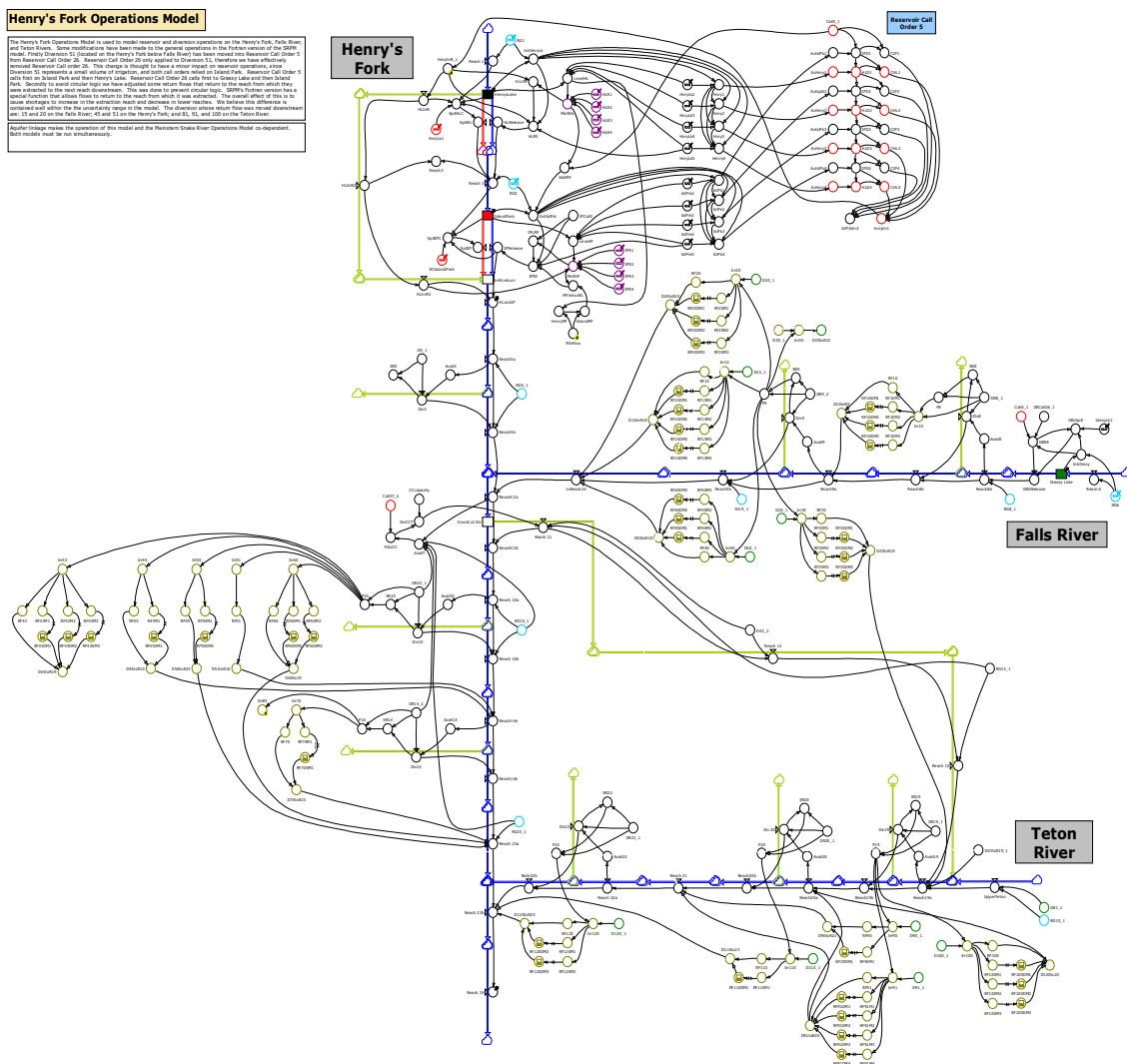


Figure B.6 Schematic of the Regulated Flow Structure for the Henry's Fork, Falls River, and Teton River

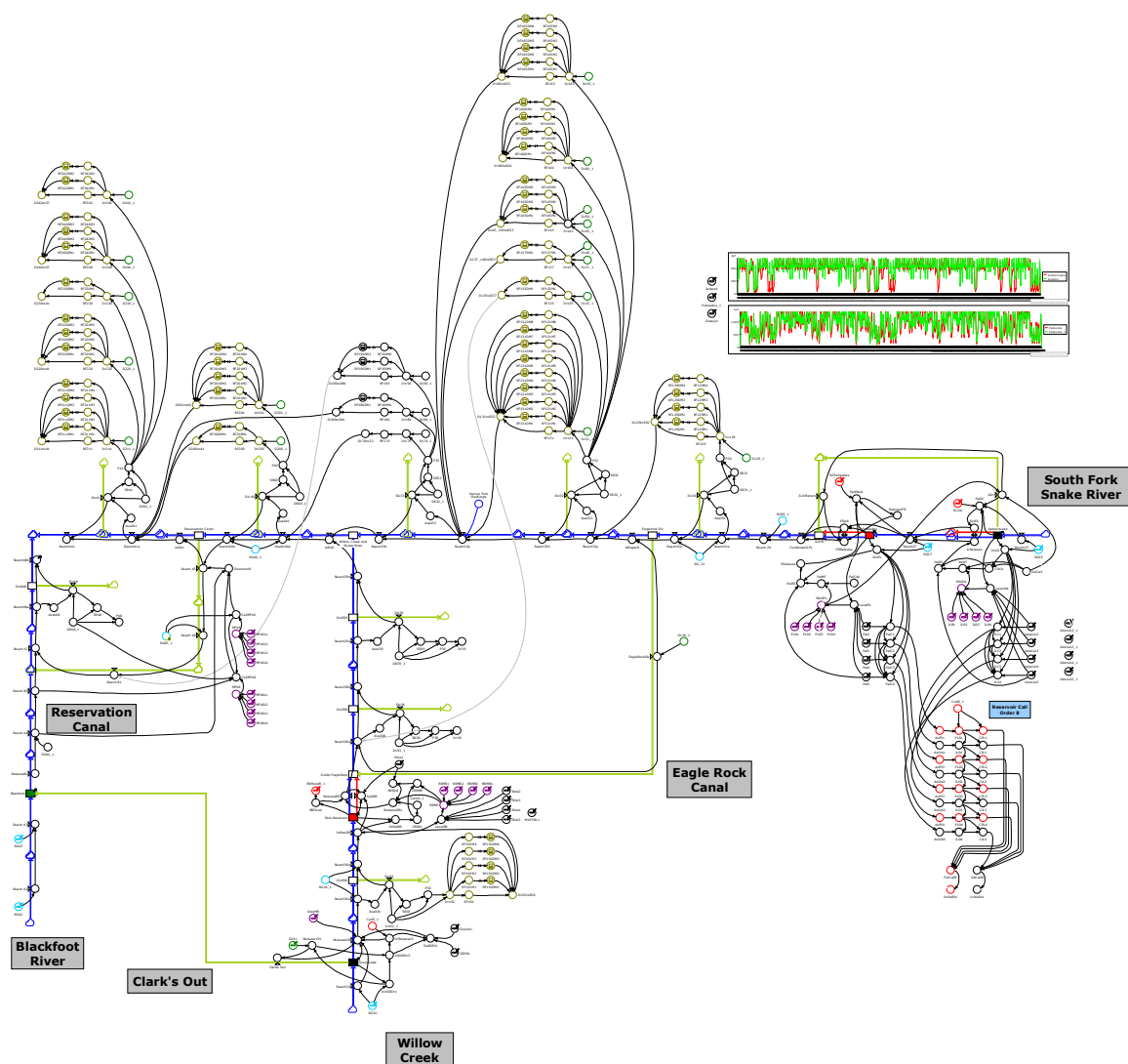


Figure B.7 Schematic of the Regulated Flow Structure for the South Fork of Snake River, Willow Creek, Blackfoot Rivers, and Mainstem of the Snake River above Blackfoot

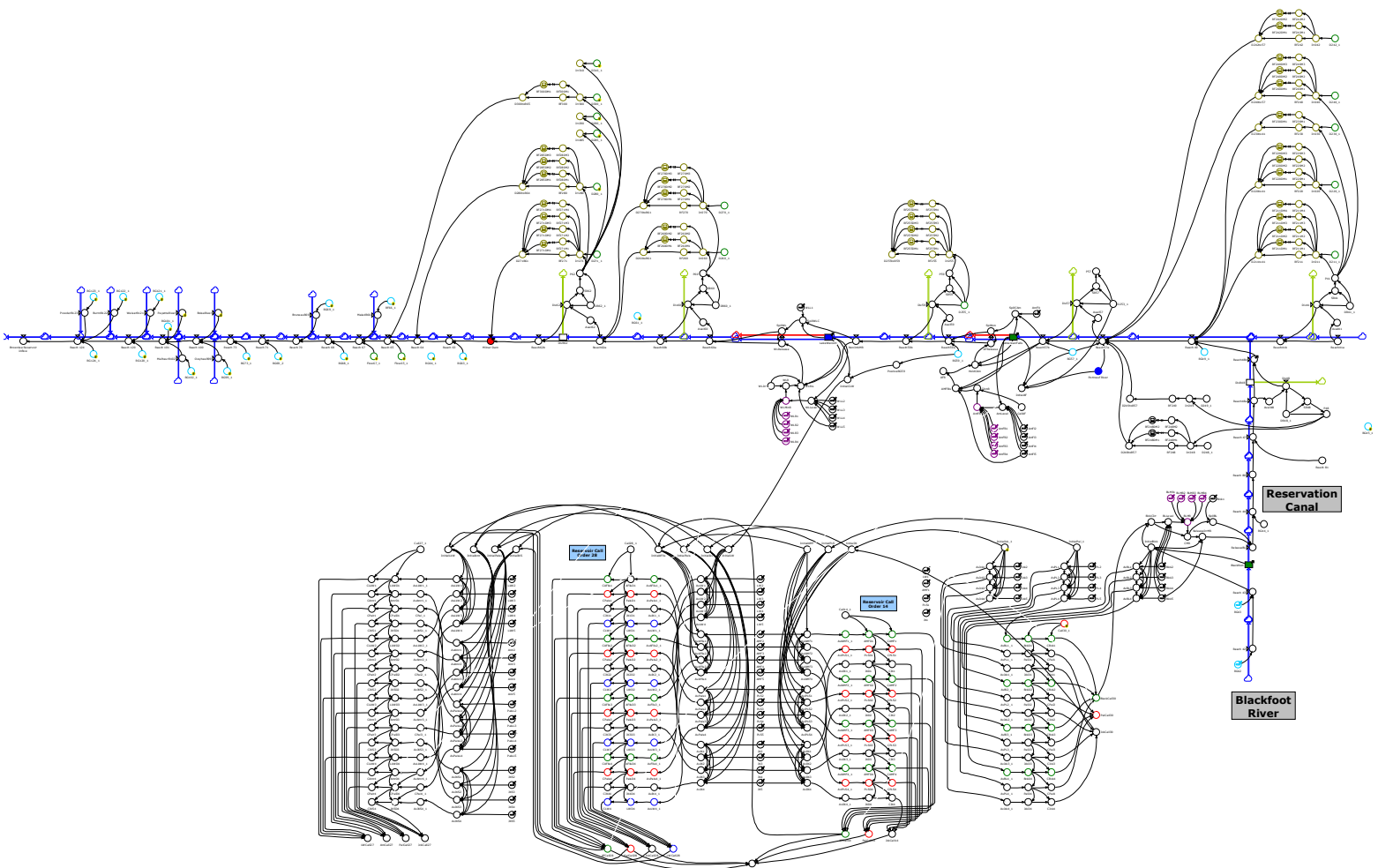


Figure B.8 Schematic of the Regulated Flow Structure for the Blackfoot River and Mainstem of the Snake River above Blackfoot

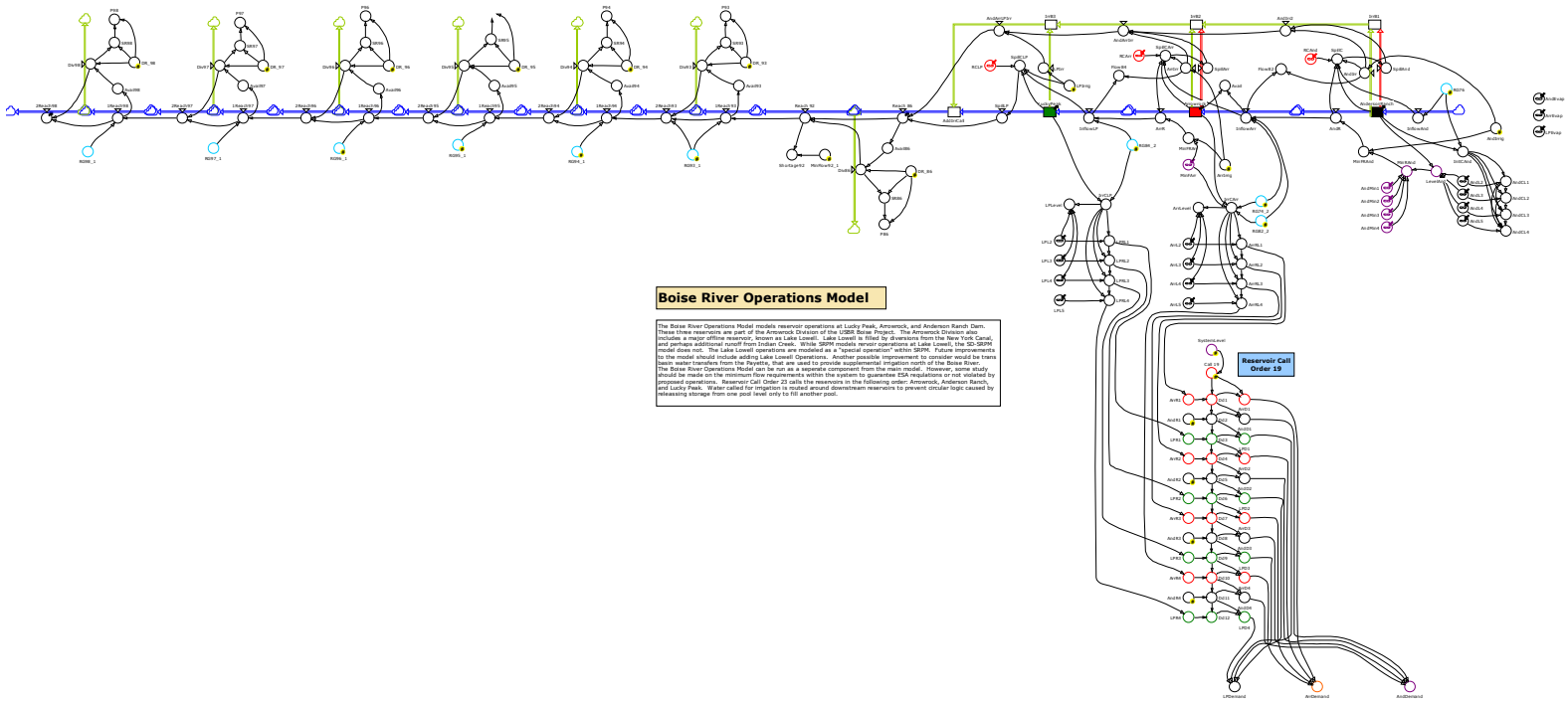


Figure B.9 Schematic of the Regulated Flow Structure for the Boise River

Payette River Operations Model

The Payette River Operations Model models reservoir operations at Lake Cascade and Deadwood Reservoir. These two reservoirs are part of the Payette Division of the USBR Boise Project. According to Ron Shurtleff, watermaster on the Payette, there is still some unallocated water at the end of the system. This portion of the Snake River system may play a crucial role in providing instream flow requirements for the ESA. Like the Boise River Operations model it can be run as an independent component.

North Fork Payette River

Deadwood River

South Fork Payette River

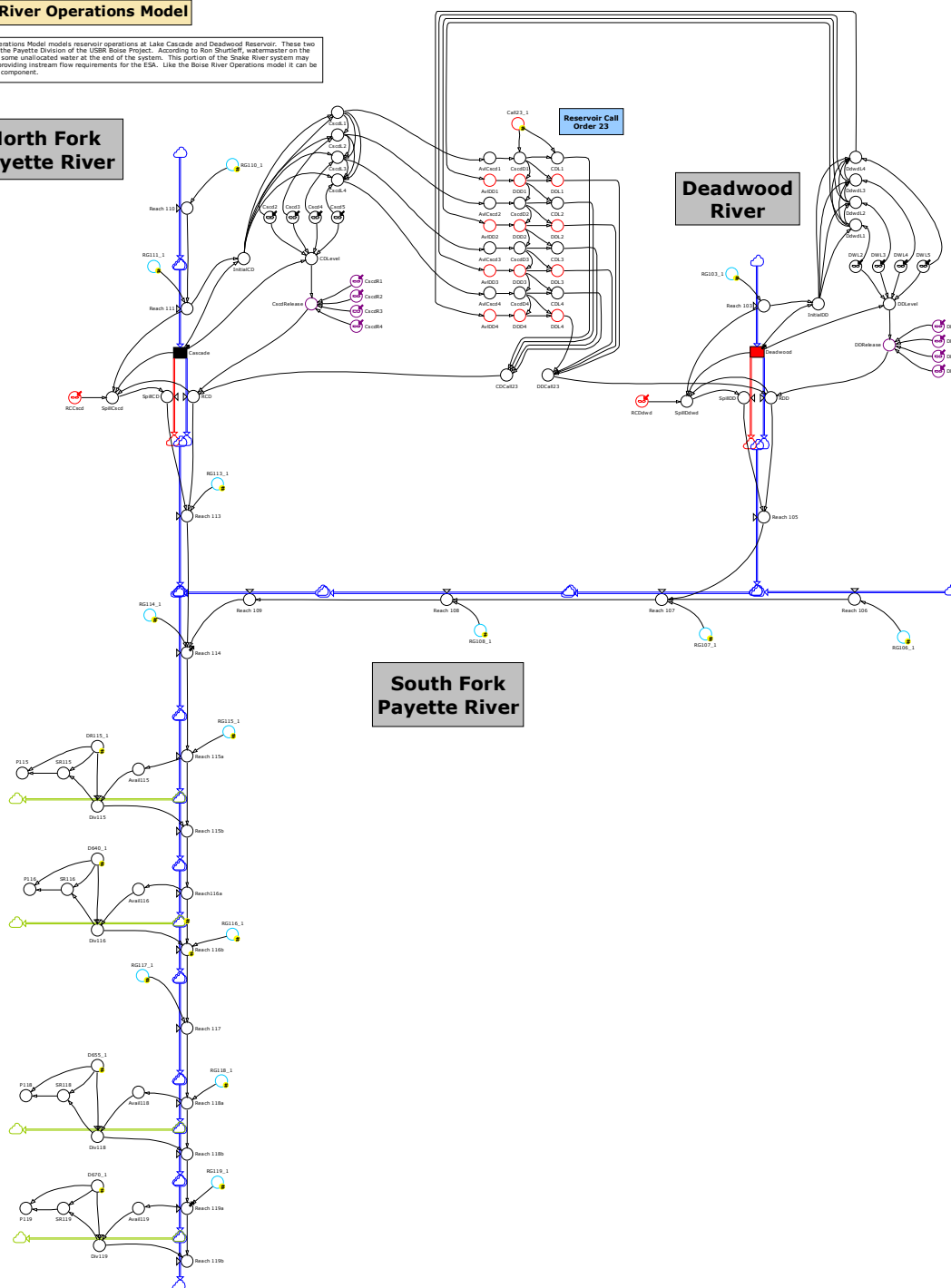
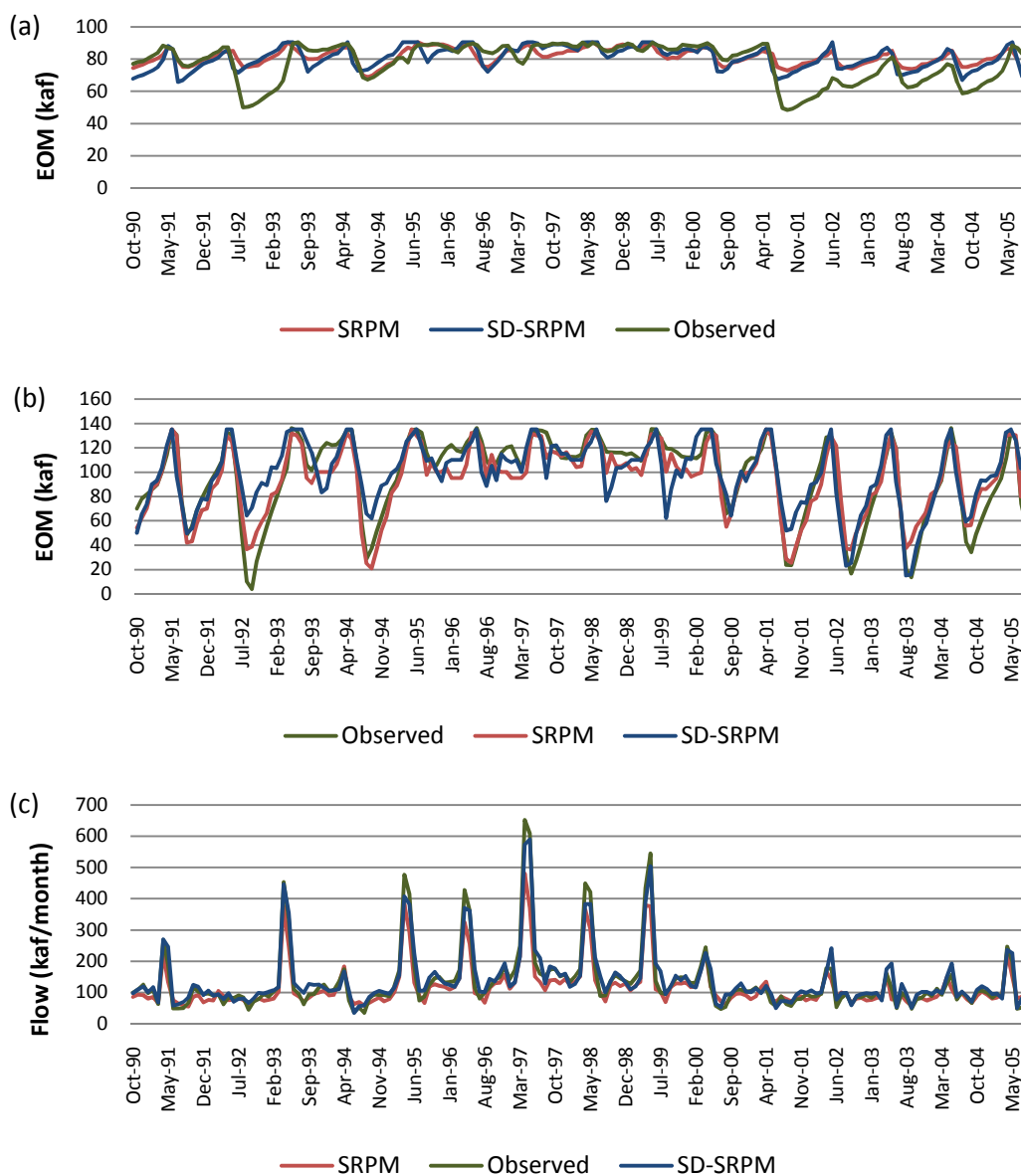


Figure B.10 Schematic of the Regulated Flow Structure for the Payette River

APPENDIX C

**Comparison between SRPM and SD-SRPM for EOM and
Regulated Flow Hydrographs**

Appendix C contains figures representing a comparison of SRPM and SD-SRPM using the original diversion file and reach gain file provided by IDWR. The diversion file represents actual diversions from 1991-2005. Observed values are based on USBR estimated reservoir content on the last day of the month and USGS gaged monthly average streamflow.



**Figure C.1 Reservoir EOM within the Henry's Fork Basin for
(a) Henry's Lake and (b) Island Park on the Henry's Fork and
(c) Flow in the Henry's Fork near Rexburg**

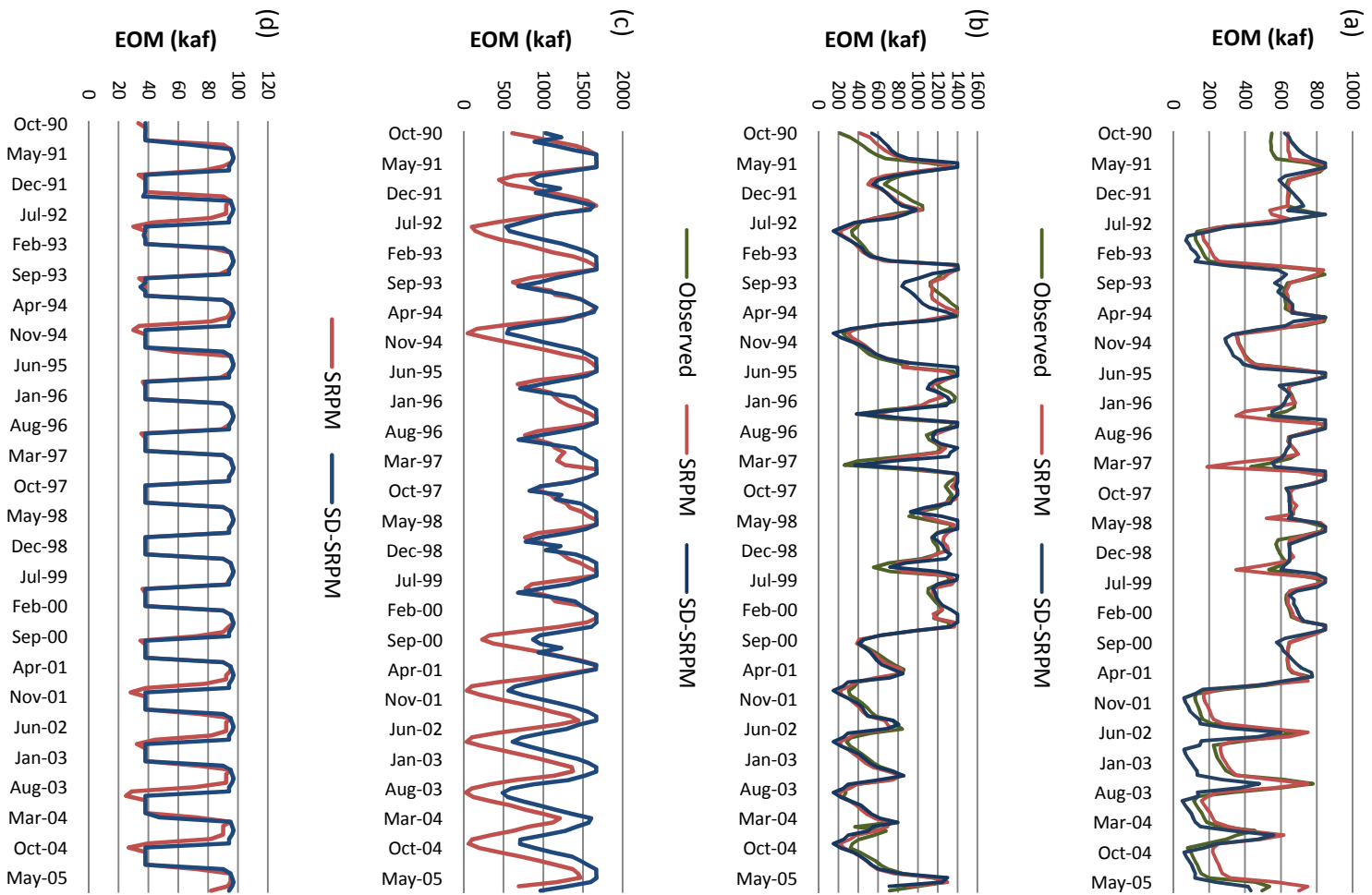


Figure C.2 Reservoir EOM within the South Fork and Mainstem of the Snake River (a) Jackson Lake, (b) Palisades Reservoir, (c) American Falls Reservoir, and (d) Lake Walcott

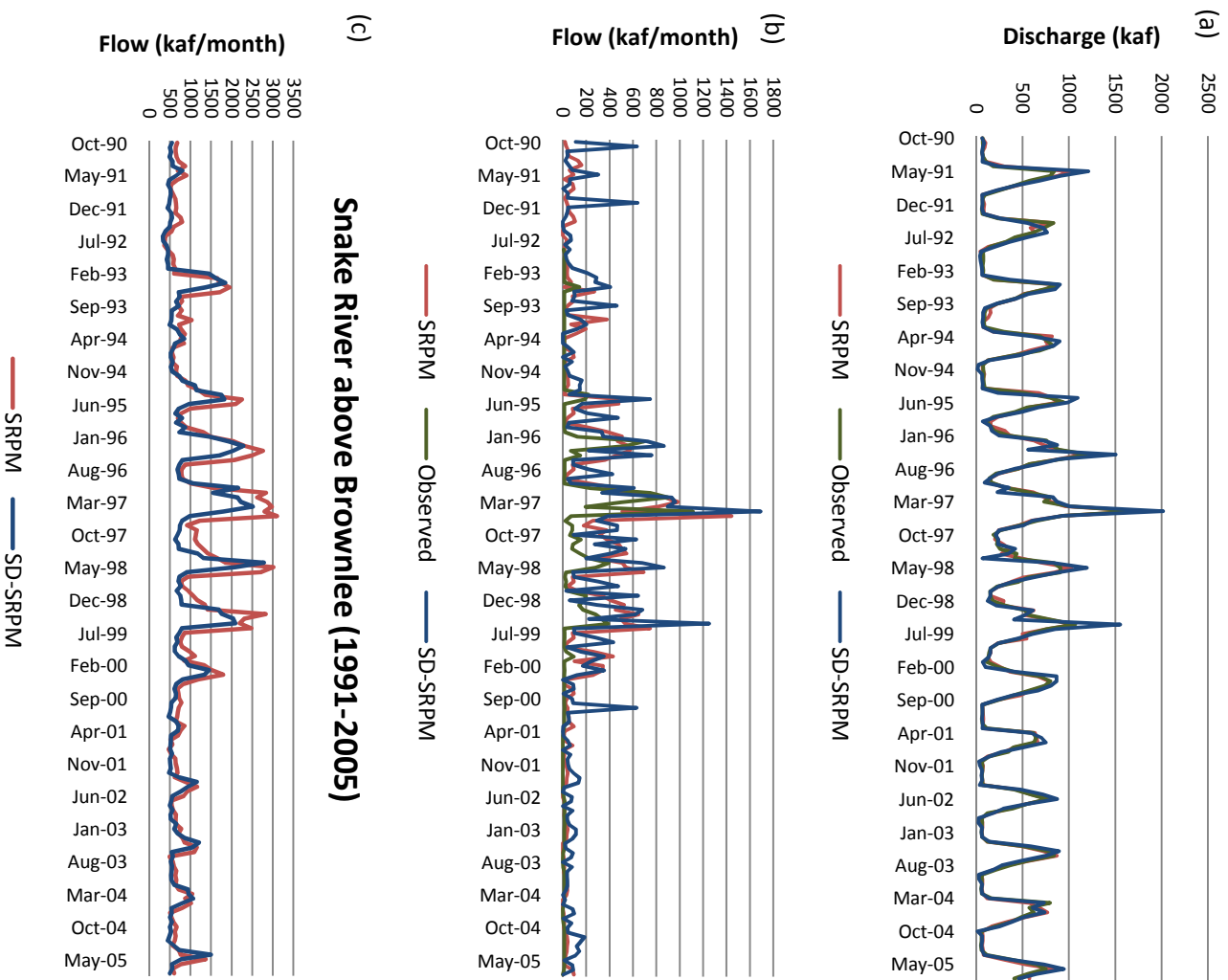


Figure C.3 Streamflow within the Snake River (a) near Irwin, (b) below Milner Dam, and (c) near Weiser

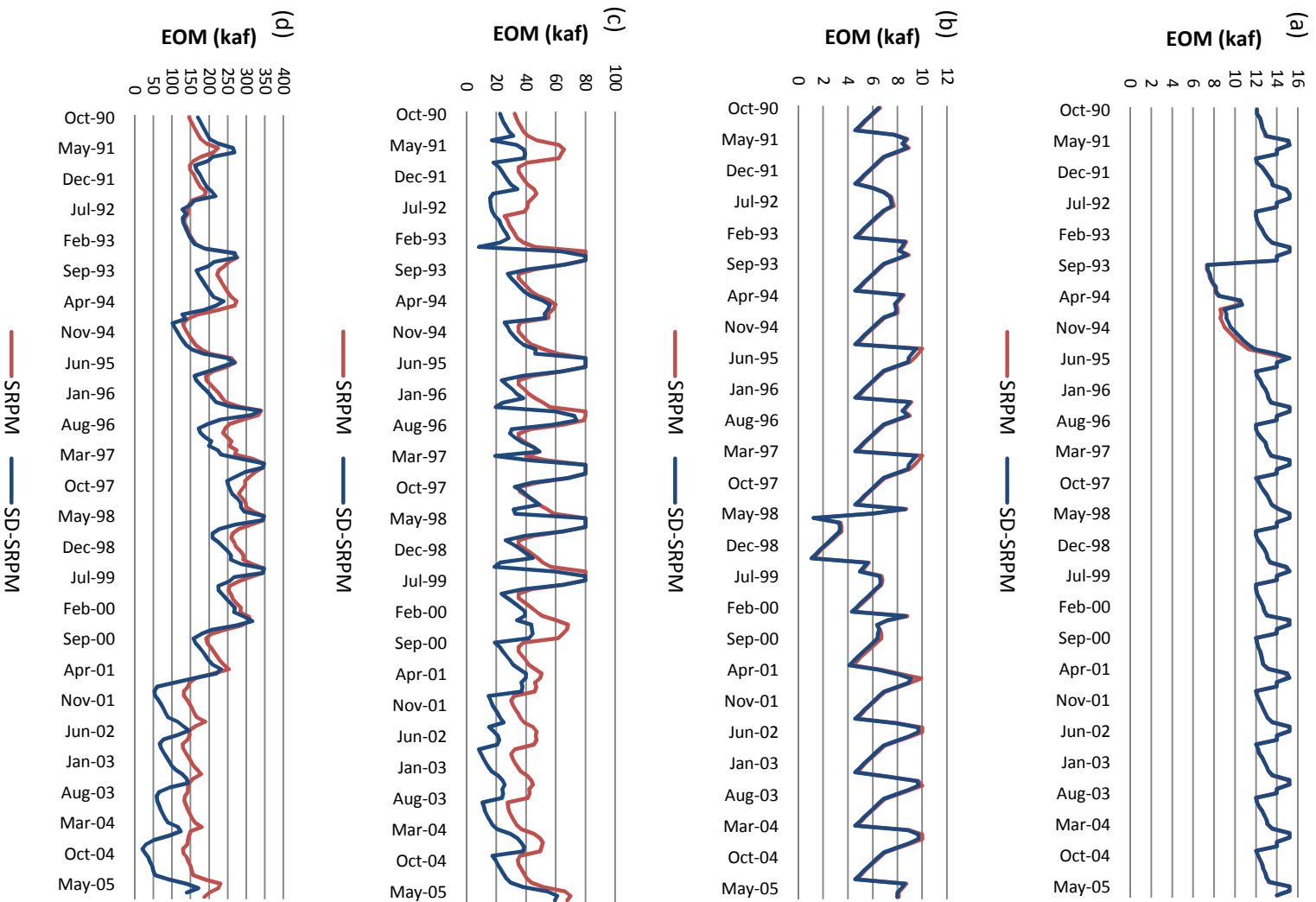
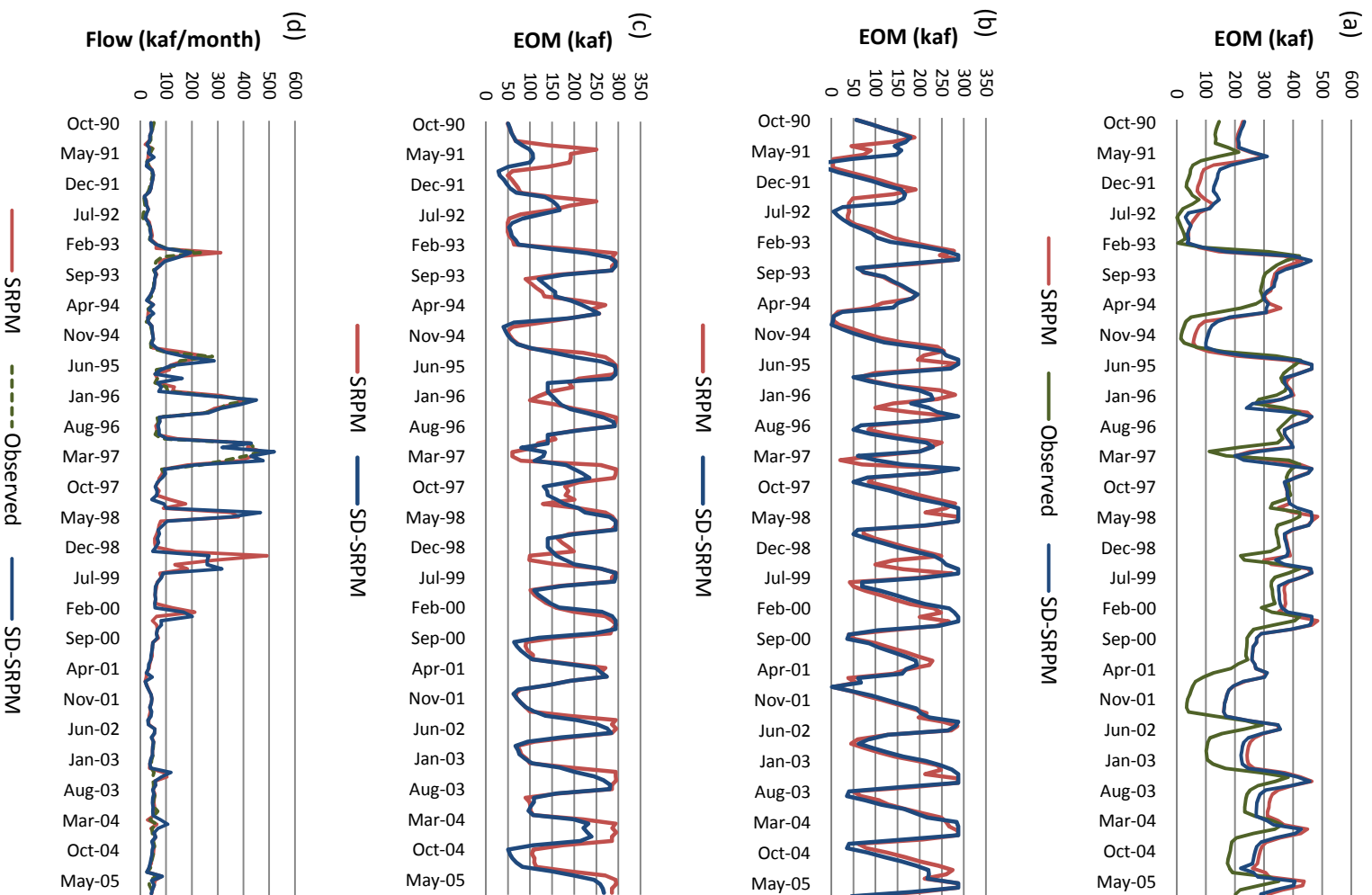


Figure C.4 Reservoir EOM within the Minor Tributaries at
(a) Grassy Lake on Falls River, (b) Grays Lake on Willow Creek,
(c) Ririe Reservoir on Willow Creek, and (d) Blackfoot on the Blackfoot River



**Figure C.5 Reservoir EOM within the Boise River Basin at
 (a) Anderson Ranch Reservoir, (b) Arrowrock Reservoir,
 (c) Lucky Peak Reservoir, and (d) Streamflow near Parma**

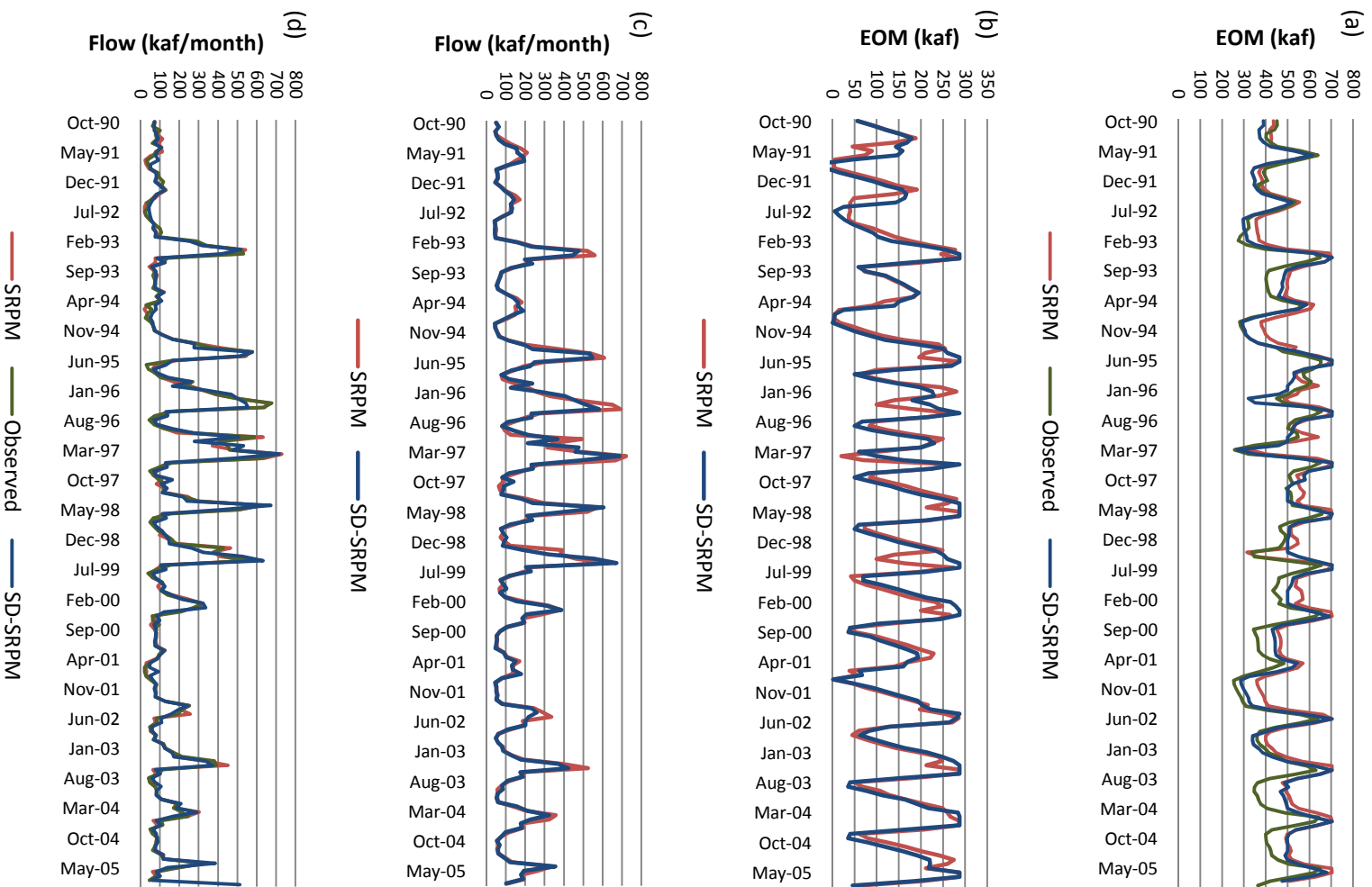


Figure C.6 Reservoir EOM within the Payette River Basin at (a) Lake Cascade and (b) Deadwood Reservoir with Streamflow near (c) Horseshoe Bend and (d) Payette

APPENDIX D

Unregulated Bias Corrected Hydrographs of Historic and Projected Flow

Appendix D contains hydrographs comparing projected, bias corrected flow to historic flow hydrographs. The following hydrographs represent the 30-year average hydrograph for the two historic periods (1931-1960 and 1976-2005) with three projected periods (2011-2040, 2041-2070, and 2071-2099). The historic hydrographs are based on data provided by IDWR. The projected flow is based on downscaled GCM data run through the VIC hydrologic model and bias corrected using quantile mapping. Details for the GCMs and bias correction technique are found in *Chapter 6*.

The figures in this appendix are arranged by location and GCM as follows: PCM1, CCSM3 and ECHO. The GCM arrangement is according to the temperature change within the model. The ECHO model represents a scenario in which precipitation in the Snake River basin declines by 15% from the historic average and temperature increases by about 10°F by 2099. The CCSM3 model represents a milder increase in temperature (about 7°F by 2099) and precipitation within the historic range. The PCM1 model is slightly wetter and cooler than CCSM3 with a temperature rise of about 5.5°F.

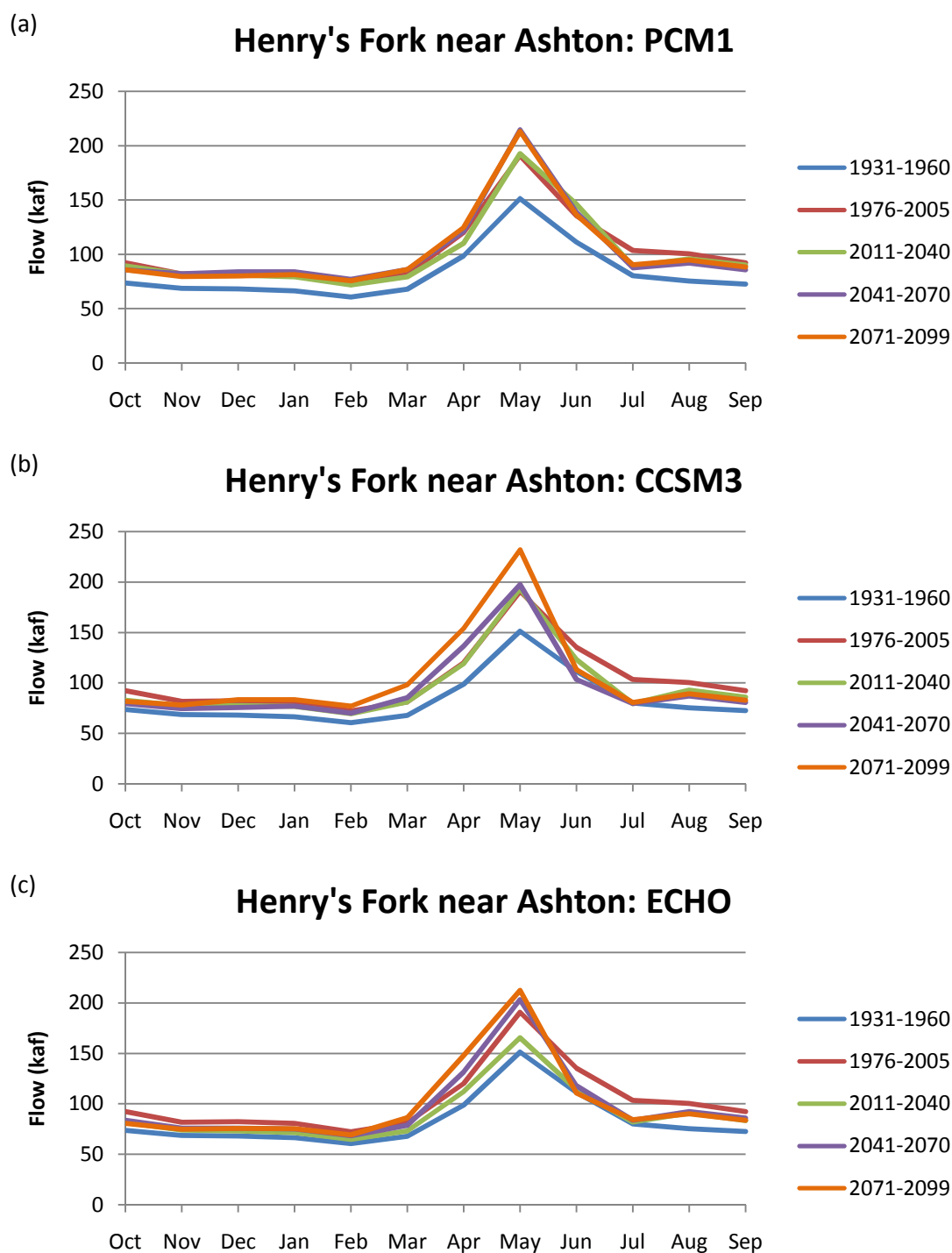


Figure D. 1 Mean, Monthly, Historic, and Projected Flow of the Henry's Fork near Ashton for the (a) PCM1, (b) CCSM3, (c) ECHO GCMs

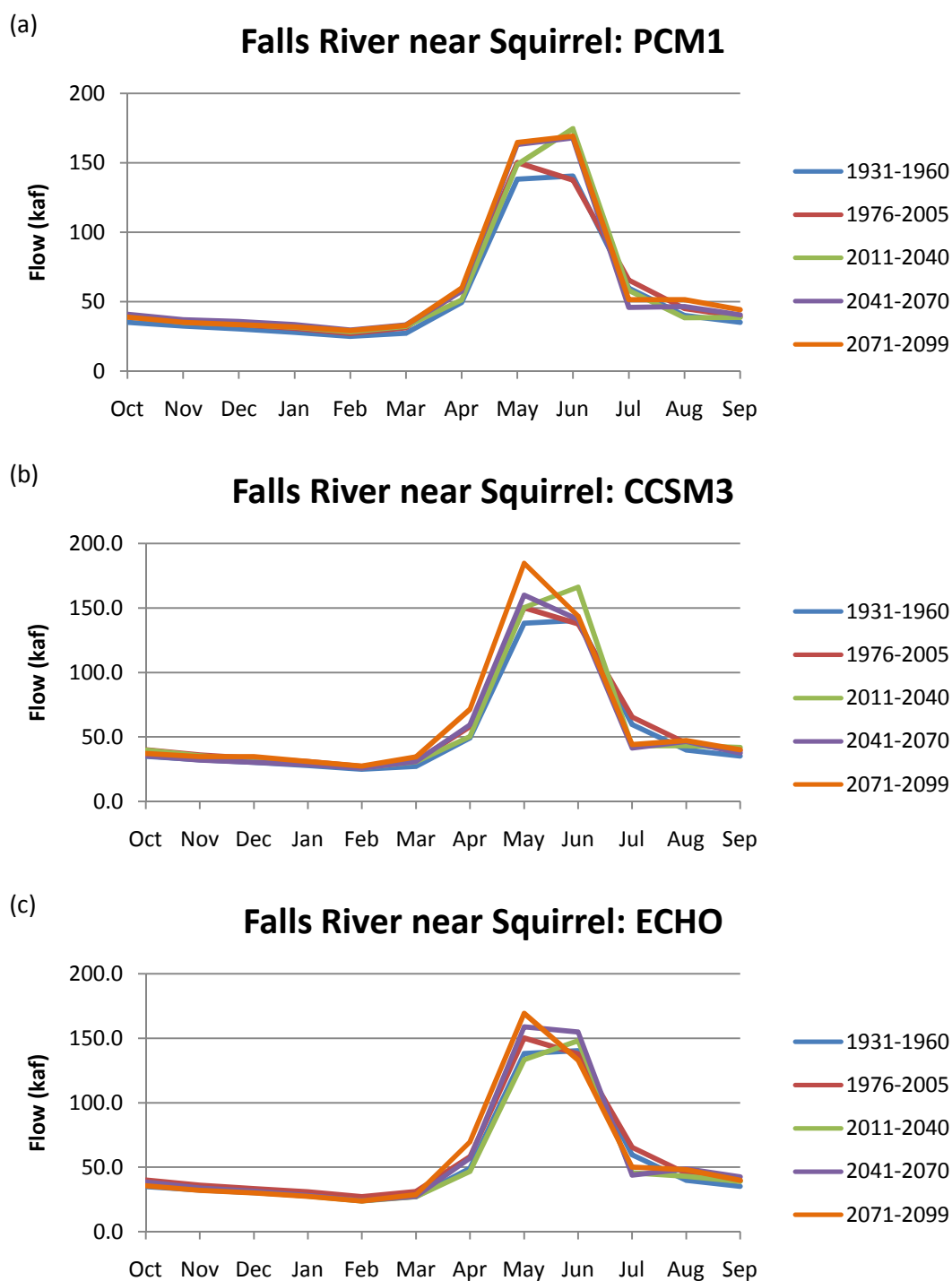


Figure D.2 Mean, Monthly, Historic, and Projected Flow of the Falls River near Squirrel for the (a) PCM1, (b) CCSM3, (c) ECHO GCMs

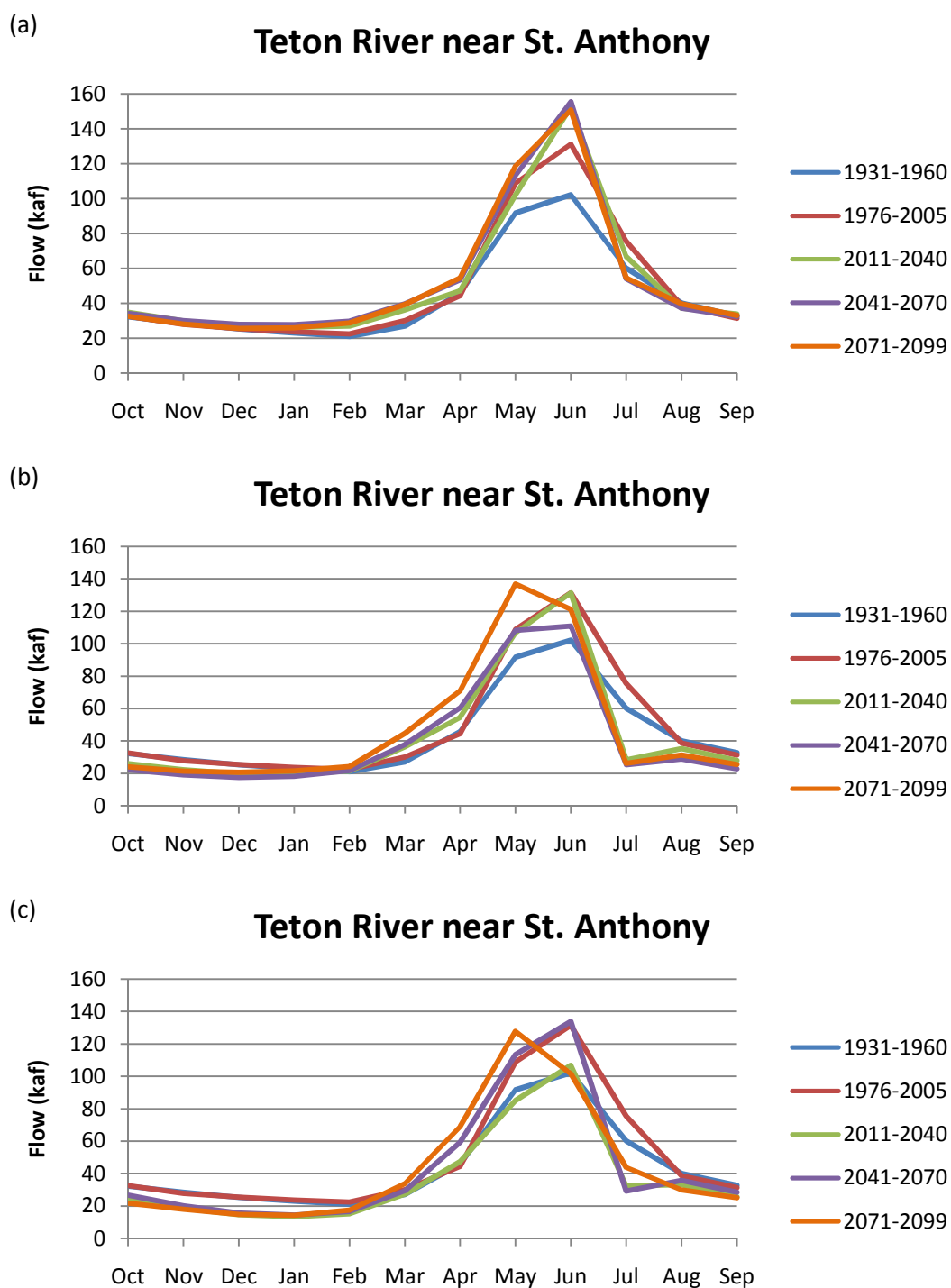


Figure D.3 Mean, Monthly, Historic, and Projected Flow of the Teton River near St. Anthony for the (a) PCM1, (b) CCSM3, (c) ECHO GCMs

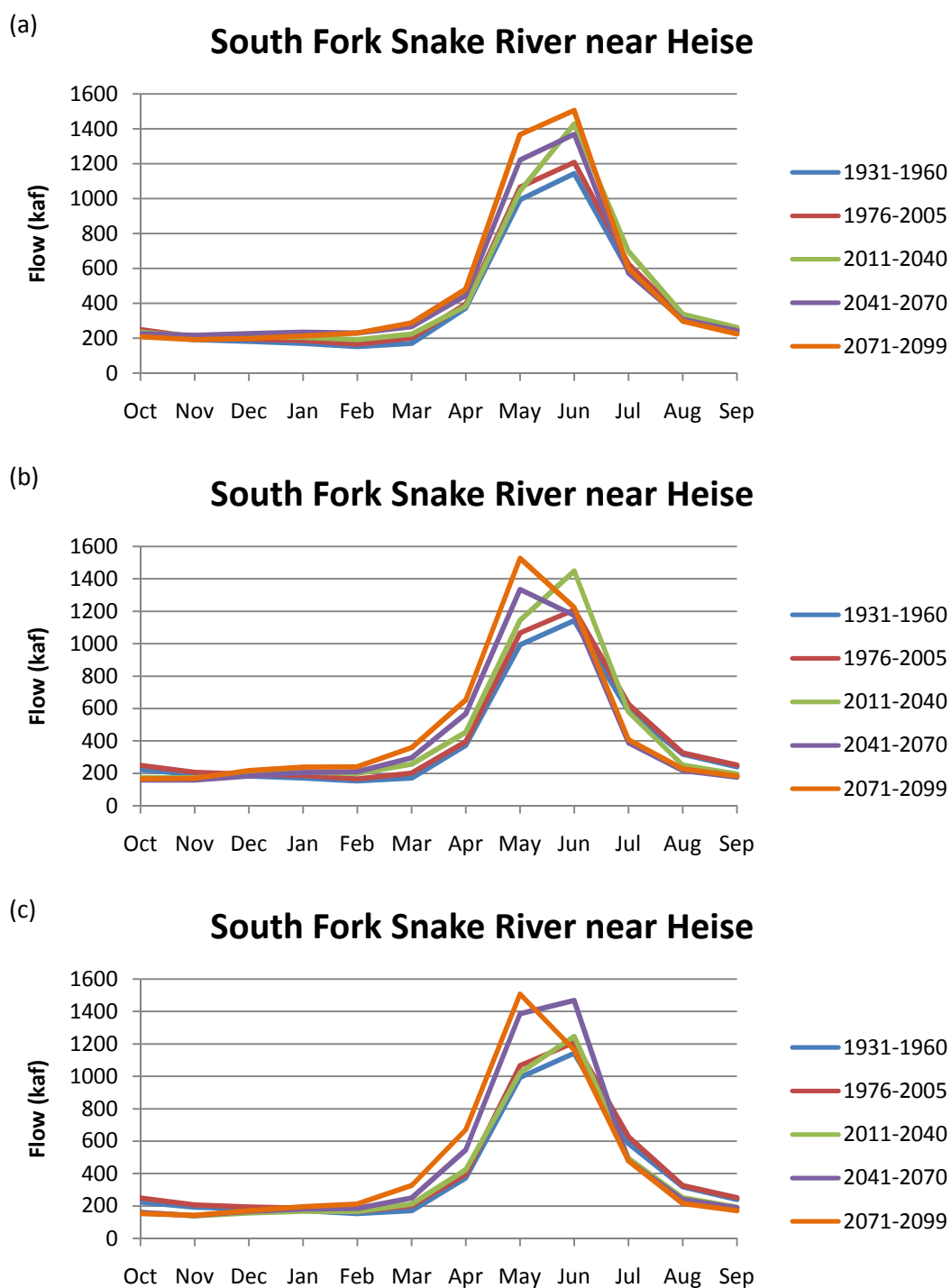


Figure D.4 Mean, Monthly, Historic, and Projected Flow of the South Fork of the Snake River near Heise for the (a) PCM1, (b) CCSM3, (c) ECHO GCMs

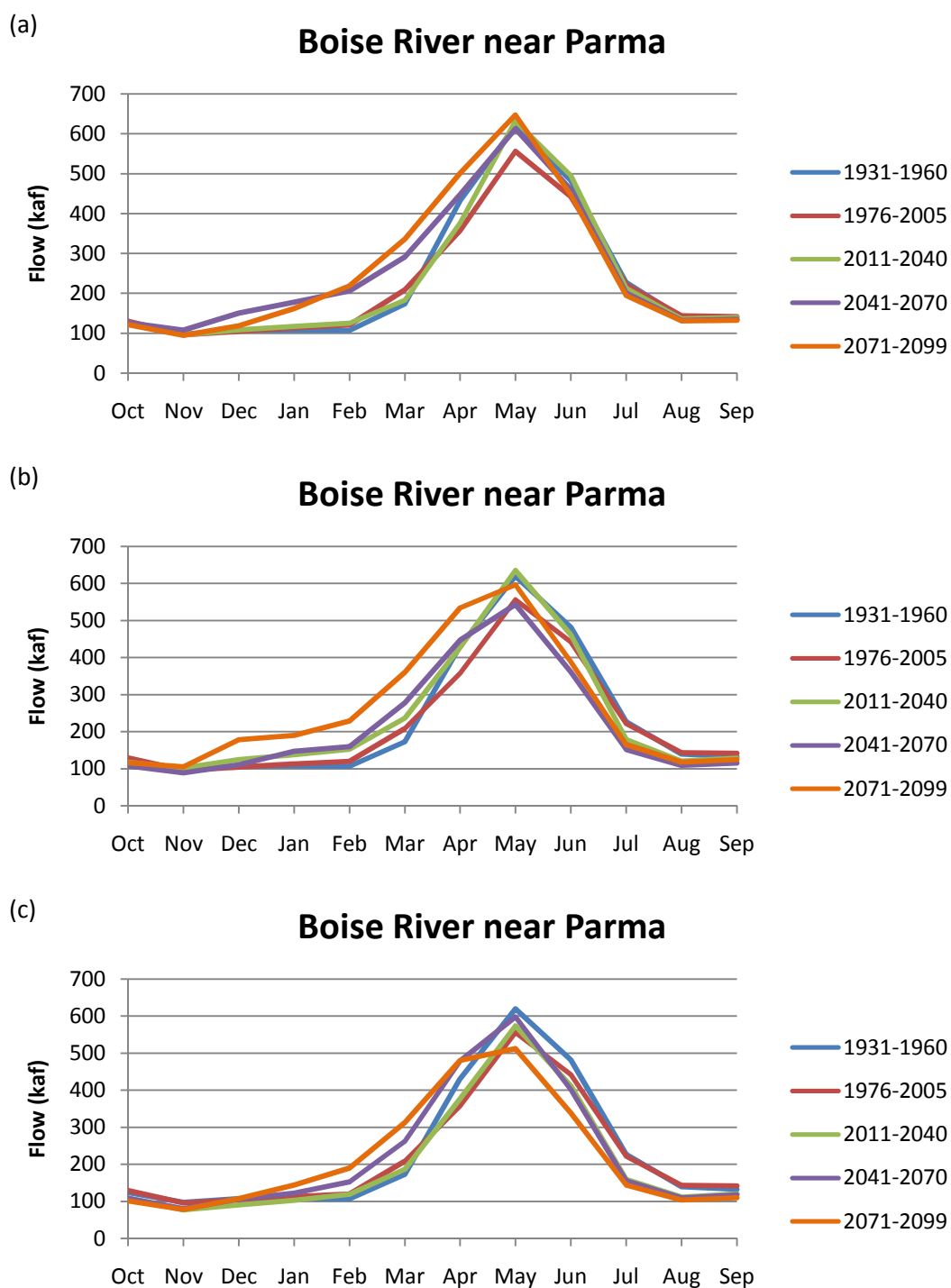


Figure D.5 Mean, Monthly, Historic, and Projected Flow of the Boise River near Parma for the (a) PCM1, (b) CCSM3, (c) ECHO GCMs

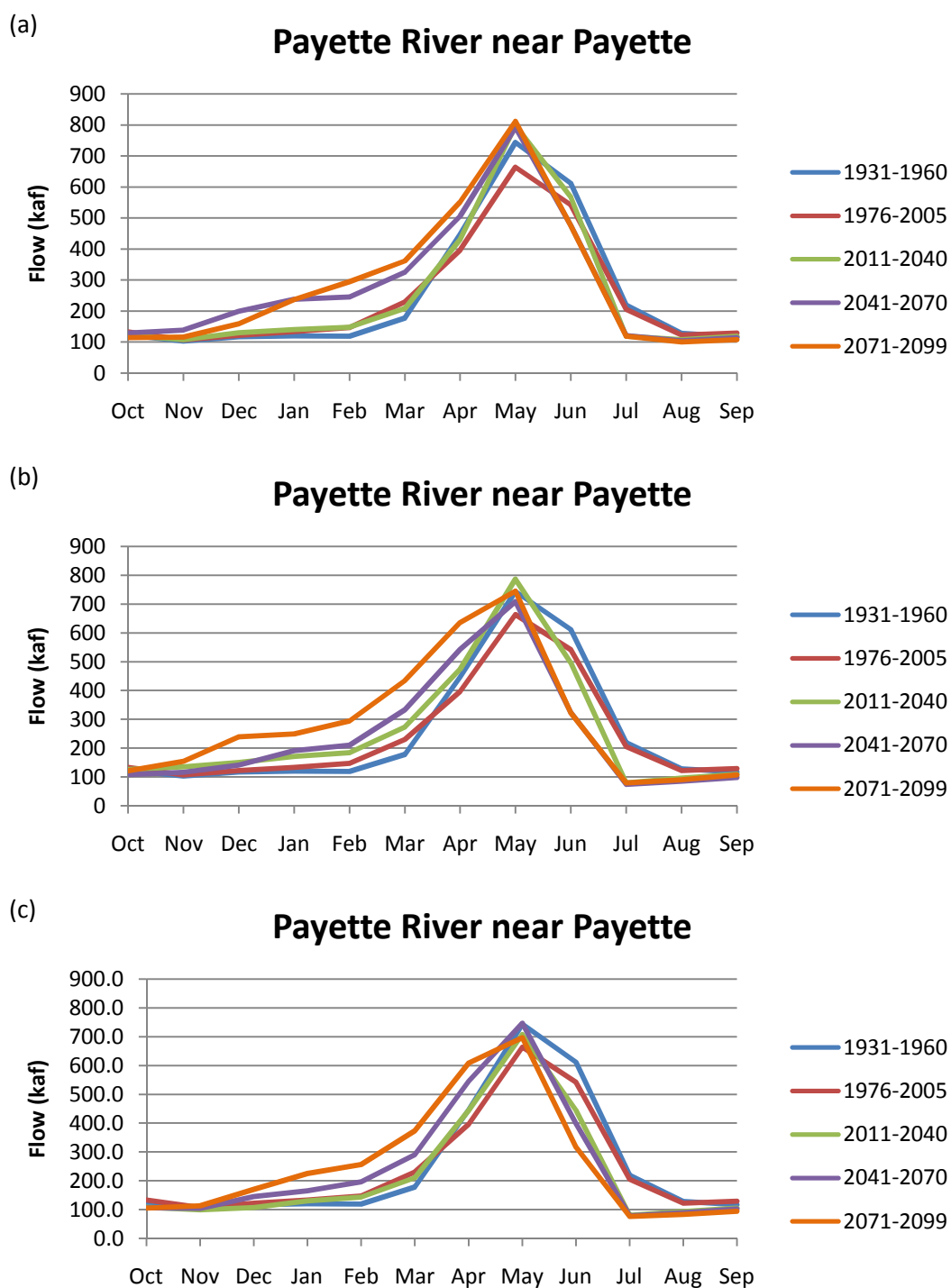


Figure D.6 Mean, Monthly, Historic, and Projected Flow of the Payette River near Payette for the (a) PCM1, (b) CCSM3, (c) ECHO GCMs

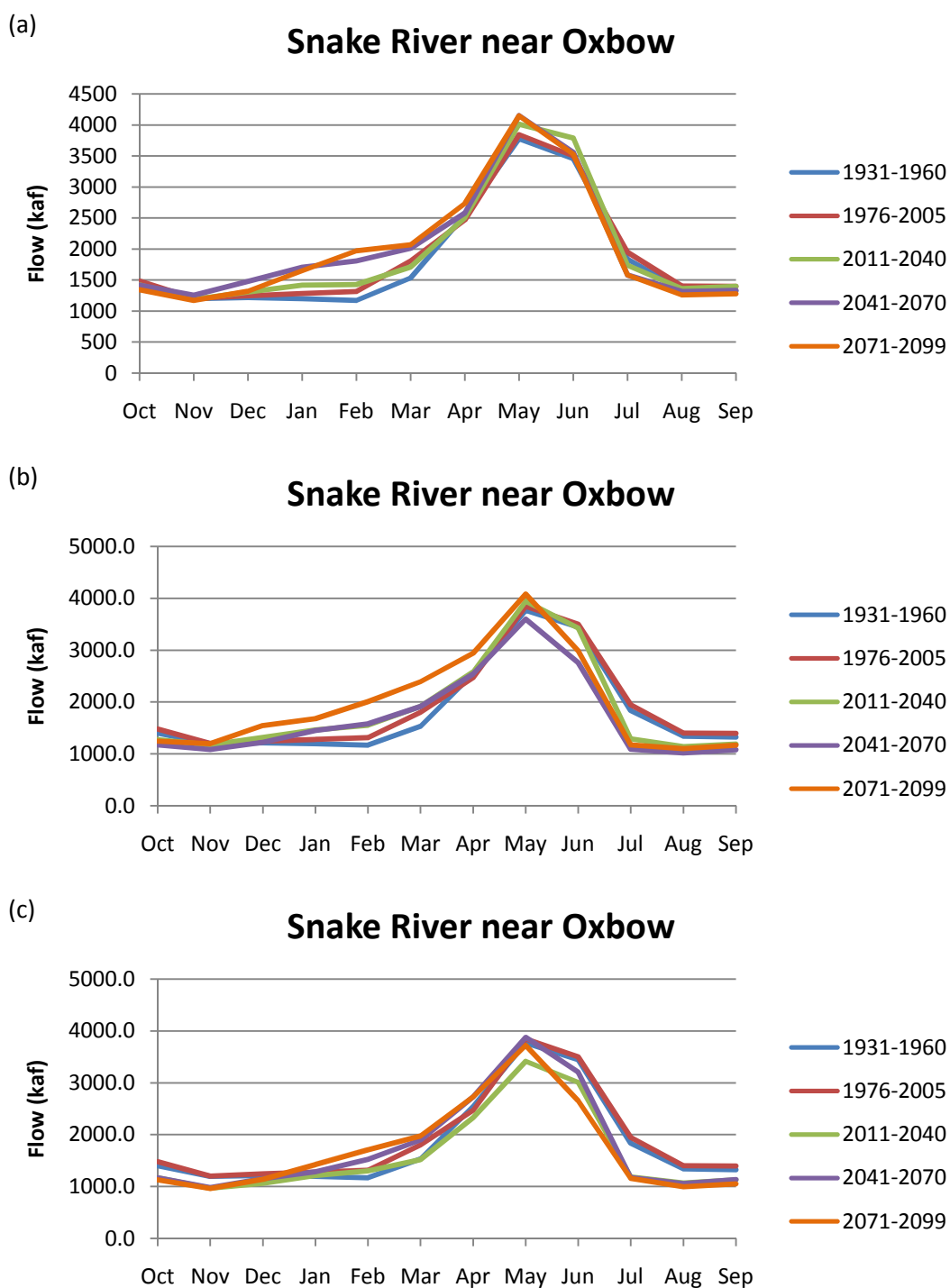


Figure D.7 Mean, Monthly, Historic, and Projected Flow of the Snake River near Oxbow Dam for the (a) PCM1, (b) CCSM3, (c) ECHO GCMs